RECAPITULATING PANCREATIC DEVELOPMENT IN INDUCING *IN-VITRO* HUMAN EMBRYONIC STEM CELL DIFFERENTIATION

by

Maria Jaramillo

B.S Biomedical Engineering, Florida International University, 2006

Submitted to the Graduate Faculty of

Swanson School of Engineering in partial fulfillment

of the requirements for the degree of

Doctor of Philosophy

University of Pittsburgh

2013

UNIVERSITY OF PITTSBURGH

SWANSON SCHOOL OF ENGINEERING

This dissertation was presented

by

Maria Jaramillo

It was defended on

June 27th, 2013

and approved by

Bridget M. Deasy PhD, Senior Scientist, CellStock LLC

Prashant N. Kumta, PhD, Professor, Department of Bioengineering

Rocky S. Tuan, PhD, Professor, Department of Orthopedic Surgery

Dissertation Director: Ipsita Banerjee, PhD, Assistant Professor, Department of Chemical and Petroleum Engineering

RECAPITULATING PANCREATIC DEVELOPMENT IN INDUCING *IN-VITRO* HUMAN EMBRYONIC STEM CELL DIFFERENTIATION

Maria Jaramillo, Ph.D.

University of Pittsburgh, 2013

Differentiation of human pluripotent stem cells into pancreatic beta cells could lead to the development of clinically relevant cells for the treatment of pathologies of the pancreas, specifically type 1 diabetes, which is the most common reason for pancreatic transplantation. Type 1 diabetes is a disease that consists in damage of insulin producing β-cells, therefore impaired regulation of blood glucose levels. While a number of groups have reported generation of differentiated phenotypes from stem cells expressing Insulin, all of these protocols have been limited by low yield and lack of mature functional cell types.

Organogenesis is a complex and dynamic process regulated by a milieu of chemical and physical signals along with interaction with neighboring cell types, all of which constitute the microenvironment niche of a developing organ. It is well recognized that in-vitro differentiation of embryonic stem cells can be best achieved by closely recapitulating the in-vivo micro-environmental niche. However, such an effort towards concerted modulation of different micro-environmental components is largely lacking in the area of pancreatic differentiation, where the primary focus till date have been on soluble chemical cues. We hypothesize that modulation of the chemical and physical micro-environment along with adequate intra-cellular signaling can

effectively modulate the functionality and fate commitment of differentiating population of stem cells. In order to test this hypothesis we developed strategies to alter physical properties of substrates, modify soluble signals during early stages of differentiation and use of novel intracellular signaling in pancreatic islet maturation.

TABLE OF CONTENTS

LIST OF TABLES

LIST OF FIGURES

1.0 INTRODUCTION

1.1 THE PANCREAS

Located beneath the liver and between the stomach and spine, the pancreas is a glandular organ that makes part of the human endocrine and digestive systems. The exocrine, or acinar part of the pancreas is composed of a system of ducts into which bicarbonate ions and digestive enzymes are secreted by centroacinar and basophilic cells respectively [1]. The endocrine portion of the pancreas, consisting of the islets of Langerhans, is responsible for production and secretion of an array of hormones whose main function is to regulate blood glucose levels. The islets of Langerhans are composed of several cell types, as illustrated in figure 1.1, each in charge of the production and secretion of a different hormone as follows: α cells produce glucagon, β-cells produce insulin, δ cells produce somatostatin and γ- cells produce pancreatic polypeptide [1].

1.1.1 α-cells

Alpha cells are make up to 20% of the endocrine pancreas and are responsible for production and secretion of glucagon. Upon low blood glucose levels, glucagon is secreted by α-cells into the bloodstream. Glucagon binds to receptors on hepatocytes where a cascade of events

is initiated that results in activation of glycogen phosphorylase which hydrolyses glycogen into glucose in a process called glycogenolysis [1]

1.1.2 β-cells

β-cells are responsible for insulin production and release, therefore are the major contributor of blood glucose regulation. β-cells are the only cells in the body capable of synthesizing large amounts of insulin. Insulin is translated as a single chain inactivated preprohormone, preproinsulin, which during insertion into the endoplasmic reticulum gets cleaved into proinsulin. Proinsulin consists of two domains connected by c-peptide, which gets cleaved by the action of several pancreatic endopeptidases, resulting in activated insulin and c-peptide, which are then packaged into secretory granules by Golgi-apparatus and then released from the cell upon appropriate stimuli [2]

Unlike most other cells in the human body, β-cells are capable of glucose intake in the absence of insulin. This is through GLUT2 transporters, which are transmembrane carrier proteins that allow passive transport of glucose into the cells [3]. Hence, when blood glucose levels are higher than intracellular levels, glucose diffuses into the β- cells trough GLUT2 transporters. Once inside the cells glucose gets phosphorylated by glucokinase, converting glucose into glucose-6 phosphate [4]. Glucose-6-phospate is used during metabolic activities of the β-cells, releasing the phosphate group which then binds to ADP increasing the amount of ATP available for cell respiration. Increase in cellular respiration increases NAD(P)H concentrations and consequently shifts the cells to a oxidative status, which increases intracellular calcium levels and consequently causes the closing of potassium channels which leads to cell depolarization and insulin-containing vesicle release [5].

1.1.3 δ-cells

δ-cells are in charge of somatostatin production and release. Somatostatin is an inhibitory hormone that acts on a variety of organs and systems including the pituitary gland and the gastrointestinal system. Its action in the pituitary gland involves inhibition of release of several hormones including growth hormone and thyroid stimulating hormone. In the gastrointestinal systems it inhibits release of hormones including insulin and glucagon [6].

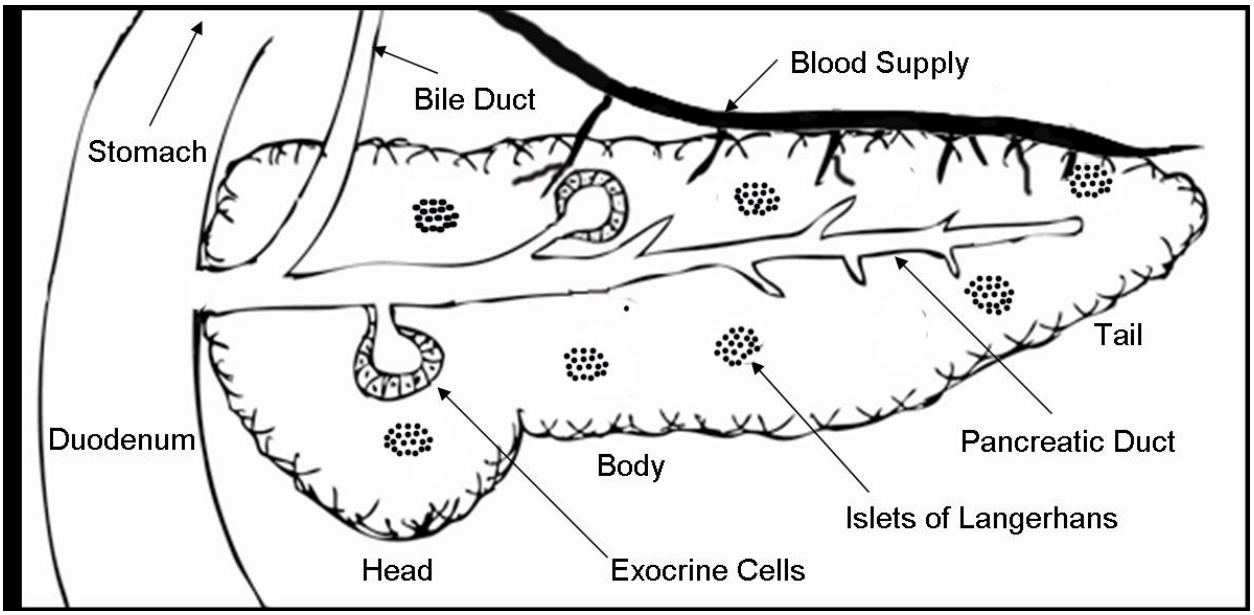

Figure 1.1 General pancreas anatomy

Exocrine cell interaction with the digestive system and endocrine cell (Islets of Langerhans) interaction with the blood stream.

1.1.4 Pancreas development

Pancreatic development starts with definitive endoderm (DE) formation which is marked by expression of several transcription factors including FOXA2, SOX17 and CER. Endoderm is formed by a flat sheet of cells which then folds forming the gut tube. Several signaling pathways,

including retinoic acid, fibroblast growth factors and TGFβ signaling, initiate specification of the pancreatic endoderm within the gut tube. Sonic hedgehog inhibition from the notochord induces expression of PDX1 in both the ventral and dorsal domain of the gut tube, although the sources of inhibition differ in each portion. This is followed by branching morphogenesis which will eventually form endocrine cells, duct cells and acinar cells. These events happen in both dorsal and ventral portions of the pancreas although the timing is different for each portion, with the dorsal development being more rapid than the ventral portion. Eventually rotation of the gut tube brings both compartments together and organization of the exocrine portion into acini and of the endocrine portion into islets occurs. At birth, the pancreas is capable of producing insulin, although glucose responsiveness differs from that seen in adult pancreas having a lower release threshold. Normal glucose stimulated insulin release is achieved within few days of birth [7,8].

1.1.5 Pancreatic disorders

Pancreatic disorders can be catalogued into two categories depending on which portion of the pancreas they affect. The main diseases that affect the exocrine portion of the pancreas are pancreatitis and pancreatic cancer, while diabetes mellitus is the ailment affecting the islets of Langerhans.

1.1.5.1 Exocrine disorders

The most common diseases affecting the exocrine portion of the pancreas are pancreatitis and pancreatic cancer. In pancreatitis, inflammation of the pancreas occurs due to injury caused by action of digestive enzymes on pancreatic tissue. Normally these enzymes are activated once they exit the pancreas, however, blockage due to infection or gallbladder stones amongst other

reasons can cause accumulation and activation within the pancreas. Depending on the causes, pancreatitis can be acute or chronic. Chronic pancreatitis is commonly caused by alcohol abuse, cystic fibrosis and hypercalcimia. In such cases, permanent damage to pancreatic structures takes place and could lead to grave complications including development of diabetes [9].

The majority of pancreatic cancer cases are classified as ductal adenocarcinomas which affect the exocrine potion of the pancreas. This cancer is characterized by poorly differentiated glandular structures believed to arise from progressive tissue changes. Prognosis of the disease is poor with a 1 year survival rate of 25%. Treatment options include surgery, chemotherapy and radiation, however, detection usually occurs late during the disease progression, therefore treatment success is limited. Current research in the area of pancreatic cancer is focused on early detection methods [10].

1.1.5.2 Diabetes Mellitus

Diabetes mellitus is a family of diseases that affect the endocrine portion of the pancreas, specifically, β-cells. It can be categorized into type 1 diabetes and type 2 diabetes according to their mechanism of action, even though type 2 diabetes itself is a whole family of disorders caused by an array of different factors [11].

Type 2 diabetes is often referred to as insulin resistant diabetes. It accounts for 90% of diabetic cases in the US and while there is a genetic component to it, it is highly linked to environmental factors such as sedentary life-style and at early stages can be treated through good nutrition and exercise. In a lot of cases type 2 diabetic patients produce normal or even elevated levels of insulin, however, it is the target tissues that are not able to properly use insulin, therefore uptake of glucose into the cells is delayed and decreased [12]. Although the exact mechanisms by which cells diminish their response to insulin are unclear, glucotoxicity, or cell

damage due to hyperglycemia is thought to be a key player in this [13]. Exercise usually reverses this insulin resistance due to the fact that skeletal muscle does not need insulin for glucose uptake, therefore normoglycemia is restored and this increases insulin responsiveness from cells throughout the body [14]. Unfortunately, type 2 diabetes patients often fail to make lifestyle changes leading to progression of the disease which often results in β-cells destruction and therefore exogenous insulin dependence.

Type 1 diabetes on the other hand is an autoimmune disorder prompting the destruction of β-cells and caused by genetic pre-disposition and often developing after viral infections. It is commonly diagnosed during childhood and leads to a series of systemic complications including cardiovascular system, kidneys, nerves and eyes. Since β-cells are destroyed in type 1 diabetes, insulin production is diminished and treatment options involve exogenous insulin supply [2].

During type 1 diabetes, glucose uptake from cells is impaired due to lack of available insulin, therefore cells need to find alternative ATP sources through breakdown of proteins from skeletal muscle, fatty acid breakdown from adipose tissue, and conversion of glycogen into glucose from the liver. Protein breakdown results in transport of amino acids to the liver, fat metabolism results in ketone conversion and glycogenolysis results in further elevated blood glucose levels, all of which have detrimental effects such as hypoxia and acidosis [12].

1.1.6 Therapeutic approaches for diabetes

As mentioned in the previous section, the first therapeutic option for type 2 diabetes consists of life-style changes such as exercise. In most cases however, poor patient compliance leads to need for pharmacological intervention such as drugs that inhibit digestion of carbohydrates, decrease glucose production in the liver, make tissues more responsive to insulin

or increase insulin secretion. In advanced cases where β-cell destruction occurs, insulin supply is necessary [15].

The main treatment option for type 1 diabetes consists of exogenous insulin supply. Along with this, constant glucose monitoring is necessary due to the fact that high glucose could lead to the events outlined in the previous section which could result in diabetic coma and possibly death; however, overuse of insulin could result in a hypoglycemic event leading to diminished glucose transport into the brain which could cause permanent brain damage and even death [12]. The complexity of this type of treatment has led investigators to develop alternative options for the treatment of diabetes in which beta cells are either repaired or replaced leading to endogenous production of insulin by the body.

The main alternative treatment is pancreatic transplantation which can be done alone or with kidney depending on the kidney function of the diabetic patient. Donor tissue comes from cadaveric patients, therefore the main limitation to this alternative is availability; hence the procedure is only performed in severe diabetes cases where insulin supply is deemed ineffective and there is permanent kidney damage [16]. A less invasive transplantation alternative involves infusion of isolated islets into the portal vein followed by immune suppression. In cases where this procedure is done, one patient may require islets from up to 3 donors, which makes this alternative highly restrictive due to availability [17].

Due to the limitations of current treatments, and high prevalence of diabetes, finding alternative cell sources for transplantation has been a prominent area of research in recent decades. Stem cells have received considerable attention in this regard and have shown promising potential as an alternate cell source. Differentiation of stem cells toward insulin-producing β cells has been attempted following approaches to recapitulate the natural process of

development. This change can be achieved by closely mimicking the native microenvironment, most commonly through the addition of soluble growth factors and molecules that direct differentiation [18]. A schematic of multi-stage protocols for differentiation of pluripotent stem cells into pancreatic cells, along with commonly used molecules and growth factors is represented in Figure 1.2

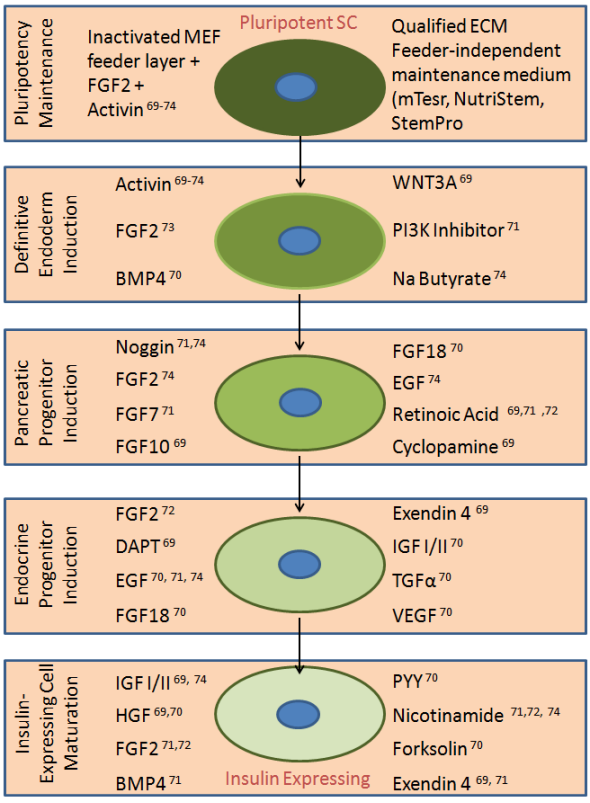

Figure 1.2 Schematic representation of multi-stage protocols for differentiation of pluripotent stem cells into pancreatic cell, along with commonly used molecules and growth factors

1.2 SPECIFIC AIMS

Diabetes is a disease affecting over 20 million people in the US. In diabetic patients the body is unable to produce or properly use insulin, which is necessary for intake of glucose into the cells, hence affecting cells' ability to produce energy [19]. The most common treatment for type I diabetes consists of exogenous insulin supply which can lead to grave complications, including a hypoglycemic event which often leads to death. While transplantation of pancreatic islets offers potential therapy, it is restricted by scarcity of donor islets[20]. Human embryonic stem cells (hESC) have two characteristics that make them an attractive alternative to whole organ transplantation: they can be maintained and expanded in an undifferentiated state indefinitely and can potentially be coaxed to differentiate into any cell type which makes them a possible unlimited cell source for transplantation[21]. Given these, it is no surprise that pancreatic differentiation of mouse and hESC has received considerable attention over the last decade. However exploitation of the full potential of embryonic stem cell requires a robust protocol for generation of mature and functional cell types, followed by efficient scaffold for transplantation

A number of groups have developed differentiation protocols that successfully derive insulin-expressing cells, however, several of these protocols have several limitations including low yield of insulin expressing cells, improper maturation, and therefore lack of functionality [22]. Most existing protocols exploit modulation of known developmental pathways trough chemical cues such as growth factors and small molecules [23]; however, other aspects of the

developmental niche have been ignored thus far, including physical and mechanical cues as well as cross-talk with different cell types of relevance to organogenesis.

Our long term goal is to develop a protocol for differentiation and transplantation of ESC into insulin producing and glucose responsive cells for treatment of type I diabetes. We propose to do this by emulating different aspects of the native microenvironment, chemically modulating previously identified contributing pathways as well as mimicking interactions with other cell types. This approach can reveal novel attributes of cell-material interactions along with cell-cell interaction. The project will enhance our understanding of how cells interact with their microenvironment during the process of differentiation. Furthermore, while we are specifically targeting pancreatic maturation a similar strategy can be adopted for other organ specific maturation as well.

The stem cell niche is the 3D microenvironment that stem cells encounter in the body and it composed of physical, chemical and mechanical cues that ultimately regulate cell fate [24]. This study aims to demonstrate how each of these microenvironmental components can be modulated to achieve hESC differentiation into cells with the potential of being used as an alternative cell source for the treatment of diabetes and other pathologies that affect the pancreas. In this study we use modulations of a different aspect of the microenvironment at different stages of differentiation as a possible strategy for induction as follows:

(a) Substrate physical properties to induce endoderm differentiation

(b) Novel use of intracellular signaling in pancreatic islet maturation

(c) Modulation of early germ layer commitment to alter functional phenotype

(d) Unique use of bioinformatics tools to analyze differentiation strategies

1.2.1 Aim 1: To evaluate the effect of substrate physical properties in early germ layer commitment

Conventionally, ESCs are differentiated by altering their chemical microenvironment through growth factors/ inhibitors/ inducers. Recently however, it was established that a mechanical microenvironment can also contribute towards cellular phenotype commitment [25]. In Chapter 2 we investigate how the cellular mechanical microenvironment of substrates affects the differentiation and phenotypic commitment of ESCs by culturing cells in a fibrin hydrogel matrix in 2D and 3D cultures.

1.2.2 Aim 2: To evaluate the effect of soluble growth factors on pancreatic maturation of hESCs

It is well understood that potential for functional maturation of the ESCs is strongly dependent on the quality of initial germ layer commitment, in our case endoderm germ layer. Past studies have established multiple pathways of inducing DE. However, the effect of pathway of endoderm induction on late stage functional maturation still remains elusive. The objective of the Chapter is to quantitatively analyze the effect of alternate DE induction pathways on the dynamics of differentiation and functional maturation to pancreatic islet cell-types.

1.2.3 Aim 3: To investigate the effect of cell-cell signaling during pancreatic maturation of hESC

Existing β-cell differentiation protocols typically achieve later stages of maturation through addition of chemical cues that modulate pathways known to induce maturation of β-cells in-vivo. Our objective in Chapter 4 is to investigate the effect of cell-cell interaction in inducing maturation of hESC derived pancreatic progenitor cells to islet cell types. We chose endothelial cells as a possible candidate since during organogenesis endothelial cells from the aorta develop in close proximity to the pancreas and has been implicated to be involved in islet development [26,27]. Furthermore, endothelial cells have been proven to increase survival and functionality of β-cells in culture and have been proven to modulate differentiation of other tissues including endodermally derived tissues.

2.0 INDUCING ENDODERM DIFFERENTIATION BY MODULATING MECHANICAL PROPERTIES OF SOFT SUBSTRATES

2.1 INTRODUCTION

ESC are pluripotent cells isolated from the inner cell mass of the blastocyst. Aside from their ability to differentiate into any tissue cell type, they can be propagated in vitro in an undifferentiated state indefinitely which makes them perfect candidates for use in the area of regenerative medicine and study of differentiation [21]. The first stage of ESC differentiation is marked by the formation of 3 germ layers with distinct molecular markers from which all tissue types will arise. Ectoderm forms mainly the skin and the nervous system. The mesoderm forms muscle, cartilage, bone as well as hematopoietic cells while endoderm mainly forms the GI tracts and both liver and pancreas [28].

Research in the last decade has established the possibility of differentiating ESCs in an in-vitro setting to not only early germ layers, but to mature organ specific cells as well. Most of these in-vitro inductions are achieved through modulations of the chemical microenvironment. More recently, researchers are studying the effect of mechanical cues such as matrix elasticity on stem cell differentiation [29,30]. Mesenchymal stem cells, when cultured on substrates of varying stiffness were reported to exhibit significant difference in their lineage commitment, which could be correlated to the physiological stiffness of the differentiated phenotype [25].

Similar studies have been performed in ESC; however, most of these studies are targeted toward osteogenic differentiation, hence using substrates with stiffness ranges that are a few orders of magnitude higher than the ones used for this study [30].

In this study, we are reporting how the physical microenvironment of soft substrates affects the early differentiation and phenotypic commitment of ESC, with emphasis on endodermal differentiation. In order to demonstrate this effect, fibrin, a biocompatible hydrogel was selected as the substrate for providing the desired variation in the physical microenvironment, primarily by modification of its gelation characteristics. Fibrin was selected primarily because of its known attributes as a biocompatible and biodegradable scaffold, which will enable future translation into clinical studies. Furthermore, fibrin is a biopolymer that plays a key role in the natural process of wound healing [31] which makes it a good candidate for stem cell transplantation [32]. Moreover, it has also been recently studied as a gel carrier system for beta-islet transplantation [33] and can also be easily coupled with chemical cues to aid differentiation [34], making it ideal for stem cell differentiation studies. Additionally, the substrate chemistry of fibrin hydrogels can be easily manipulated to achieve a broad range of soft substrates, making it suitable for the present study.

The overall objective of this study is to investigate the effect of physical properties of soft substrates on specific characteristics of ESC. The ESC cultures differentiated on fibrin gel were analyzed in detail to ascertain their proliferative potential and differentiation patterning behavior in response to variations of substrate mechanical properties. Two different culture configurations were analyzed: cells seeded on top of pre-formed fibrin gel (2 dimensional) and cells embedded inside the fibrin gel (3 dimensional). To the best of the authors' knowledge this is the first report illustrating the effect of physical properties of soft substrates on endodermal differentiation of

ESC. This can have a significant impact in the derivation of hepatic or pancreatic cells from ESCs, to be used in the treatment of hepatic disorders and diabetes respectively.

2.2 RESULTS

2.2.1 SEM characterization of fibrin microstructure

Appropriate characterization of ESC interaction with a substrate microenvironment requires a thorough understanding of the microstructural features of the substrate under various conditions. Figure 2.1A and 1B illustrate SEM images of the fibrin gels taken at two very high values of fibrinogen concentrations of 1 and 8mg/ml, respectively selected as representative concentrations. It was observed that for a fixed fibrinogen concentration, there was a decrease in fiber diameter as thrombin concentration increased (Figures. 2.1A: a, b, c) and the fibers appeared to be less bundled. It can also be seen that there was no significant difference in fiber diameter between 1x and 2x compared to 0.25x. The difference in diameter also appeared to become less significant as fibrinogen concentration increased.

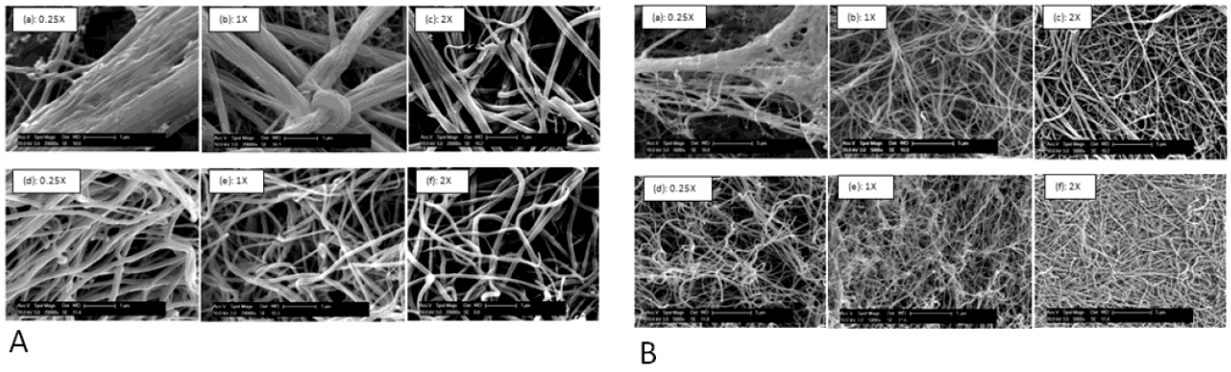

Figure 2.1: Microstructure of fibrin gels of varying fibrinogen thrombin concentrations.

(A) Effect of varying fibrinogen concentration as well as fibrinogen to thrombin ratios on the microstructure of the gels imaged at a high magnification of 20KX. In (a)-(c) 1 mg/ml of fibrinogen at fibrinogen to thrombin ratios of 0.25X, 1X, and 2X respectively. In (d)-(f) 8 mg/ml of fibrinogen at fibrinogen to thrombin ratios of 0.25X, 1X, and 2X respectively. (B) Effect of varying the fibrinogen concentration as well as the fibrinogen to thrombin ratios on the microstructure of the gels observed at a low magnification of 5KX. In (a)-(c) 1 mg/ml of fibrinogen at fibrinogen to thrombin ratios of 0.25X, 1X, and 2X, respectively. In (d)-(f) 8 mg/ml of fibrinogen at fibrinogen to thrombin ratios of 0.25X, 1X, and 2X, respectively.

As fibrinogen concentration decreased for a fixed fibrinogen to thrombin (F/T) ratio, the fibers formed more bundle type thicker structures, as can be seen in Figure 2.1A: e compared to 1A: b. As a result, each fibril appears to have a larger fiber diameter: ~ 0.5-0.75 mm for 1mg/ml fibrinogen compared to~0.1 mm for a fibrinogen concentration of 8mg/ml at a fixed F/T ratio of 1x.

Table 2.1 Concentration of Thrombin in NIH units for all fibrin hydrogel conditions

Fibrinogen Concentration	0.25x*	1x#	2x@
1 mg/ml	0.1	0.4	0.8
2 mg/ml	0.2	0.8	1.6
4 mg/ml	0.4	1.6	3.2
8 mg/ml	0.8	3.2	6.4

* Fibrinogen/Thrombin = 10.
\# Fibrinogen/Thrombin = 2.5.
@ Fibrinogen/Thrombin = 1.25.

Furthermore, at a fixed fibrinogen concentration, the substrate appeared to have a more open pore structure with a larger pore size as thrombin concentration decreased from 2x to 1x and 0.25x, as can be seen for both 1 and 8mg/ml fibrinogen concentrations in Figures 2.1B: a-c and d-f, respectively. To better analyze the effect of thrombin concentration on the porosity of the substrate, ImageJ software was used to quantify the average pore size of the gel at fixed fibrinogen concentrations. SEM images were binary and ImageJ software was used to estimate the average size of spaces between fibers. This value was obtained for each fibrinogen concentration and was normalized to the values obtained for gels synthesized with the same fibrinogen concentration at a F/T ratio of 2x. As illustrated in Figure 2.2, pore size decreased with increasing thrombin concentrations for both 1 and 8 mg/ml values of fibrinogen concentrations. However, the effect of thrombin concentration on pore size was much stronger between 0.25x and the higher ratios, while between 1x and 2x, the changes were minimal as can be seen in Figure 2.1.

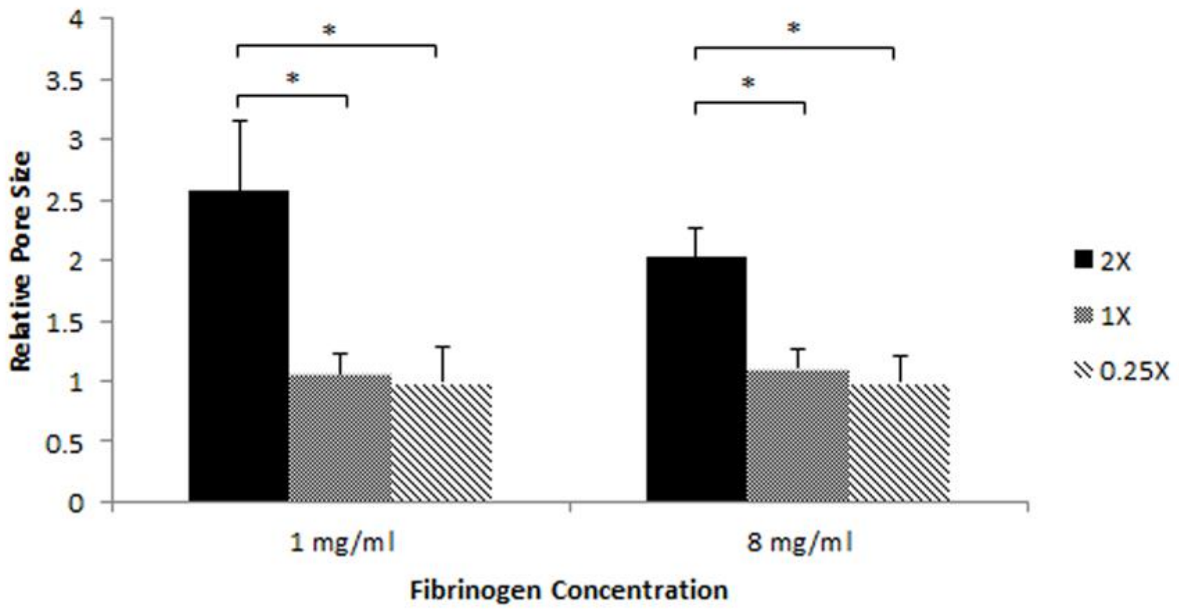

Figure 2.2: Average pore size

calculated using ImageJ for 1 mg/ml and 8 mg/ml fibrinogen concentrations and all three fibrinogen to thrombin ratios normalized to 2X for both fibrinogen concentrations. * p<0.05 compared to highest stiffness group.

2.2.2 Rheological characterization of fibrin hydrogels

The effect of microstructural variations of the gel on the macroscopic property of the gel substrate was investigated by conducting a rheological characterization of the gel. Table 2 illustrates the storage modulus (G'), a measure of energy stored by the sample under oscillatory deformation conditions, while Table 3 illustrates the loss modulus (G"), a measure of energy dissipated under vibratory conditions. Both storage and loss moduli showed little dependence on frequency of oscillation, indicative of a solid-like behavior: therefore, their values at a frequency of 0.5Hz was arbitrarily chosen as a representative value.

After being cleaved by plasmin, fibrinogen is converted into the monomeric form of fibrin and self-assembles to form an insoluble fibrin clot that is stabilized by the crosslinking of factor XIII. In the current study, the scaffold storage modulus was varied by two orders of magnitude from 4 Pa, corresponding to a fibrinogen concentration of 1mg/ ml, and an F/T ratio of 0.25x to 247 Pa, corresponding to a fibrinogen concentration of 8mg/ml and an F/T ratio of 2x. Furthermore, upon increasing thrombin concentration for a fixed fibrinogen concentration, gel stiffness increased by as much as 76 Pa (8mg/ml of fibrinogen for F/T ratios of 0.25 and 2x). Mechanical stiffness was varied by either keeping the fibrinogen concentration fixed or by selecting four different fibrinogen concentrations: 1mg/ml representing the low range and 8mg/ml representing the high range. Similarly, for a fixed fibrinogen concentration, the thrombin concentration was varied correspondingly to F/T ratios of 0.25, 1 and 2x, representing low, medium and high units of thrombin, respectively. Based on this, rationale, it was thus possible to prepare fibrin gels that exhibited a wide range of mechanical stiffness.

Moreover, despite altering the F/T ratio, conditions with the same thrombin concentration and different fibrinogen concentrations also existed. Similarly, after increasing fibrinogen concentration, gel stiffness also increased by as much as 95 Pa (4mg/ml fibrinogen with F/T 2x and 8mg/ml fibrinogen with F/T 1x). The three cases in which fibrinogen concentration was doubled were as follows: 1) 1mg/ml fibrinogen with an F/T ratio of 2x and 2mg/ml of fibrinogen with an F/T ratio of 1x; 2) 2mg/ml of fibrinogen with an F/T ratio of 2x and 4mg/ml of fibrinogen with an F/T ratio of 1x; and 3), 4 mg/ml of fibrinogen with an F/T ratio of 2x and 8 mg/ml of fibrinogen with an F/T ratio of 1x). Gel stiffness nearly doubled in all three cases, while thrombin concentration remained fixed except at low fibrinogen concentrations as illustrated in Table 2.

Table 2.2: G' values in Pa for various fibrinogen concentrations and all crosslinking conditions at a frequency of 0.5 Hz

fibrinogen concentration	0.25x	1x	2x
1 mg/ml	4.0 ± 0.9*	14.1 ± 4.0*	24.8 ± 4.5
2 mg/ml	13.0 ± 0.9*	35.8 ± 8.7	42.0 ± 7.1
4 mg/ml	72.1 ± 6.0*	89.2 ± 9.1	97.9 ± 11.9
8 mg/ml	171.1 ± 20.3*	193.9 ± 17.7*	247.3 ± 15.5

* $p < 0.05$ compared to highest stiffness group.

Table 2.3: G'' values in Pa for various fibrinogen concentrations and all crosslinking conditions at a frequency of 0.5 Hz

fibrinogen concentration	0.25x	1x	2x
1 mg/ml	0.7 ± 0.1*	1.5 ± 0.3	2.7 ± 0.6
2 mg/ml	3.3 ± 0.4	4.6 ± 1.6	4.8 ± 1.7
4 mg/ml	9.4 ± 1.4	10.8 ± 3.0	11.5 ± 2.5
8 mg/ml	24.7 ± 4.6*	28.2 ± 2.8	33.7 ± 3.9

In comparing this trend where thrombin concentration was doubled for a fixed fibrinogen concentration (1-2x for all fibrinogen concentrations), a much lower relative increase in storage modulus was observed, except at lower fibrinogen concentrations. This suggests that fibrinogen concentration was more influential on the manipulation of gel moduli, except under dilute conditions. Interestingly, the storage modulus for all conditions was not exclusive and an overlap in modulus was observed between the two conditions. More specifically, the moduli of gels prepared with 1mg/ml fibrinogen and an F/T ratio of 1x and 2mg/ml fibrinogen with an F/T ratio of 0.25x were both~14 Pa, indicative of the influence of other microstructural forces affecting mechanical stiffness such as fiber diameter, porosity and orientation.

2.2.3 Effect of substrate stiffness on embryonic stem cell proliferation

ESCs plated on soft fibrin substrates were found to attach well under all substrate conditions and were alive and proliferating. However, cells did not spread out significantly and retained a spherical clumped-up morphology.

Observation of the cells after three days of culture consistently showed the formation of cell clusters (Figure 2. 3). When cell morphology was compared across substrates of different thrombin concentrations for the same fibrinogen concentration, it was typically observed that substrates with lower thrombin concentrations resulted in larger cell clusters compared to their more crosslinked counterparts.

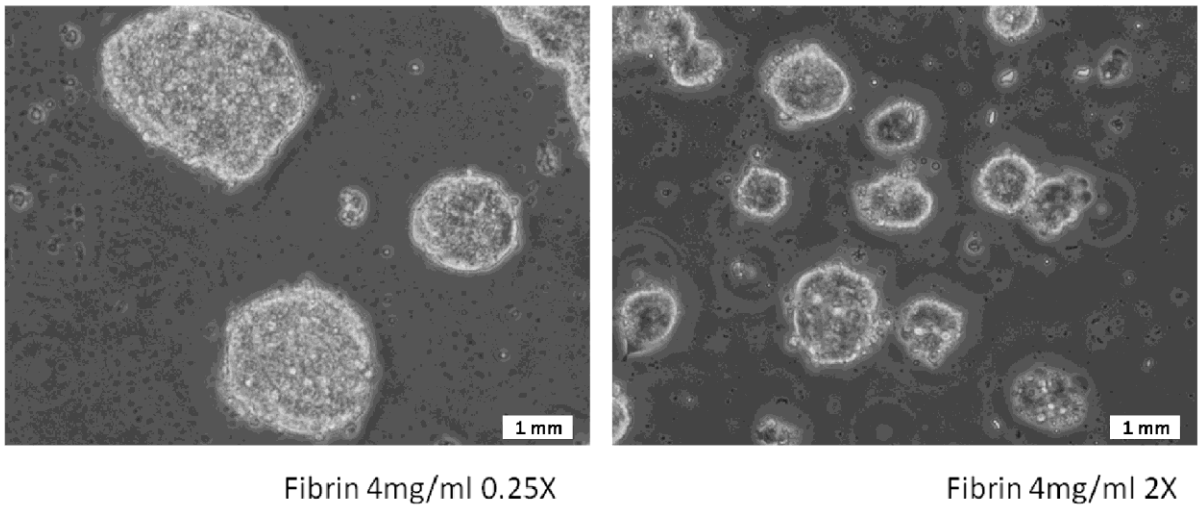

Figure 2.3: Aggregation of cells on fibrin substrates.

Representative images of cells plated on gels of identical fibrinogen concentration, but varying cross-linking fibrinogen/thrombin ratio: 0.25X (Left) and 2X (Right). Cells attach, but do not spread out, instead, they form cell clusters. Cell cluster size greater in gels with lower cross-linking ratio.

Since differences in cell cluster size can be attributed to differences in cell proliferation rate, proliferation analysis was performed by Alamar blue assay 24 h after plating the cells on fibrin gels. A duration of 24 h was chosen primarily to minimize the effect of fibrin degradation by the cells and to avoid the effect of differentiation on proliferation. The effect of thrombin concentration of the substrates on cellular proliferation is illustrated in Figure 2.4. For each fibrinogen concentration, the proliferation rate was normalized to the condition with the lowest F/T ratio. It was consistently observed that for a specific fibrinogen concentration, ESCs cultured on lower crosslinked substrates exhibited a higher proliferation rate compared to parallel cultures on a more crosslinked structure.

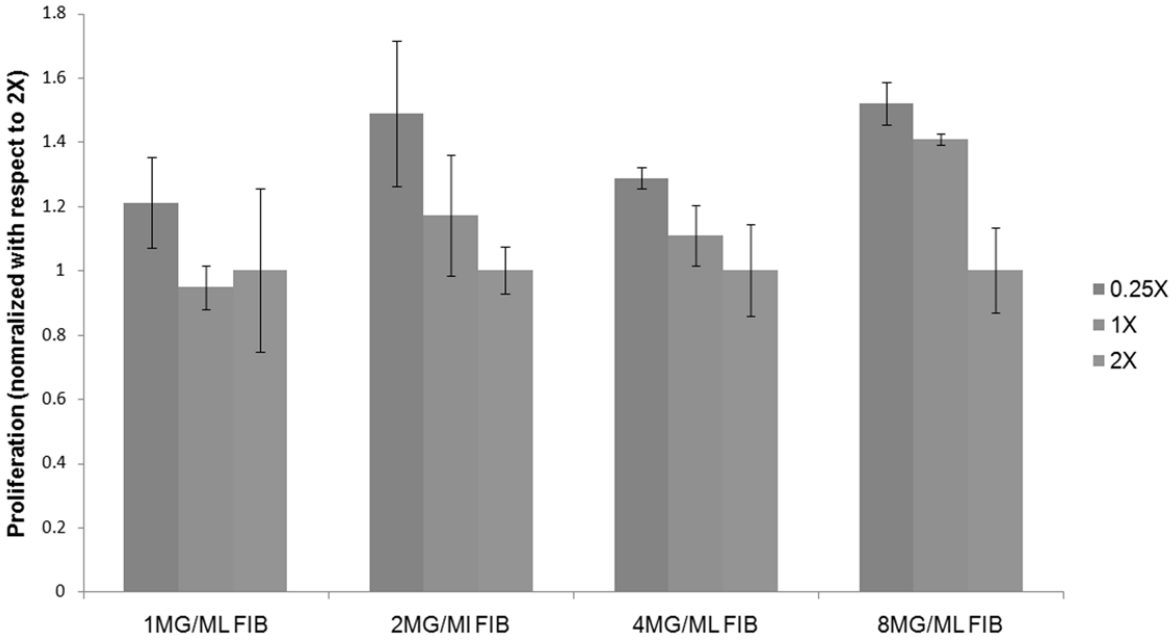

Figure 2.4: ES cell proliferation on fibrin substrates of varying compositions

Comparison of the proliferation of mouse ES cells plated on gels of different fibrinogen concentration and varying cross-linking ratio after 24 hours of plating. Y-Axis represents alamar blue fluorescence. All results normalized with respect to the lowest cross-linking ratio for each group. At all fibrinogen concentrations proliferation was found to decrease as the cross-linking increased. * $p<0.05$ compared to highest stiffness group.

2.2.4 Effect of substrate physical properties on embryonic stem cell differentiation

2.2.4.1 Substrate Stiffness

ESCs were plated on the gels and allowed to spontaneously differentiate for five days, after which samples were analyzed by qRT-PCR for three different marker for each of the germ layers and for pluripotency assessment. The markers used were: undifferentiated markers *REX1*,

OCT4 and *SOX2* [35-37]; early endoderm markers *AFP*, *SOX17* and *HNF4* [38-40]; early mesoderm markers *BRACH, GSC* and *FGF8* [41-43]; and early ectoderm markers *Nestin, FGF5* and *BMP4* [44-46]. During differentiation, cells were cultured in DMEM/FBS without further lineage specific induction.

The effect of substrate properties on ESC differentiation was analyzed by comparing the relative variation of all germ layer markers across the entire range of substrate stiffness. Figure 2.5A illustrates the sensitivity of each germ layer along with pluripotency to changes in substrate stiffness. It was observed that pluripotency markers maintained similar expression levels in all substrates. As to individual germ layers, Figure 2.5A shows that mesoderm and ectoderm markers were relatively insensitive to changes in substrate stiffness in the specific stiffness ranges examined. Endoderm markers, however, were found to respond strongly to changes in substrate properties. It was observed that substrates of lower stiffness of~13 Pa resulted in stronger endoderm upregulation. However, a higher stiffness range of 171 Pa was observed to upregulate both *AFP* and *SOX17*. Interestingly, the other germ layers were also slightly elevated under higher stiffness conditions, indicating an overall increase in differentiation under those conditions. Moreover, preferential upregulation of endoderm markers was observed only at lower stiffness conditions. Of the endoderm markers, the magnitude of upregulation of *AFP* was thousands of folds stronger than that of *SOX17*, while both *SOX17* and *AFP* elicited a similar trend in expression.

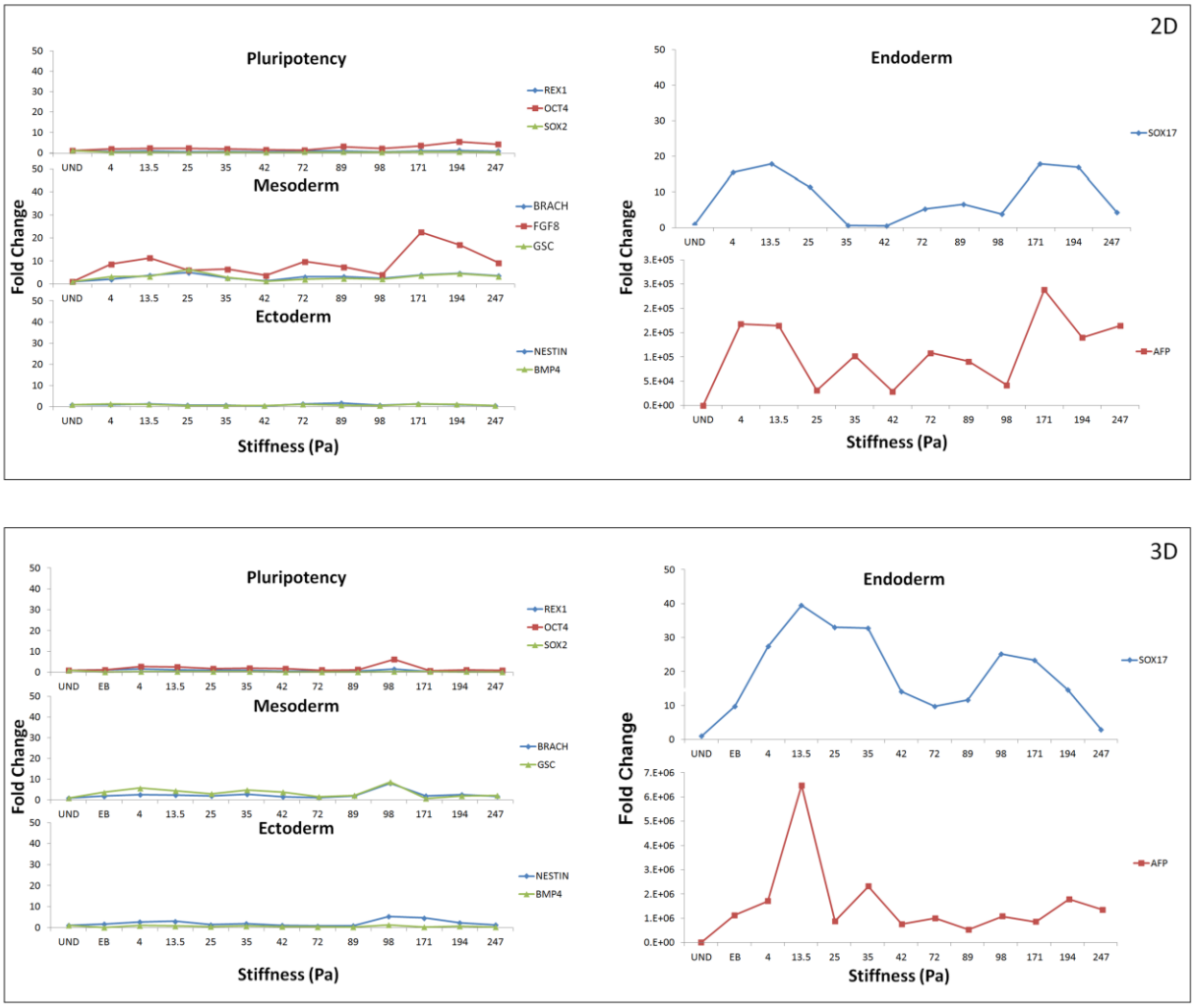

Figure 2.5: The effect of changing substrate stiffness on the ESC differentiation in 2-dimensional (a) and 3-dimensional (b) configurations. Results are normalized with respect to undifferentiated cells. Most significant effect was observed in the up-regulation of endoderm markers *SOX17* and *AFP* in lower range stiffness gels. Effect was more prominent in 3-dimensional configurations.

2.2.4.2 Substrate Composition

As earlier mentioned, fibrin substrate properties were modified by changing both fibrinogen concentration and F/T ratio. As a result, it was important to analyze the effect of gel composition on stem cell differentiation. Differentiation patterns were compared across different thrombin concentrations for a fixed value of fibrinogen concentration (Figures 2.6a, b). Very

high fibrinogen concentrations of 1 and 8mg/ml were chosen to assess differentiation patterns across a wide spectrum of fibrinogen concentrations. For ease of comparison, the fold changes in gene expression levels were represented by normalizing to 2x crosslinking for each fibrinogen concentration.

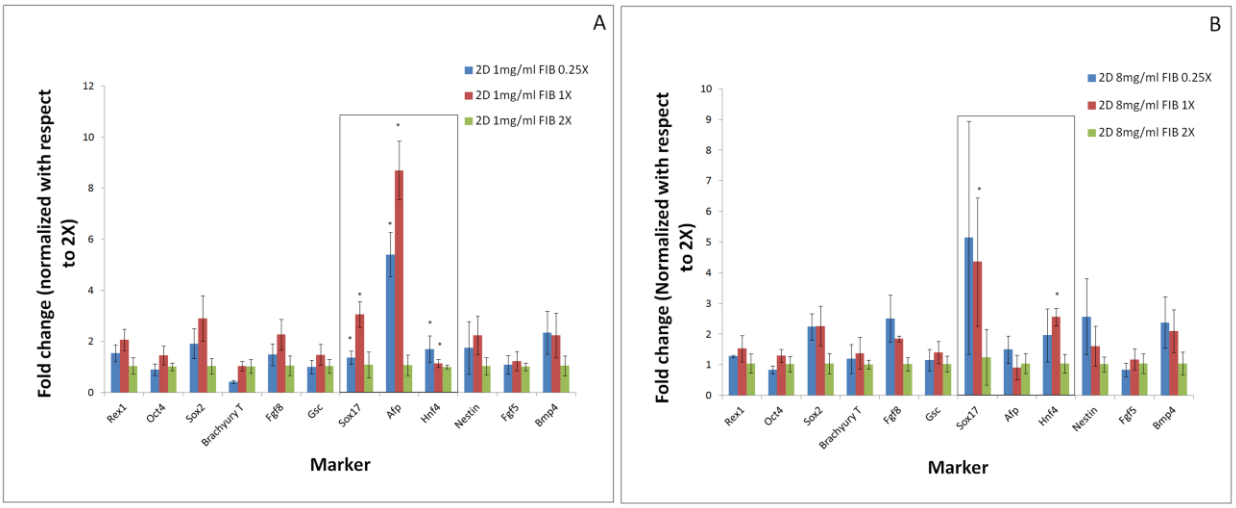

Figure 2.6: The effect of substrate cross-linking ratios on 2D ESC differentiation analyzed at extreme fibriniogen concentrations of 1mg/ml (a) and 8mg/ml 1mg/ml (b) in 2-dimensional configuration. Results are normalized with respect to highest cross-linking ratio of 2X. Most significant effect was observed in the up-regulation of endoderm markers when compared between cells differentiated on gels of lower cross-linking (0.25X, 1X) and higher cross-linking (2X) ratio. * p<0.05 compared to highest stiffness group.

Analogous to Figure 2.5, the mesoderm and ectoderm markers were found to be relatively insensitive to changes in crosslinking ratio in the 1mg/ml fibrinogen concentration (Figure 2.6a). In contrast, the endodermal markers, particularly *SOX17* and *AFP*, were found to be extremely sensitive to changes in crosslinking ratio. For 1mg/ml fibrinogen concentration, we observed approximately 5- and 9-fold increases in *AFP* expression levels for softer gel conditions of ratios 0.25 and 1x, respectively, compared to the stiffer gels synthesized at 2x. *SOX17* expression levels exhibited a moderate 3- and 5-fold increase when thrombin

concentration was lowered from 2 to 1x in both fibrinogen concentration groups, respectively. Similar patterns were found across all fibrinogen concentrations, where lowering the crosslinking ratio resulted in stronger expression of endoderm markers (Appendix figs. 2.1, 2.2).

While the above analysis focuses on the effect of changing crosslinking ratios for fixed fibrinogen concentrations, it was worthwhile to compare the effect of changing fibrinogen concentrations for a fixed cross-linking ratio, since both cases resulted in differences in substrate stiffness (Table 2.2). Figure 2.9 represents the changes in gene expression levels when the F/T ratio remained constant (1x) while the concentration of fibrinogen varied between 1 and 8 mg/ml (Figure 2.9A). It was observed that lower values of fibrinogen concentration preferentially favored endoderm differentiation.

2.2.4.3 Substrate Microstructure

In all analyses, we consistently observed that endoderm upregulation correlated with lower substrate stiffness conditions and was achieved either by lowering the crosslinking ratio for fixed fibrinogen concentrations or by lowering fibrinogen concentrations for a fixed crosslinking ratio. To further analyze whether substrate stiffness was uniquely controlling the differentiation patterning, we examined two fibrin substrates of similar stiffness but of various fibrinogen and thrombin concentrations and analyzed ESC differentiation patterns on them. As illustrated in Tables 2.1 and 2.2, gels synthesized with 1mg/ml fibrinogen with an F/T ratio of 1x and 2mg/ml fibrinogen with an F/T ratio of 0.25x resulted in a similar gel stiffness value of~14 Pa. ESCs differentiated on these two conditions were analyzed for their differentiation patterns, as illustrated in Figure 2.10. Of interest, it was observed that the mesoderm and ectoderm markers elicited quite similar behavior under these conditions, although endoderm markers were strongly altered. These results indicate that while substrate stiffness strongly influenced

differentiation patterns, it was clearly not the sole player in this complex process. Careful observation of the fibrin gel under these two conditions by SEM (Appendix figure 3) revealed significant differences in their microstructural characteristics despite comparable stiffness values. Analysis revealed that some of the major structural differences included differences in fiber density, fibrin and pore size. Following this analysis, it is reasonable to suggest that along with macroscopic stiffness, microstructural features are also likely to influence differentiation patterns. A more detailed characterization of the gel microstructural features and its possible correlation with ESC differentiation is currently being investigated by our group.

2.2.4.4 Culture Configuration

Experiments were performed by plating cells on pre-formed fibrin gels in 2D configurations. However, to better elucidate the effects of stiffness, composition and microstructure in ESC differentiation, ESCs were also cultured in 3D configurations in which ESCs were suspended within the fibrin substrate during synthesis of the gels.

Similarly to 2D experiments, the effect of substrate properties on ESC differentiation was analyzed by comparing the relative variation of all germ layer markers across the entire range of substrate stiffness. Figure 2.5B illustrates the sensitivity of each germ layer along with pluripotency to changes in substrate stiffness. Pluripotency, mesoderm and ectoderm markers were relatively insensitive to changes in substrate stiffness in the specific stiffness ranges considered in this study. Endoderm markers were found to respond strongly to changes in substrate property. It was observed that substrates of lower stiffness (~ 13 Pa) resulted in stronger endoderm upregulation. In contrast to 2D configurations, the positive effect of higher stiffness range was less obvious in 3D cultures, where the strongest effect was in the lower range of 13 Pa. Both *SOX17* and *AFP* elicited a similar trend in expression; the magnitude of

upregulation of *AFP* was thousands of folds stronger than that of *SOX17*, with the upregulation under 3D culture being more dominant than 2D configuration. An additional control of ESC differentiation through EB formation was included in the 3D cultures to account for the possible effect of biochemical induction arising from differential swelling of the gels. As illustrated in Figure 2.5, the magnitude of upregulation in softer substrates was much stronger than that of EB, which suggests that the substrate played a more significant role than biochemical induction through the media.

We also studied the effect of substrate composition in 3D configurations (Figure 2.7). When the fibrinogen concentration was maintained constant and thrombin ratios were varied, the 3D culture resulted in a much stronger effect on *SOX17* expression levels, which was upregulated by 3- and 7-fold for gel conditions of 0.25 and 1x respectively, compared to the stiffer gels synthesized at 2x for the 1mg/ml fibrinogen gels. In the case of the 8mg/ml gels, an even more pronounced effect was found with 5- and 15-fold upregulation in the 1 and 0.25x conditions, respectively. Furthermore, in the 8mg/ml fibrinogen conditions, the endoderm marker *HNF4* also exhibited a significant upregulation comparable to *SOX17*. Additionally, while the 2D cultures led to somewhat elevated expression levels of many of the germ layer markers, 3D cultures were consistently more specific for endoderm markers along with *FGF* and *Nestin*. Hence, while the overall effect of softer substrate (~ 13 Pa) was more pronounced than the stiffer substrates, lower crosslinking always resulted in stronger endoderm expression compared to higher crosslinking for invariant fibrinogen concentrations in the entire range of substrate stiffness considered in this study.

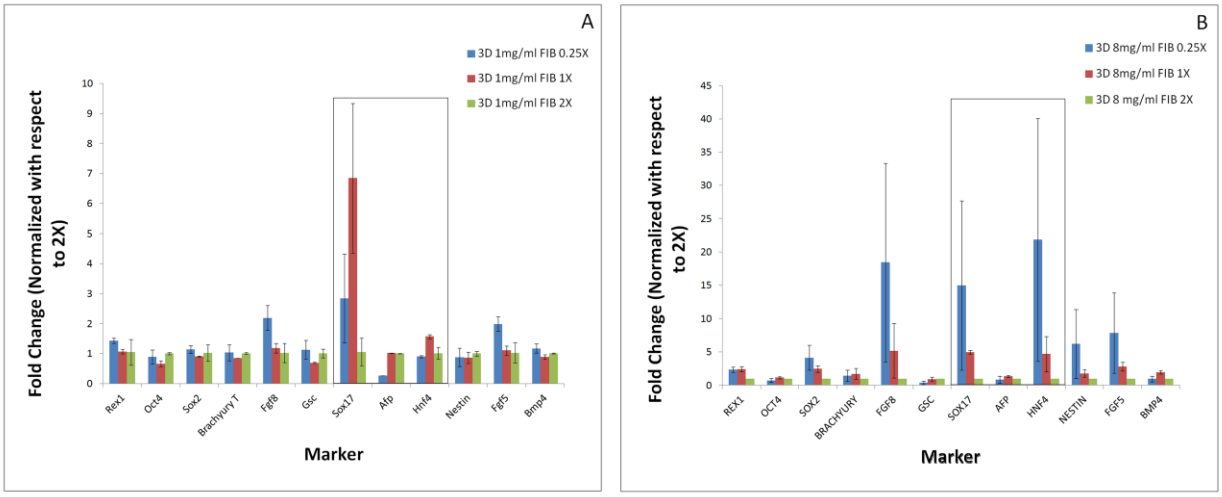

Figure 2.7: Effect of substrate crosslinking ratios on 3D ESC differentiation analyzed at extreme concentrations of 1 mg/ml (a) and 8 mg/ml 1 mg/ml (b). Results are normalized to highest crosslinking ratio of 2x. Most significant effect was observed in the upregulation of endoderm markers compared to cells differentiated on gels of lower crosslinking (0.25x, 1x) and higher crosslinking (2x) ratios. * p<0.05 compared to highest stiffness group.

To further analyze the differentiated cell population for its protein expression levels, immunohistochemical analysis was performed for the case eliciting the strongest upregulation in gene expression: the 3D culture for SOX17 and AFP expression. As illustrated in Figure 2. 8, the differentiated cells cultured in the softer substrates that resulted in highest upregulation of both *AFP* and *SOX17* (1mg/ml, 1x) stained strongly for both SOX17 and AFP. High co-expression of these markers was also observed in the cell clusters formed. Parallel analysis of differentiated cells on gels of higher thrombin concentrations of 2x showed negligible stain (data not included).

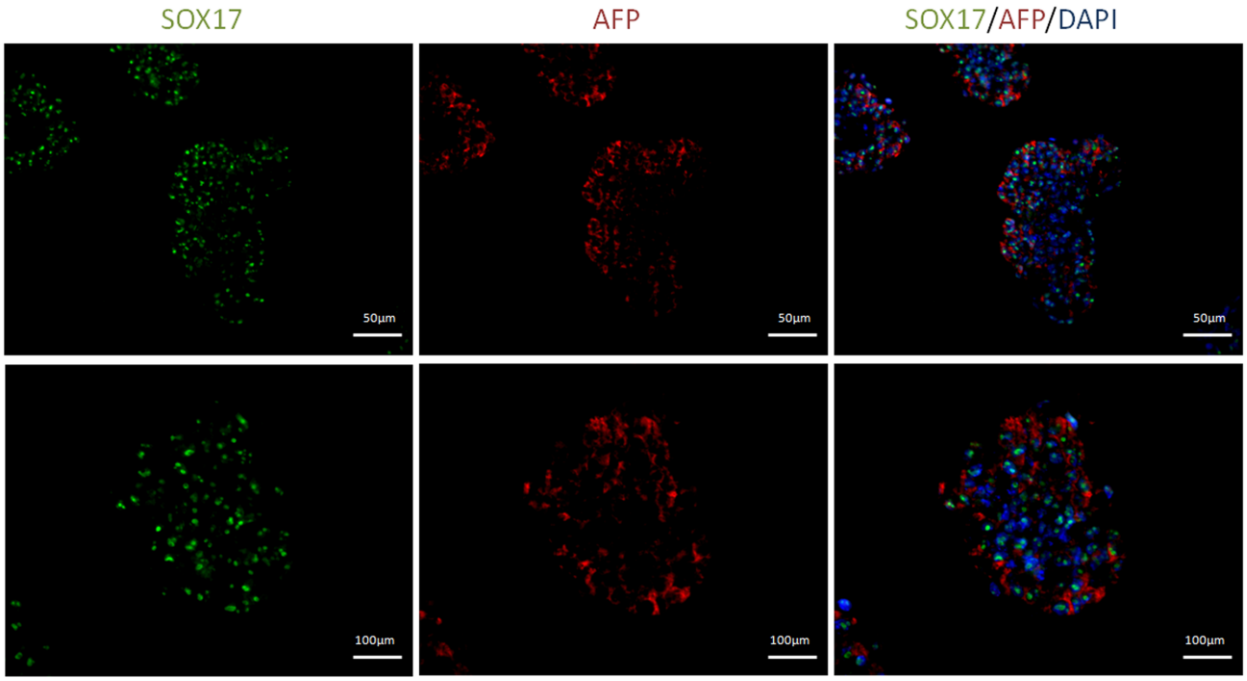

Figure 2.8: Immunocytochemistry images of endoderm markers

For cells plated at 1 mg/ml and 1x. High expression of endoderm markers AFP (Red) and Sox17 (Green) was observed in the cell clusters that were found to be highly co-expressed

When crosslinking ratios were maintained constant and fibrinogen concentrations were modified, we once again found that lower values of fibrinogen concentration (Figure 2.9b) preferentially favored endoderm differentiation and this effect was more accentuated in the 3D culture compared to the 2D culture, with upregulation of endoderm *AFP* and *SOX17* being 4 and 17x higher in 1mg/ml fibrinogen gels, respectively.

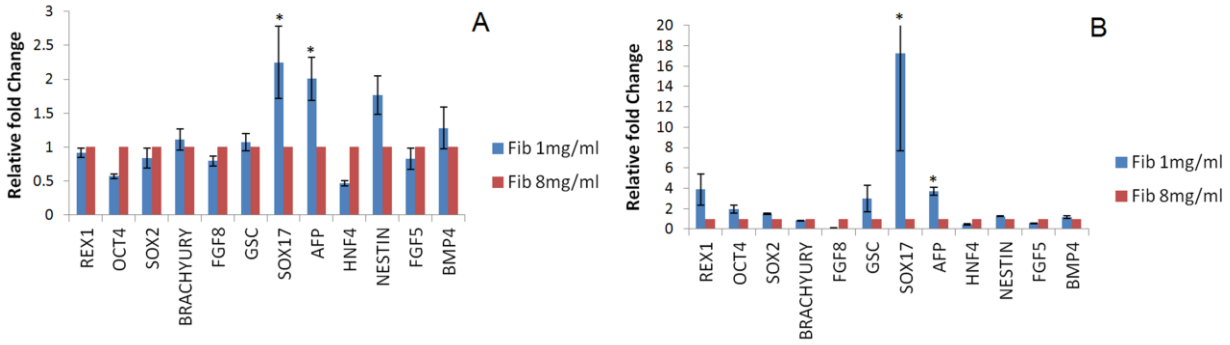

Figure 2.9: Pluripotency and germ layer markers of ESC cells differentiated in substrates of various fibrinogen concentrations with same crosslinking ratios

(A) 2D and (B) 3D cultures. Significant upregulation of endoderm markers was found when cells were differentiated on gels obtained at lower fibrinogen concentrations. * $p<0.05$ compared to highest stiffness group.

2.3 DISCUSSION

In this paper we present an analysis of the effect of mechanical microenvironment on the embryonic stem cell (ESC) culture and differentiation. ESCs were maintained on soft fibrin substrates of varying physical characteristics, modulated by altering both of its components – fibrinogen and thrombin involved in the formation of fibrin gels.

Analysis of the microscopic architecture of the fibrin gels using SEM reveal a strong effect of both fibrinogen concentration and crosslinking on fiber diameter, fiber bundling and relative pore size, as demonstrated in Figures 2.1 and 2.2. Such findings are in agreement with previously published data [47,48]. Mechanical characterization of the fibrin gels was performed using plate rheometer to measure both the storage and loss modulus as summarized in Table 2.2.

In comparing Table 2.2 and 2.3, it should be noted that G'>>G" for all of the samples considered which suggests as expected a more solid-like than liquid-like behavior for all the conditions consistent with low loss characteristics of the solids. The results illustrate that increase in fibrinogen or thrombin concentration results in an increase in substrate stiffness. While a higher response is observed by increasing the fibrinogen concentration, chemical variation is also greater, which lead us to focus on the effects of varying thrombin concentration for most of our observations.

The ESCs were cultured for 5 days on these substrates, at the end of which the cells were analyzed for their proliferative and differentiation potential. Since we are interested in early germ layer commitment, differentiation was performed over a relatively short period of time. Our first observation after cell plating was that instead of spreading out, the cells form clusters which vary in size depending on the thrombin concentration, as seen in Figure 2.3. An explanation can be that the fiber thickness decreases as the substrate becomes more cross-linked, thus decreasing pore size, and exhibiting a higher modulus as shown in Figures2.1 and 2.2, and Tables 2.2 and 2.3. A similar trend is consistently observed across all four fibrinogen concentrations analyzed.

Cell proliferation assay also confirmed that gels synthesized with lower thrombin concentrations facilitated increased proliferation in comparison to stiffer substrates (Figure 2.4). A similar trend has also been reported with mesenchymal stem cells and fibroblasts grown in fibrin gels [49,50]. Studies using neural stem cells showed that when plated in 3D hydrogel cultures, there was a significant increase in proliferation as the stiffness of the scaffolds decreased [51]. Similar results were obtained for neural cells in 2D matrices with varying elasticity [25].

Analysis of differentiation patterning of the cells cultured on the substrates revealed that while mesoderm and ectoderm remain relatively insensitive to changes in substrate physical properties, the endoderm markers elicit quite a strong response. More specifically, substrates in the range of 13Pa show strongest preferential upregulation of the endoderm markers under both 2D and 3D culture configurations. The overall effect of the substrate, however, was more pronounced in 2D than in 3D cultures. At this point we would like to note that a similar study has been recently reported, however, the mentioned study used substrates with stiffness ranges that were four orders of magnitude higher, and their results were targeted towards osteogenic differentiation [30]. While evaluating the effect of the substrate composition, it was observed that for a fixed fibrinogen concentration, cells in softer gels are preferentially up-regulating endoderm related markers as compared to more cross-linked counterparts. Figures 2.6 and 2.7 are extreme representative case study for fibrinogen concentration of 1 mg/ml and 8mg/ml while similar analysis on substrates of different fibrinogen concentrations consistently exhibited a similar trend of softer substrates leading to a stronger upregulation of endoderm related markers. Notwithstanding the variability in the extent of the particular effect, overall there was remarkable consistency in preferential upregulation of endodermal expression in less crosslinked substrates for both two- and three-dimensional culture configurations. For 2D configuration, the ESCs cultured on 0.25X showed stronger upregulation compared to 1X, while the difference between 1X and 2X is more subtle. The three dimensional culture overall shows a clearer trend of higher upregulation with softer substrates.

A careful observation of the gels synthesized with lower thrombin concentrations show that even though no mesoderm markers exhibit significant upregulation, in some cases FGF8 is quite strongly upregulated. An explanation can be that FGFs, apart from being a mesodermal

marker, also plays a role in the endothelial development and are important angiogenic factors [52,53]. The upregulation of these markers can probably be attributed to differentiation into endothelial cells, explained by the fact that softer matrices result in larger cell clusters. Larger cell clusters results in insufficient transport of nutrients and oxygen to the center of the structures, which results in hypoxia and may trigger the creation of blood vessels, resulting in upregulation of FGF markers.

Overall we consistently observe that for a particular fibrinogen concentration, gels obtained at lower thrombin concentrations favor endodermal differentiation of the cultured ESC. As revealed by the microstructural characterization of the gels, increasing the concentration of thrombin results in a dense network of thinner fibers which are less bundled (Figure 2.2). Such microstructural features manifest in increased substrate stiffness as a result of increased cross-linking for the same fibrinogen concentration (Table 2.2). Based on the mechanical characteristics of the gel and the biological characterization of the cells on the fibrin substrates, it is reasonable to suggest without any uncertainty that lower substrate stiffness values preferentially favor ESC differentiation towards the endodermal lineage.

Even though substrate stiffness is clearly playing an important role in cellular lineage commitment, it is certainly not the only factor, as revealed in Figure (2.10). Comparison of two substrates of varying fibrinogen concentration and fibrinogen to thrombin ratios but comparable substrate stiffness revealed that mesoderm and ectoderm markers were almost invariant under these two conditions, indicating these germ layers to be insensitive to the substrate properties at the initial stage of differentiation and within the substrate ranges presented in this study. Endoderm layer however varied significantly between these conditions, which establish that substrate stiffness, although important, is not the sole player in the process of germ layer

commitment. Careful analysis of the substrate micorstructural features revealed that even though the macroscopic stiffness properties are similar, the gels differ substantially in their microstructural features. These results warrant a more detailed analysis of the effect of substrate microstructural features on differentiation, which are currently being investigated by the authors. It is important to note that there is variability in the results obtained from different experiments as observed by the error bars attributed to population heterogeneity and variable response to global inductive cues [54,55]. However, despite the variability, all experiments consistently showed the similar trend of softer substrates preferentially favoring differentiation towards endodermal lineage.

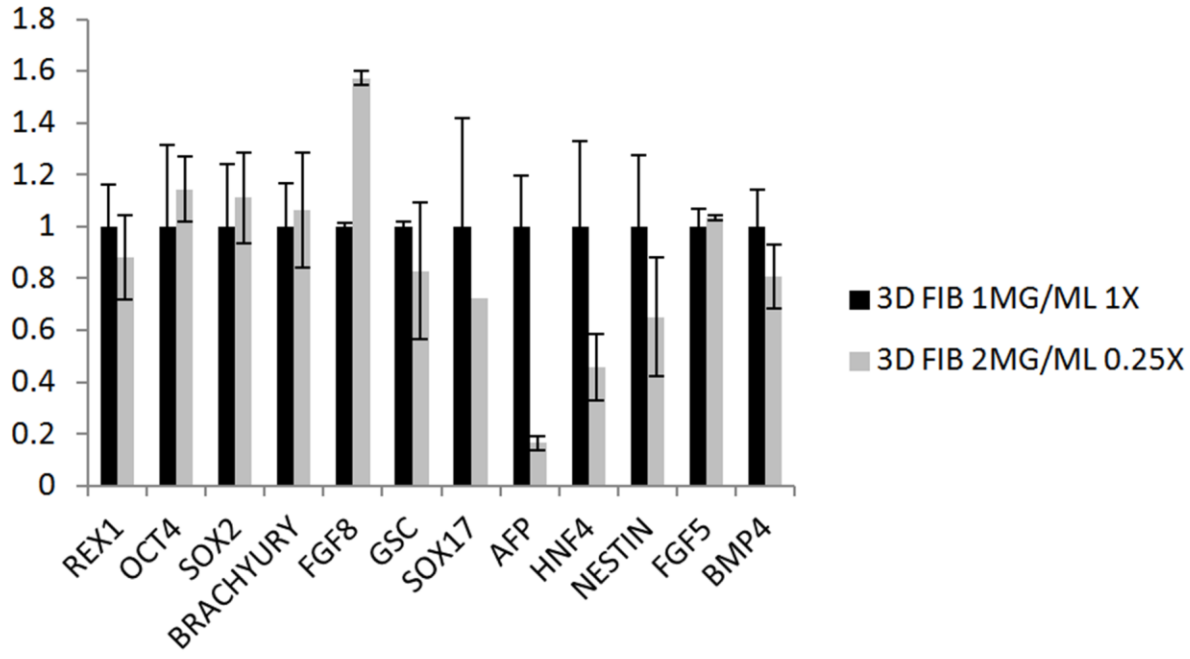

Figure 2.10: Comparison between substrates of same stiffness but different composition.

1 mg/ml fibrinogen obtained at F/T crosslinking ratio of 1x and fibrinogen concentration of 2 mg/ml obtained at F/T crosslinking ratio of 0.25x. Figure shows expression of most markers to be equivalent in both groups except for that of endoderm markers. Results normalized to 1 mg/ml fibrinogen 1x crosslinking ratio

This paper presents a thorough analysis of the effects of varying substrate mechanical properties on the embryonic stem cell proliferation and differentiation potential. The mechanical properties of the fibrin substrate are varied by systematically altering (i) the fibrinogen concentration and (ii) the thrombin concentration. SEM analysis of the synthesized gels illustrate the variation of microscopic gel microstructure, such as the fiber thickness, porosity and the overall effective area of fibrin strand available for cell anchorage as a result of altered fibrinogen and thrombin concentrations . Detailed mechanical characterization of the different substrates reveals that variation of substrate concentration or cross-linking results in substantial modulation of the substrate stiffness.

Analysis of the ESC cultured on different substrate conditions clearly illustrate the strong influence which substrate mechanical properties assert on cellular proliferation and differentiation potential. Overall, the ESCs cultured on softer substrates, as a result of lower thrombin concentrations, were found to be more conducive to proliferation as well as differentiation. For both the 2-dimensional and 3-dimensional culture configurations analyzed in this work, the substrates with lower thrombin concentrations elicited a somewhat elevated expression level of most of the gene expression markers tested. However, the level of up-regulation strongly depended on the specific germ layer. It was consistently observed that differential expression of endodermal markers are the strongest in gels obtained with lower cross-linking compared to highly cross-linked gels, an effect which was further accentuated in 3-dimensional culture as compared to 2-dimensional culture. The presented results are indicative of the fact that lower substrate stiffness values are favoring the preferential differentiation of the ESCs towards endodermal lineage. However, substrate stiffness is not the sole player controlling differentiation, which is probably dependant on both gel microstructure and chemical

composition. Furthermore, among the germ layers tested, early mesoderm and ectoderm layers were found to be less responsive to substrate properties.

2.4 MATERIALS AND METHODS

2.4.1 Gel synthesis

Soft fibrin hydrogels comprising 1, 2, 4, and 8 mg/ml of fibrinogen, respectively, were synthesized. The fibrinogen to thrombin ratios of 10, 2.5, and 1.25 mg/U (fibrinogen/thrombin) were synthesized for each fibrinogen concentration as previously described [56] and shown in Table 2.1. For convenience these ratios are referred to as 0.25X, 1X, and 2X respectively, corresponding to increased cross linking with increased thrombin concentration throughout the text. The fibrinogen to thrombin ratio, rather than simply either the fibrinogen or the thrombin concentration, was altered in order to ensure that a wide of a range of stiffness values could be studied for the fibrinogen concentrations chosen. This was systematically done to ensure a complete range of low, medium and high concentrations of fibrinogen and thrombin, respectively as outlined in Table 2.1, 1 mg/ml representing a low fibrinogen concentration and 8mg/ml correspondingly representing a high fibrinogen concentration. Thrombin concentrations were selected to represent three F/T ratios of low (1.25), medium (2.5) and high (10) corresponding to low, medium and high units of Thrombin.

2.4.2 Rheology measurments

Gel discs of 35 mm diameter, prepared as described for 2D gel synthesis, were deposited onto glass slides which were pre-rinsed with DI water. The samples were then allowed to gel fully at 4 ˚C. After complete gelation, they were fully immersed in the same media used for differentiation studies. The glass slides were then secured to the Peltier cell of a TA Instruments AR2000 stress-controlled rheometer, which was kept at 37 ˚C throughout the measurements.

A frequency sweep was then performed, using a 25 mm stainless steel in parallel plate geometry with sandpaper glued to the plate to avoid slippage. The samples were subjected to an oscillatory strain described by equation (1), where is the amplitude of the oscillatory strain (5%), f is the frequency and t is the time. Frequencies employed ranged from 0.1 to 100 rad/s.

$$\gamma = \gamma_o(2\pi ft) \quad (1)$$

The stress required to achieve the specified strain was measured and the components of the complex modulus, the storage (G'), and loss (G'') moduli were accordingly determined.

2.4.3 Scanning electron microscopy (SEM)

The fibrin gel microstructure was analyzed using SEM. The gels were prepared for SEM analysis as described previously in the 2D gel synthesis section above. Preparation of samples was performed as previously described [56]. SEM images were collected using a Philips XL30 field emission gun SEM (FEI Company). Further image analysis was then performed using the ImageJ software (acquired from http://rsbweb.nih.gov/ij/).

2.4.4 aintenance and differentiation of ES cells

Murine ESD3 cells were cultured according to previously published methods [57].

2.4.5 Cell culture in 2D

For differentiation of the ESCs on fibrin substrate, the cells were tripsynized, washed and re-plated in appropriate configurations. For the 2D culture 30,000 cells in 200ul media were plated on top of the pre-formed fibrin gels prepared on wells of 48 well plates and polymerized overnight at 4oC temperature.

2.4.6 Cell culture in 3D

For 3D cell culture format 100,000 cells were re-suspended in the fibrinogen solution before adding thrombin and plated on wells of 48 well plates. The gel with the entrapped cells was then allowed to polymerize for one hour at a temperature of 40C , after which the culture media was added and subsequently the culture was incubated. For both cases, the cells were maintained in DMEM medium (Invitrogen) supplemented with 10% FBS, 4mM L-glutamine (Cambrex) and 100U/ml penicillin, with media being changed every day. As control embryoid bodies were formed in rotary culture by adding 100,000 cells in ultra low attachment 35mm dishes with same media described above. The dishes were placed in a rotator in the incubation and maintained at constant speed of 40 RMP

2.4.7 QRT-PCR Analysis

The mouse ESC (ESD3) cultured in the two- or three-dimensional configurations were harvested by trypsin after five days of culture and RNA was extracted using the NucleoSpin kit according to the manufacturer's protocol. The sample absorbance at 280nm and 260nm was measured using a BioRad Smart Spec spectrophotometer to obtain RNA concentration and quality. Reverse transcription was performed using ImProm II Promega reverse transcription kit following the manufacturer's recommendation. qRT-PCR analysis was performed for pluripotency and early germ layer markers using the primers listed in Appendix Table 1. Each sample was then run in replicates, and average values were accordingly used for analysis.

2.4.8 Cell proliferation assay

The proliferative potential of ES cells was analyzed using the Alamar Blue assay. For the two dimensional culture, 15,000 ESD3 cells were plated on fibrin gels of different configurations. 24 hours after plating, the culture media was replaced by fresh media containing 10% Alamar blue and incubated for 4 hours. Fluorescence reading was obtained from a multi-well reader (BioTek Synergy 2, Winooski, VT) at an excitation wavelength of 570nm and emission wavelength of 585nm according to the manufacturer's instructions. Results were normalized with respect to the values obtained for the gels with the highest thrombin concentration, or most cross-linked (2X) condition.

2.4.9 Immunohistochemical analysis

Staining was performed on differentiated cells. The fibrin gels containing cells in 3D format were formed on cover-slips in wells of a 24 well plate. Staining was performed following the company recommendations .The antibodies used were *AFP* goat polyclonal antibody and *SOX17* rabbit polyclonal antibody (Santa Cruz). The secondary antibodies used were donkey anti-rabbit IgG Texas Red (Santa Cruz) and Alexa Fluor® 488 donkey anti-goat IgG (Invitrogen). Confocal images were taken using an Olympus Fluoview 1000 system.

2.4.10 Statistical analysis

Each experiment was performed twice with duplicates each time. Average and standard error were found and Student t-test was performed for significance and correspondingly, reported in the results section.

3.0 POTENTIAL FOR PANCREATIC MATURATION OF DIFFERENTIATING HUMAN EMBRYONIC STEM CELLS IS SENSITIVE TO SPECIFIC PATHWAY OF DEFINITIVE ENDODERM COMMITMENT

3.1 INTRODUCTION

Diabetes affect over 20 million people in the US [19]. In diabetic patients the body is unable to produce or properly use insulin. The most common treatment for type I diabetes consists of exogenous insulin supply. Other treatment alternatives include transplantation of cadaveric pancreas or isolated pancreatic islets [20], but the main limitations remains in the lack of available donor tissue. hESC have been suggested as an alternative transplantable cell source for treatment of diabetes [58]. However exploitation of the full potential of hESCs requires a robust protocol for generation of mature and functional cell types. Pancreatic differentiation of hESCs has received considerable attention over the last decade. While there has been some success in deriving insulin (*INS)* positive cells from hESC, typically the differentiated cells are limited in yield and functionality [59]. Most differentiation protocols involve a stage-wise directed differentiation strategy that mimics stages of pancreatic organogenesis by modulating pathways known to be involved in pancreatic development [58]. The first critical stage of pancreatic differentiation is the commitment to definitive endoderm (DE). Studies over the last decade have established multiple alternate pathways for DE induction of hESCs. While all these

alternate routes yield efficient DE, it is not obvious how sensitive pancreatic maturation will be to such early pathways of DE induction. Thus, the method of DE induction remains somewhat arbitrary, being assessed only by the presence of DE markers and not by its potential for pancreatic maturation.

In this work we are addressing this issue by evaluating the sensitivity of late stage pancreatic maturation on initial pathways of DE induction. We induced DE differentiation of hESCs by activation of the Nodal pathway through Activin A, in combination with modulation of one of the following pathways: WNT, BMP, PI3K and FGF. All of these pathways have been identified as key players at multiple stages of pancreatic development. Activin A, a TGF-β family protein has been long identified to mimic nodal, which results in mesoderm and DE formation [60]. FGF plays critical roles in several stages of pancreatic development. In the ventral pancreatic endoderm, FGF signaling comes from the adjacent endothelial mesoderm and at high concentrations specifies hepatic development at the expense of pancreatic differentiation [61]. Conversely, in the dorsal pancreatic endoderm, FGF signaling comes from the notochord and works as a sonic hedgehog (SHH) inhibitor, therefore inducing expression of PDX1 and further pancreatic development [61]. Additionally, BMP4 signaling from the septum transversum acts synergistically with FGF2 to induce hepatic differentiation at the expense of ventral pancreas development [62]. However, BMP4 signaling has been found to act synergistically with Activin and FGF2 to promote mesendoderm differentiation in human pluripotent stem cells [63] and has been used in combination with Activin for DE induction in pancreatic differentiation studies [64,65]. Similarly, inhibition of WNT signaling by proximal mesoderm has been implicated in proper pancreatic and hepatic progression from the foregut [62]; while activation of WNT induces mesendoderm formation in pluripotent stem cells from

mouse and human sources [66-68]. Lastly, PI3K was first reported as a negative regulator of cellular differentiation, and its inhibition has more recently been linked to proper endoderm formation under high nodal signaling conditions [69]. Studies have also linked PI3K suppression at later stages with proper endocrine specification [70].

Due to the high complexity of these pathways and their role in pancreatic progression, a more thorough analysis of their effects is needed. The aim of this study is to compare previously identified pathways of DE induction, analyze their pancreatic potential, compare differentiation of these derivatives with existing reports on in-vivo pancreatic organogenesis and identify markers that can be useful indicators of pancreatic differentiation at early stages of the differentiation program

3.2 RESULTS

3.2.1 Pancreatic differentiation of hESC

A multi-stage directed differentiation protocol was used to induce the hESCs to pancreatic lineage (Figure 3.1). The first step was to induce DE through multiple alternate pathways, which was achieved by exposure to Activin in combination with one of the four other growth factors and molecules that modulate alternate pathways for DE induction.

While Activin alone can induce DE, it is typically combined with different molecules to increase the efficiency of induction. In pancreatic differentiation studies, DE is most commonly achieved by combination of Activin A with WNT3A [71], BMP4[64], PI3K inhibitor[72] or FGF2[73].

After 4 days of DE induction, Activin A and other inducers were removed and all groups were exposed to the same subsequent signals as follows (Figure 3.1): for pancreatic progenitor (PP) induction Cyclopamine was added alone for two days and in combination with retinoic acid for two additional days; cells were then exposed to nicotinamide alone for 2 days and nicotinamide and DAPT for up to one week for the maturation stage.

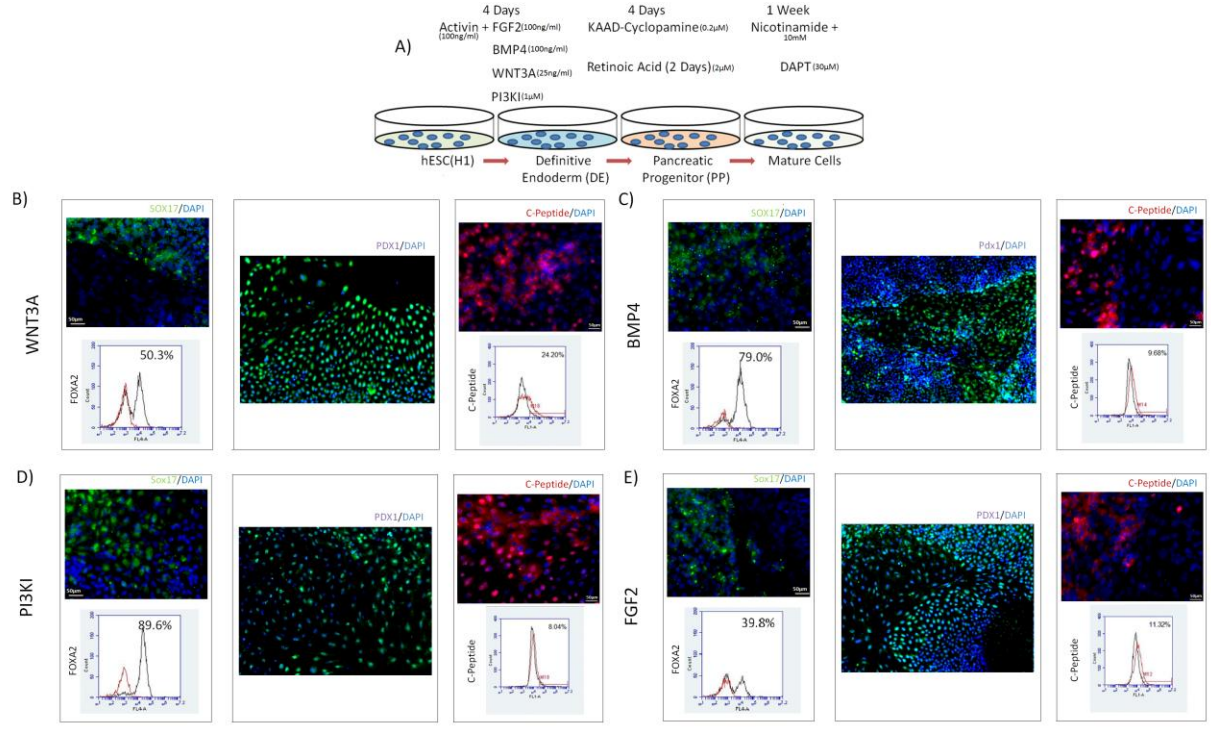

Figure 3.1: Multi-stage Differentiation System.

(A) Schematic representation of multi-stage differentiation system. Detailed media formulation found in Supp table 1. DE was induced by modulation of nodal pathway simultaneously with one of four alternate pathways. PP was achieved by SHH inhibition along with retinol signaling. Maturation was induced by notch inhibition. Differentiation using WNT3A (B), BMP4 (C), PI3KI (D) or FGF2 (E) at DE stage. ICC pictures show nuclear staining of *SOX17* (green) and Flow cytometry shows yield of FOXA2 after DE induction, followed by nuclear PDX1 ICC pictures (purple) after PP induction and cytoplasmic C-Peptide ICC (red) expression yield as measured by flow cytometry after maturation.

3.2.2 Pancreatic maturation of hESCs is sensitive to initial pathway of endoderm induction

Morphological examination of the matured cells exposed to alternate DE induction pathway revealed heterogeneous populations of cells in all conditions (Figure 3.2A), containing groups of cobblestone like cells indicative of endoderm morphology; however, PI3KI cells appeared to be larger than other groups. To determine if this was attributed to cell confluence, and to analyze the system more thoroughly, we studied proliferation, apoptosis and dynamics of cell cycle under different induction conditions. Cell death at DE stage was comparable for all conditions except PI3K inhibition, which elicited high cell death. Figure 2B represents the number of dead cells floating in the media. Number of cells that remained attached was also quantified and found to be roughly 10% for all groups except for PI3KI which showed 20% (data not shown). This is evident in Figure 3.2C which shows a drop in cell number in PI3KI-DE. However, cell cycle dynamics (Fig 3.2D-E) confirms a proliferative population, with similar dynamics between PI3KI and WNT3A condition. Analysis of the cell cycle clearly indicates a maturing population of cells, transitioning from a dominant S phase to a dominant G1 phase, representative of mature cells [21]. As expected, undifferentiated hESC (time = 0) have a short G1 phase as exhibited by a low sub-population (~27%) in the phase, with subsequent increase in G1 residence time with differentiation (Fig. 3.2D). While the residence times of the S and G2/M phases are not expected to significantly change with differentiation, the fraction of the population in these phases decreases to compensate for the increased G1 phase (Fig. 3.2E, F). In contrast with PI3KI and WNT3A condition, BMP4 and FGF2 treated cells elicited a slower overall cell cycle dynamics, which was however not reflected in the proliferation data (Fig 3.2C) showing an almost identical behavior between WNT3A, BMP4, and FGF2.

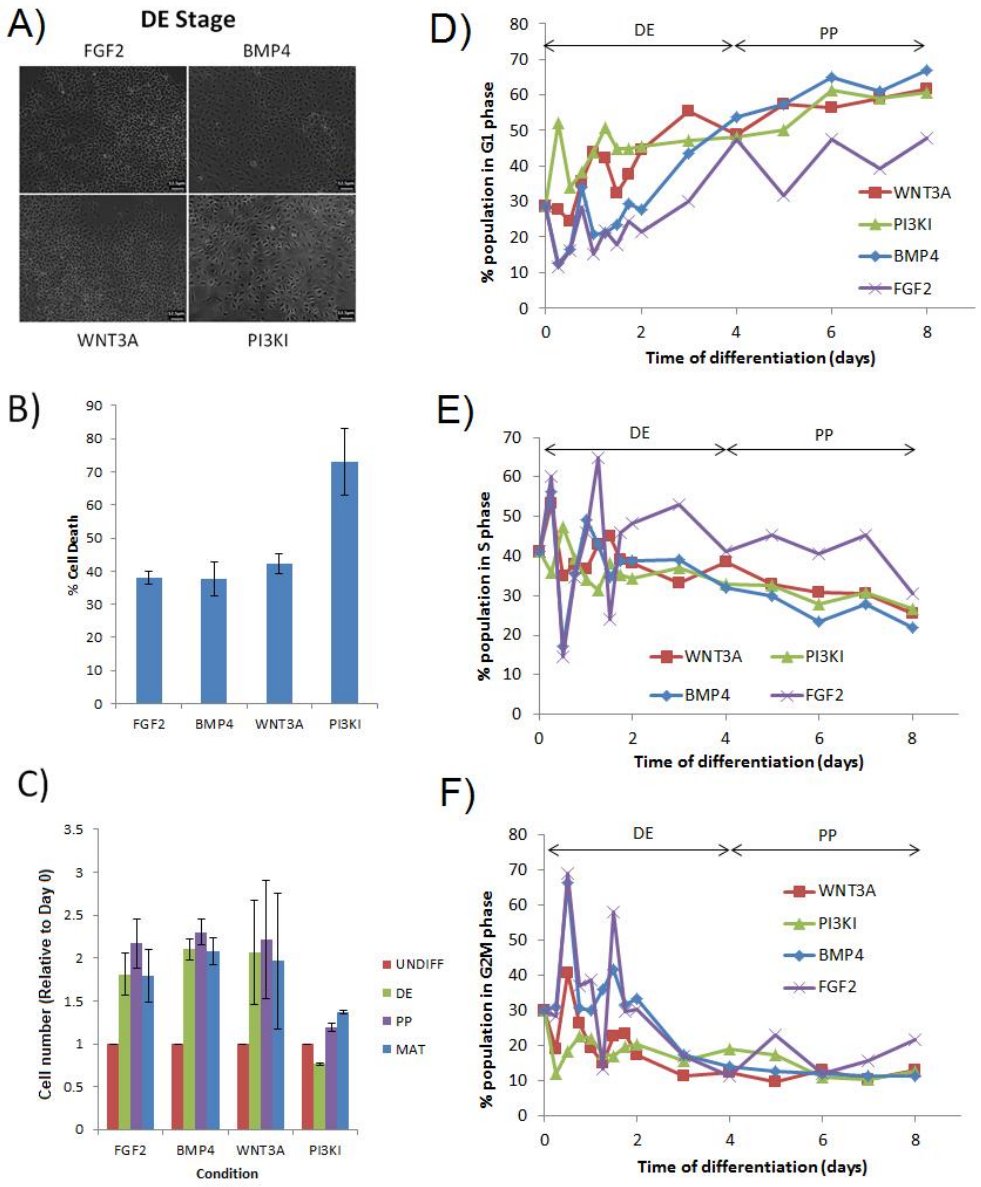

Figure 3.2: Cell proliferation, death and morphological analysis of the cells

(A) DE induction showing heterogeneous populations under all conditions (Scale bar: 12.5µM), and (B) Cell death after 24h of DE treatment. Death was comparable in all groups, except for PI3KI which resulted in considerably higher death (C) Cell number at the end of each stage of differentiation shows an increase in cell number at the end of each stage, except for maturation stage, which only increased for PI3KI treated cells. (D-F) Cell cycle analysis of the differentiating cellular population under different conditions, as analyzed and quantified by flow cytometry. Shown is the fraction of the population in the G1 (D), S (E), and G2/M (F) phases of the cell cycle. Data are represented as mean +/- STDEV

In order to confirm differentiation after DE induction, immunocytochemistry (ICC) and flow cytometry for SOX17 and FOXA2 was performed for all groups after 4 days of treatment. Both transcription factors were found to be expressed in all groups (Fig 3.1A-D) with yield of FOXA2 positive cells ranging from 40-90%. qPCR was performed to examine expression of stage specific markers CXCR4, SOX17, FOXA2 and CER. As illustrated in Fig. 3.3A, upregulation of these markers was obtained under all differentiating conditions, with PI3KI consistently eliciting the highest upregulation achieving close to 50 fold increase in CXCR4, 400 fold increase in SOX17, 10 fold increase in FOXA2 and 500 fold increase in CER.

Upon pancreatic induction, all the induction conditions show expression of PP marker PDX1 by ICC (Fig 3.1A-D). This was further confirmed by qPCR for PDX1, which showed that with the exception of BMP4 all other conditions strongly expressed PDX1 (Fig. 3.3B). A notable increase of other PP markers were also observed, particularly ISL1. BMP4 treated cells, however, consistently showed either comparable or lower upregulation of PP markers than the other groups. BMP4 treated cells additionally showed downregulation of PAX6.

At the last stage of differentiation, ICC and flow cytometry confirmed expression of C-peptide for all groups with yields ranging from 9-24% (Fig 3.1A-D). Detailed gene expression for mature β cell markers (Fig 3.3C) revealed the highest INS mRNA upregulation under WNT3A and FGF2 conditions both of them achieving over 10,000 fold increase compared to undifferentiated cells, with no statistical difference between them. While BMP4 condition showed the lowest (11 fold) upregulation of INS, it was the highest in upregulation of GLUC mRNA (Fig. 3.3C).

The above analysis clearly indicates that initial pathway of endoderm induction plays a crucial role in subsequent maturation of the cells towards pancreatic lineage.

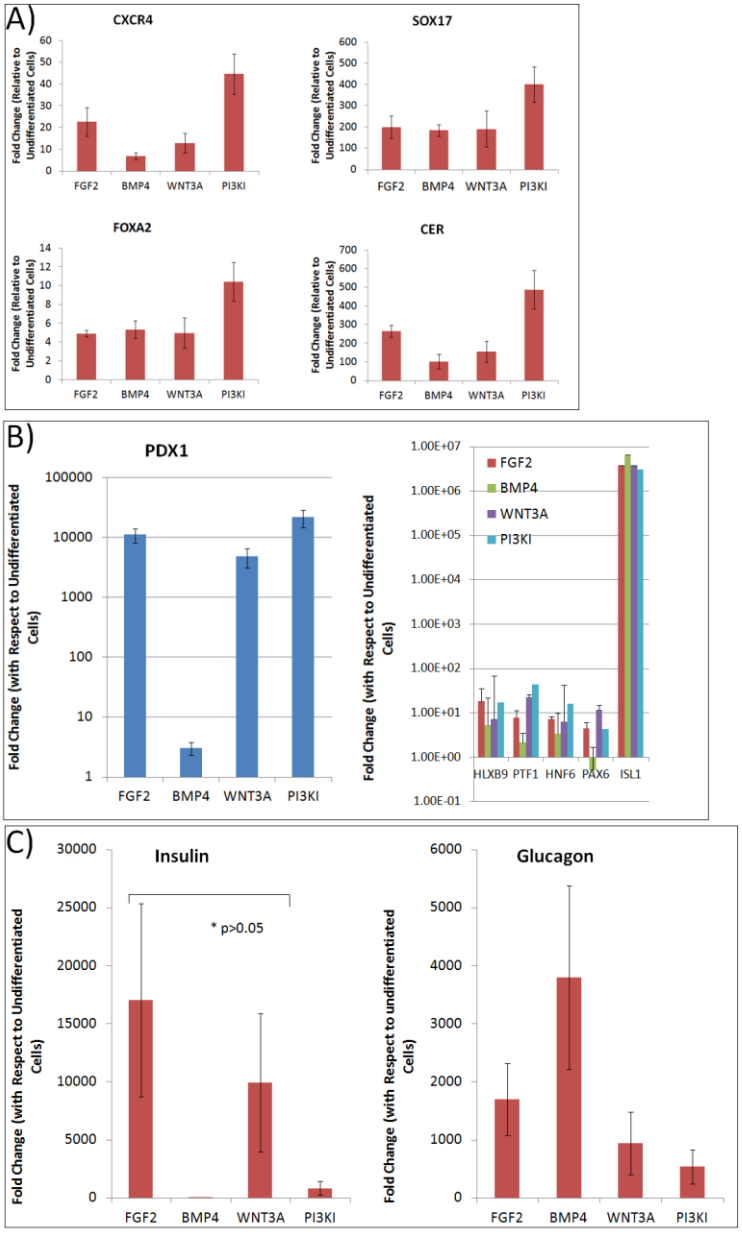

Figure 3.3: Stage Specific Marker Expression.

(A) DE specific markers after DE induction under all differentiation conditions. Upregulation was obtained for all groups with PI3KI consistently yielding highest expression. (B) PP specific markers after PP induction for all DE derivatives with upregulation obtained for most markers under all conditions, except for BMP4 which consistently resulted in lowest upregulation. (C) Pancreatic hormone expression after maturation for all groups with WNT3A and FGF2 groups achieving highest upregulation of *INS* ($p > 0.05$), while BMP4 obtained lowest *INS* upregulation but highest *GLUC* expression. Data are represented as mean +/- SEM

3.2.3 Alignment of *in-vitro* differentiation with *in-vivo* organogenesis

Research over the last decade has established the advantage of directed differentiation of hESCs following the sequence of *in-vivo* development. Hence there is an increased emphasis on aligning the *in-vitro* differentiation dynamics to *in-vivo* organogenesis events. Accordingly, we analyzed the alternate pathways of DE induction and subsequent maturation in the light of differentiation dynamics.

Pancreatic development can be broadly divided into 7 stages, each characterized by specific transcription factors: (1) Primitive gut endoderm (PGE) from which pancreas, lung, thyroid, thymus, parathyroid, and liver are derived[74], followed by (2) prospective pancreatic endoderm (PPE) containing prospective ductal, endocrine and exocrine pancreatic cells. The next step is the (3) pancreatic progenitor (PP) stage marked by the transient expression of PTF1 and is followed by appearance of (4) NGN3 expressing early endocrine progenitors (EEP) which develop into (5) endocrine progenitors (EP) from which all the islet cell types develop, including α, β, γ, δ or ε cells. From here disappearance of NGN3 expression marks emergence of (6) immature β- cells which mature into functional, (7) *INS* expressing β-cells[7]. To draw a parallel to our 3-stage differentiation protocol we combined some of the developmental stages as follows: DE stage includes endoderm, PGE, and PPE; PP stage includes PP and EEP induction; finally, the maturation stage includes EP induction, immature β- cells and β- cell maturation. Figure 4A illustrates a qualitative measure of the expression level of stage specific transcription factors across different stages of development as gathered from literature [7,74]. Figure 4 (B-E) presents parallel transcription factor dynamics for hESC differentiation under different DE induction conditions as observed in a representative sample with *INS* expression closest to the mean. For the purpose of this study, we defined presence the of a marker as a 10 fold or higher

upregulation as observed in qPCR in order to account for experimental error. Overall, all of the FGF2, WNT and PI3KI conditions were found to exhibit similar trends as *in-vivo* development, only with some minor differences. For example, *PTF1* is known to be an early and transient marker of pancreatic commitment, preceding *PDX1* expression. While both FGF2 and WNT conditions show a gradual increase in *PTF1*, under PI3KI conditions *PTF1* comes up very late even though *PDX1* expression is detected much earlier, even at the DE stage. On the other hand *PAX6*, which is expressed early in α cells and later in the entire islet [75] and has been suggested to be a key component of glucagon secretion [76], is prominent in PI3KI conditions from an early stage (DE) and increases with maturation. BMP4 condition, however, was found to be an outlier, as it did not align with either *in-vivo* sequences or any of the other conditions.

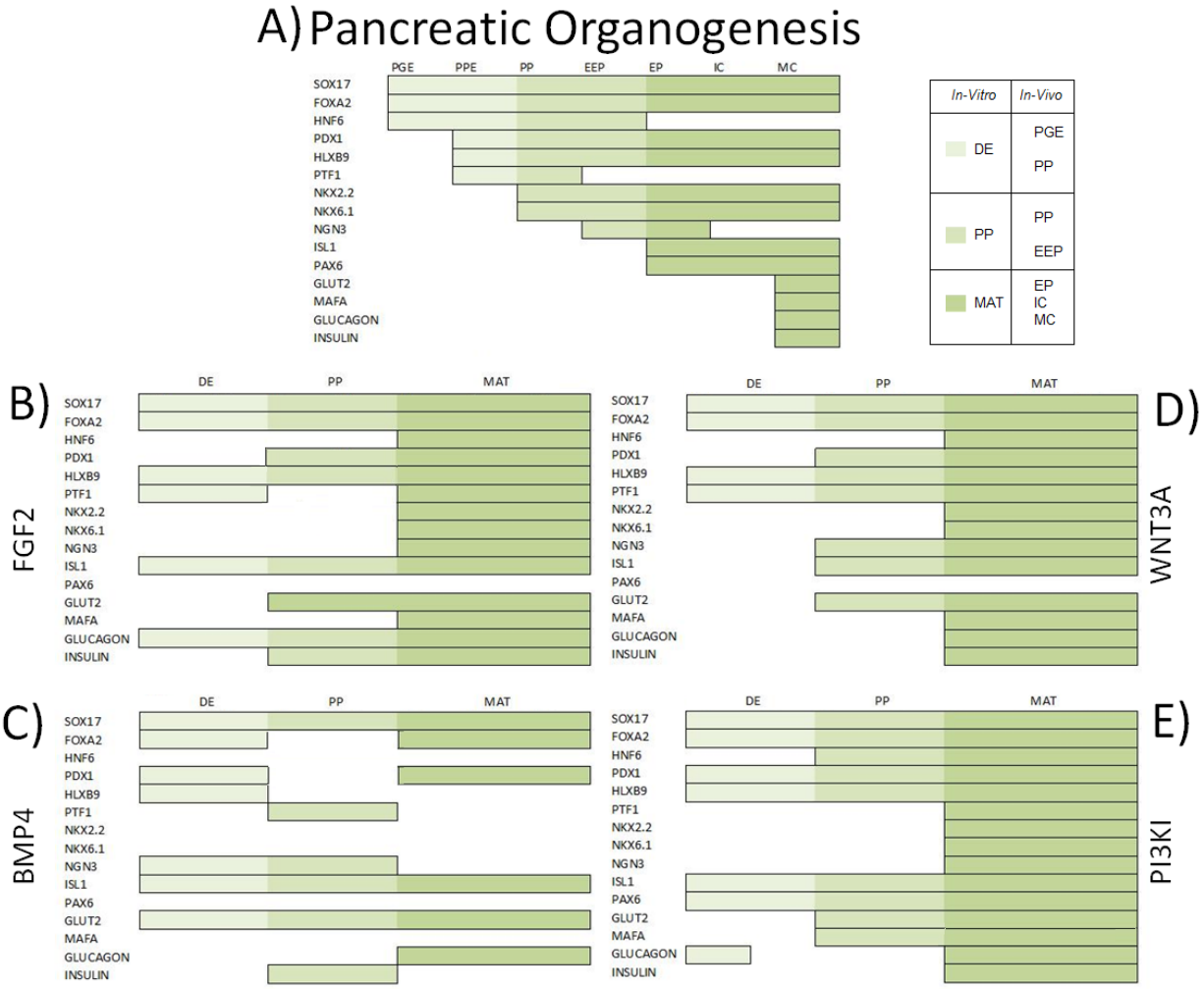

Figure 3.4: Marker Progression.

A representative sample (based on *INS* expression) for each group was analyzed and compared to in-vivo (A) pancreatic development [24] in order to identify which DE pathway modulation(s) lead to better resemblance to pancreatic organogenesis. Similarities can be observed when DE induction is achieved by modulation of (B) FGF2, (C) BMP4, (D) WNT3A and (E) PI3KI while we observed that marker progression greatly differs under BMP4 induction. The different stages of pancreatic development were grouped to represent the 3 stages of the differentiation protocol. Primitive gut endoderm (PGE) and prospective pancreatic endoderm (PPE) represent DE induction (light green) pancreatic progenitor (PP) and early endocrine progenitors (EEP) represent PP induction (medium green) and endocrine progenitors (EP), immature β- cells, mature β-cells (MC) represent the maturation stage (dark green).

3.2.4 BMP4 induced DE cells exhibit a divergent maturation dynamics

Analysis by hierarchical clustering: In order to resolve the differentiation dynamics further, we performed hierarchical clustering of 15 stage specific transcription factors measured over 4 time points under the 4 DE induction conditions. Figure 3.5A shows a heat map of transcription factor dynamics. . Hierarchical clustering of the transcription factor dynamics identified four clusters of TFs, of which the most striking was the one formed under BMP4 induction (NKX2.2, PAX6, HNF6, PTF1, NKX6.1). These factors were rapidly down-regulated with differentiation induction, the highest expression being in the undifferentiated cells. It is important to note that the data is Fig 3.5A is presented as relative expression; hence even though the absolute gene expression for undifferentiated cells were the same under all conditions, the differences in the heatmap arises from the normalization.. The aforementioned cluster branched separately from all the remaining clusters indicating the difference in transcriptional activation following BMP4 treatment. Overall, many of the PP markers were higher at the DE stage under BMP4 treatment while the later markers were not upregulated upon maturation. On the other hand FGF2, WNT3A, PI3KI treatments followed the pancreatic organogenesis closely as shown by clusters 2 to 4. On closer inspection, it was found that 67% of the markers assayed for are regulated in a similar manner under FGF2 and WNT3A pathway modulation, representing the largest similarity between the pathways studied. PI3KI leads to 47% and 40% similarity with WNT3A and FGF2 respectively, and the 3 pathways regulate 33% of the genes in a similar way. BMP4 treatment results in the most dissimilar gene patterning, sharing only 7% similarity with

FGF2 and 20% with both WNTA and PI3KI. Additionally, the magnitude of upregulation of genes assayed for, including *INS*, was comparable for these FGF2 and WNT3A conditions at all stages of differentiation. Taken together, these results suggest similarity in pancreatic maturation stages when FGF and WNT pathways were modulated for initial endoderm differentiation.

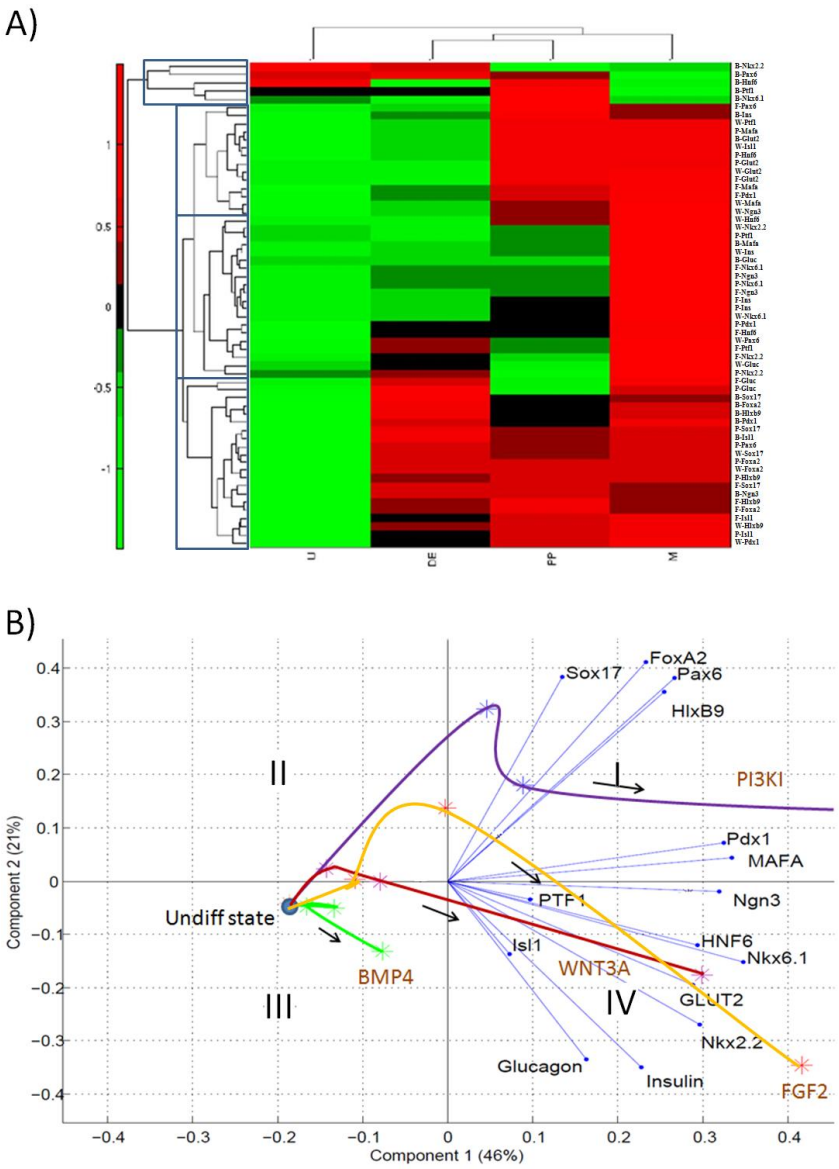

Figure 3.5: Transcription factor dynamics.

(A) Heat map for the entire data set of genes and conditions illustrating marker progression throughout differentiation stages. BMP4 induction condition typically was found to cluster separately from the rest. Hierarchical clustering was performed on the mean centered and variance scaled data of transcription factor dynamics across all the four DE induction conditions. (B) Biplot of transcription factor dynamics assessed by principal component analysis on the mean data-set. The first component shows a demarcation of the undifferentiated and differentiated states. The second component divides the markers according to their expected appearance during *in vivo* differentiation. The PI3KI curve moves closer to the DE markers, BMP4 curve does not perform well and the WNT3A and FGF2 curves show successful pancreatic maturation.

In the hierarchical clustering formulation each of the markers was treated separately under each induction condition giving rise to a total of 60 marker-condition pairs. However, in order to compare the dynamics of differentiation it will be advantageous to look at the dynamics in the same space of transcription factors. Hence, we projected each of the induction condition in the same space of the transcription factors using principal component analysis (PCA). However, PCA will extract new orthogonal directions from the original space which are combinations of these markers.

Analysis by principal component analysis: PCA allows visualization of multidimensional data in a new orthogonal coordinate space of PCs and often the first few PCs explain most of the variation in the data. In our case, we found that the first two components explained 67% of the variation in the data which is significant for biological systems as the remaining can often be attributed to noise. Figure 5B shows a biplot where the time points for each of the four induction conditions are plotted in the PC space with the original variables i.e. TFs overlayed onto the plot. The first PC divides the region into the undifferentiated state (III) and differentiated state (I & IV). The second PC further splits it into early markers (I & II) and the late markers (IV). Ideally, to mimic pancreatic development, the cells must proceed from the III quadrant (undifferentiated state) to IV (mature hormone expressing cells) via I (DE stage). Except BMP4, all the other induction methods closely follow this path. It is found that WNT3A and FGF2 follow similar paths ending up closer to the *INS* and *GLUC* axes while PI3KI deviates significantly. PI3KI treatment still favors the DE markers like *SOX17* and *FOXA2* and some late markers like *PAX6*, *HLXB9* and *PDX1* during the final stages. However, PI3KI derivatives fail to perform well with

respect to the important mature markers like *INS* and *GLUC*. BMP4 derivatives perform very poorly with respect to *INS* expression, although we see that they proceed to the *GLUC* axis during the final stages.

Diverse analysis of the experimental data leads to a similar conclusion: BMP4 induction is less suitable for pancreatic β cell maturation. This is primarily because of low *INS* expression in the mature phenotype along with lack of timely upregulation of intermediate transcription factors known to be associated with β-cell development. However, a similar treatment condition resulted in high *GLUC* expression, perhaps indicating its suitability for α-cell maturation.

3.2.5 K-means clustering of individual pathways reveal WNT3a to be more consistent with development

Our next goal is to determine which of the remaining conditions are more suitable to drive pancreatic maturation. One way to assess this is to find representative TFs that show coherent expression dynamics. To address this question we scrutinized each of the pathways individually through K-means clustering of each induction condition. As shown in Figure 6A, *SOX17, FOXA2, HLXB9* were co-regulated under WNT3A, FGF2 and PI3KI conditions. These markers indicate the DE and dorsal pancreatic endoderm. This combination of *SOX17, FOXA2* and *HLXB9* was repeated in all the above induction conditions and therefore, indicating that each of these treatments is efficient for activating the primary DE transcriptional machinery but the later stage transcriptional activation is different. These markers were consistently expressed through all the differentiation stages. In addition, PI3KI and FGF2 clusters also contained *ISL1*. However, no other coherent cluster was obtained for the PI3KI condition indicating lower alignment with developmental dynamics towards the later stages of maturation.

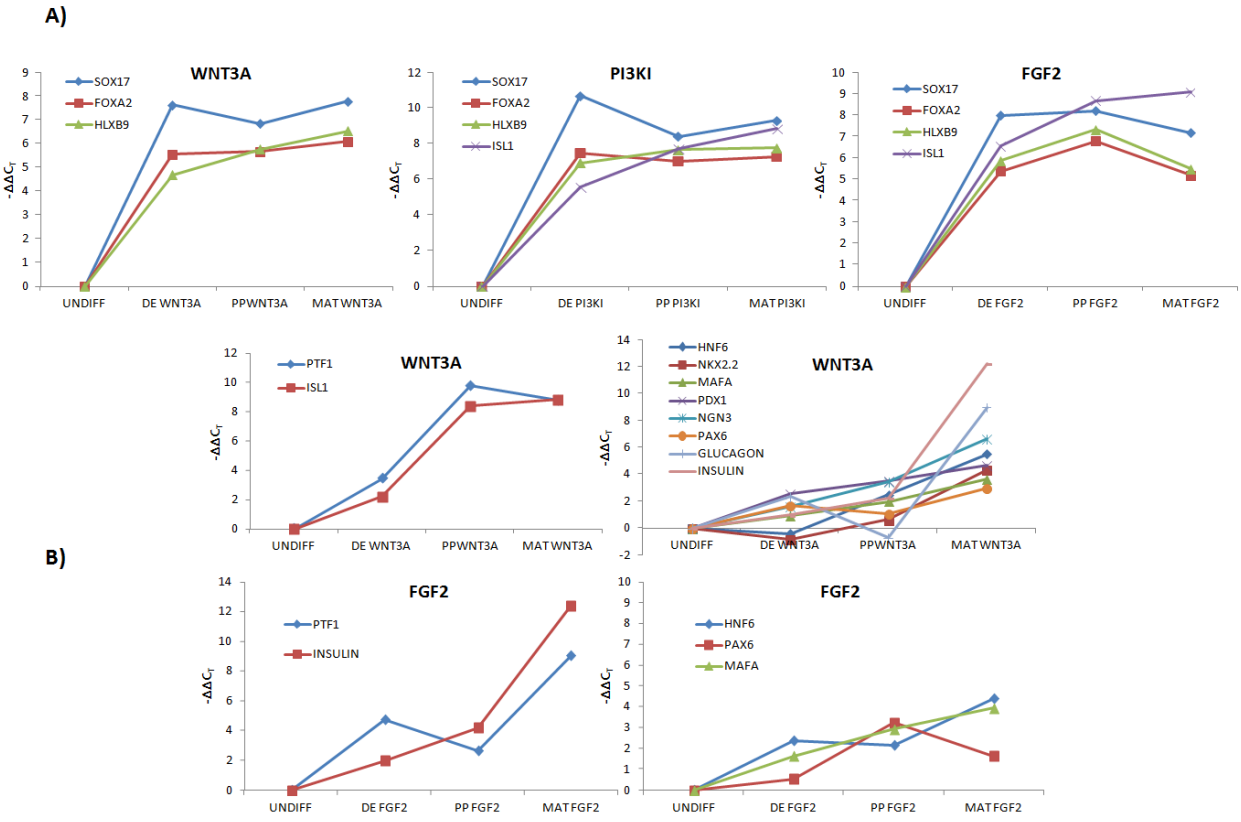

Figure 3.6: Significant K-means clusters.

Clusters obtained for each induction condition. (A) WNT3A (B) PI3KI (C) FGF2 and (D) BMP4. The k-means clusters show close similarity of our induction conditions WNT3A and FGF2 with pancreatic organogenesis and PI3KI with DE commitment. The markers *SOX17, FOXA2, HLXB9* are closely regulated under all the induction conditions.

Additional clusters containing many later markers were obtained for WNT3A and FGF2 as shown in Figure 6B. One among these was *PTF1* and *ISL1* under WNT3A which arise in the pancreatic precursor cells during the early bud-stage. Other late markers like *PAX6*, *PDX1*, *MAFA*, *GLUC*, *INS*, *NGN3*, *HNF6*, and *NKX2.2* which are expressed in the NGN3+ cells maturing to the β cell stage [77] were also identified under WNT3A treatment. These later markers show continuous rise in expression across the stages. Therefore, it reinforces the observation that early WNT3A induced cells were found to closely shadow the *in vivo*

embryonic transcriptional dynamics. For FGF2, clusters containing small number of late markers were identified as shown in Figure 6B. Two groups were identified, one containing *PTF1* and *INS* and the other containing *HNF6*, *PAX6* and *MAFA*. However, FGF2 contained far less coherent markers at the later stages than WNT3A.

The above analysis indicates that modulation of activin with WNT and FGF2 are likely routes to pancreatic β cells, although WNT pathway is identified to be the most suitable because of the co-regulation of important markers during each stage of the differentiation process. Furthermore, this comparison reveals that even though the expression of DE and PP markers are quite similar for all the induction conditions at the end of DE stage, they deviate significantly upon maturation. This is suggestive of cellular 'memory' of pathway of initial induction even after phenotypic maturation.

3.2.6 PP markers, and not DE markers, are reliable predictors of islet maturation

The above results establish that different pathways of endoderm induction have a significant influence on its mature phenotype and functionality. Another way of looking at it is that efficiency of endoderm commitment, as analyzed by current markers, is not indicative of an efficient pancreatic maturation. The next question thus is whether any of the early or intermediate stages can reveal the potential for cellular maturation to islet cell types.

We addressed this by performing partial least squares regression (PLSR) analysis on the mean TF expression data, to identify which early TFs, if any, were predictors of *INS* expression. Here we are seeking the TFs that showed the most significant correlation to INS expression over all the time points of the differentiation trajectory. The correlation of each of the TFs with *INS* for each induction condition is represented in Figure 3.7 as associated regression coefficients. It

is found that most of the PP markers show high degree of correlation to *INS* expression while there is no significant dependence on the DE markers analyzed. None of the early DE markers analyzed show a positive correlation to *INS* across all the induction conditions. The intermediate PP stage markers like *PTF1*, *PDX1*, *HNF6*, *NKX2.2*, *NKX6.1*, *NGN3* are better predictors of *INS*. Also, WNT3A and FGF2 conditions gave positive coefficients with most of the PP and mature markers indicating that these conditions are optimal for *INS* expression. It is also observed that under BMP4 and PI3KI, the markers NKX6.1, PTF1 and NGN3 gave strong positive correlations indicating that these markers are in fact strongly associated with INS even under low INS upregulation. In addition, we analyzed the expression of PP markers after DE induction and we found high expression of HLXB9, PTF1 and ISL1 at this early stage under some of the conditions for the selected sample. Interestingly, PTF1 resulted in high upregulation under FGF2 and WNT3A, which resulted in highest INS upregulation. This observation combined with the fact that PTF1 expression is highly correlated to INS expression under many conditions from PLSR suggests that analysis of PTF1 expression after DE induction could be used as a determinant of pancreatic potential.

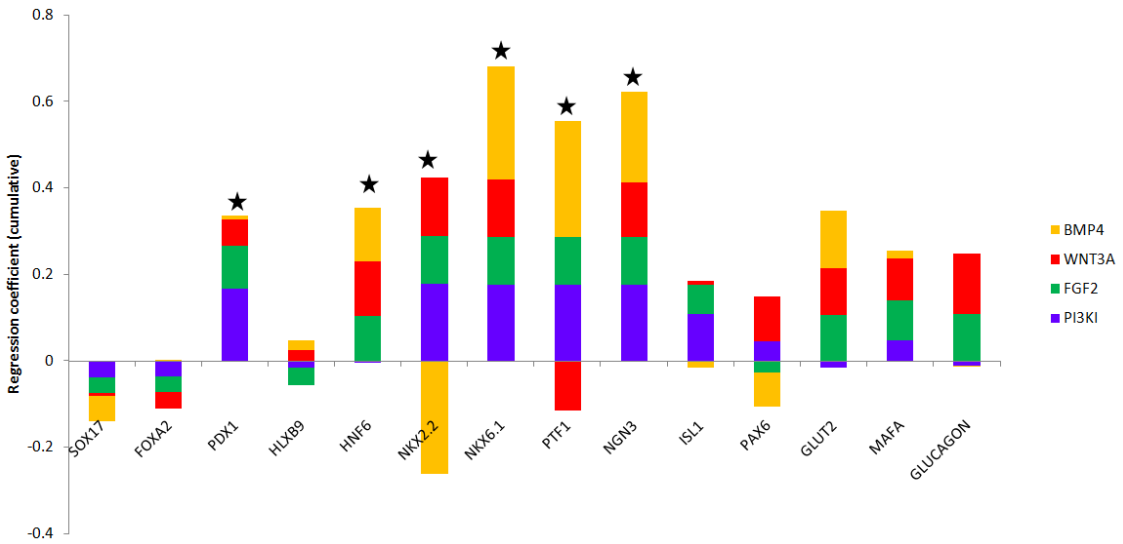

Figure 3.7: Predictors of *INS* expression.

Partial least squares regression performed on the mean expression. Most PP markers show high degree of correlation to *INS* expression while there is no significant dependence on the DE markers. WNT3A and FGF2 conditions gave positive coefficients with most of the PP and mature markers indicating that these conditions are optimal for *INS* expression.

3.3 DISCUSSION

This study analyzes and compares the potential of pancreatic maturation of DE derivatives, obtained from hESC following alternate pathways. Our primary goal was to determine if potential for pancreatic maturation was sensitive to the pathway of initial DE commitment. And if so, determine which pathway is most supportive of pancreatic maturation.

We chose to analyze those DE induction pathways which have been most commonly reported in literature for pancreatic differentiation of pluripotent stem cells. There have been reports of successful DE induction following alternate routes, which have not been considered in

the current study. For example, identification of small molecules has shown great promise as a cost effective alternative to expensive growth factors. While these molecules have not been directly compared in our protocol, many of these molecules modulate similar pathways as discussed here. Some examples include 1m and CHIR99021 which act by inhibiting GSK3β through WNT3A [78,79]; and IDE1 and IDE2 which modulate nodal pathway through activation of TGF-β signaling pathway, similar to Activin [80]. In addition, we have recently reported the sensitivity of endoderm differentiation to substrate physical properties, when cultured on fibrin [81] and alginate gel [82]. However, the exact mechanism involved in such induction of differentiation through insoluble cues has not been elucidated yet.

Importantly, we found that the yield of mature *INS* expressing cells was sensitive to the pathways for initial DE induction. Our analysis suggests that BMP4 signaling is not conducive for pancreatic β cell differentiation of hESCs. Even though other studies have used BMP4 to achieve DE differentiation with subsequent maturation to pancreatic lineage [63,64,83], in our studies BMP4 derived DE derivatives were found to exhibit a stronger potential for *GLUC* expression when subjected to our maturation protocol. Several reasons could be attributed to this difference in the results. It is important to highlight that while these studies also use BMP4 at early stages of differentiation there are obvious differences in the entire differentiation protocol. Phillips et al [63,83] reported the use of BMP4 in combination with activin in early stages of differentiation; however, in later stages they use FGF, IGF, HGF, VEGF, amongst other factors. Their differentiation protocol is based on pancreatic differentiation from adult pancreatic ductal cells, while our protocol is based on recapitulation of events present during *in-vivo* pancreatic organogenesis.

Earliest effect of BMP pathway modulation during pancreatic development occurs at early stages, where in combination with Activin and FGF2, BMP4 signaling specifies DE induction [63]. Also, at the earliest stages of differentiation, BMP4 accelerates the down-regulation of pluripotency genes and up-regulation of mesendodermal genes like *BRACH* [65]. However, later effects of BMP4 are inhibitory of pancreatic differentiation and strong inducers of hepatic differentiation [62]. In our experiments we see BMP4 to consistently induce lowest upregulation of DE, PP and mature β cell markers which could indicate residual BMP4 signaling from DE induction even after removal of BMP4 from media. This is consistent with several pancreatic differentiation studies that use BMP4 at DE induction stage, but use noggin, a BMP pathway inhibitor, at later stages of differentiation [84,85]. From marker progression analysis (Figure 3.4) we see that in BMP4 treated cells, *NGN3* peaks early during DE induction with maintenance throughout the PP stage and decreases during the maturation stage. A recent study has implicated temporal regulation of *NGN3* as an important determinant of cell type specification with early expression favoring α cell induction [86]. In agreement with this, we also see BMP4 cells do express highest levels of GLUC, while exhibiting a very low upregulation of INS. These results link BMP4 signaling to differentiation of α-cells in vitro suggesting that DE specification signaling may prime cells to mature endoderm tissue types.

In a parallel work we tested possible combinations of growth factors for inducing DE and found the combination of Activin, FGF2 and BMP4 to give a high up-regulation of *SOX17* and *CXCR4* compared to using FGF2 or BMP4 alone [87] (Appendix figure 4). Recent work by Yu *et al*. [88] gives an explanation for this effect, with FGF2 sustaining Nanog expression and helping the BMP4 induced differentiation to shift towards endoderm as opposed to extra embryonic lineages . In a previous study by Vallier *et al.*, using Activin in combination with

FGF2 and BMP4 resulted in similar differentiation into mesendoderm [89]. Based on this we decided to mature the endoderm cells derived under combination of FGF2 and BMP4 towards pancreatic maturation. However, the level of *INS* upregulation upon maturation remained comparable to that of BMP4 treatment alone (Appendix figure 5). Thus, FGF2+BMP4 under high Activin seems to work well for DE induction, but may not be optimal for further maturation to the pancreatic lineages.

Our analysis further indicated modulation of WNT pathway to be most supportive of pancreatic maturation. Several studies establish WNT canonical pathway as a potent endoderm inducer and its presence has been shown to stimulate expression of endoderm markers [7,90,91] while inhibition of WNT pathways induces increase of cardiac markers [92]. WNT is therefore added during *in-vitro* differentiation of hESCs particularly during the initial stages of mesendoderm induction. Canonical WNT pathway is found to co-operate with the Activin (SMAD) signaling pathways for the expression of mesendoderm specific genes [93]. However, WNT signaling must be suppressed at the later stages during differentiation to the posterior foregut endoderm [94,95]. Our results show WNT3A DE derivatives to result in high *INS* expression levels and highest yield of C-Peptide positive cells. In agreement with this, in a previous study, Nostro *et al*. found that at low concentrations, increasing canonical WNT pathway activation at the endocrine development stage gave higher up-regulation of *INS* [85].

In addition WNT3A, FGF2 shared most similarities in terms of gene expression patterns and magnitudes, suggesting similar transcriptional regulation. Also, the results of PCA showed that the trajectory of differentiation was very similar for these two conditions. Interestingly, both these conditions also lead to highest expression of *INS* mRNA levels with no statistical difference between them. While gene expression patterns were similar between WNT3A and

FGF2, cell cycle analysis reveals substantial differences (Fig 3.2). The length of the G1 phase for WNT3A treated cells increased at a faster rate than for FGF2, as shown by the higher proportion of the population in the phase. This longer G1 phase time is indicative of a more mature phenotype [96]. Therefore, while both conditions give desirable mature gene expression, WNT3A is the preferred route for maturation based not only on gene expression but cell cycle behavior.

The conclusion that WNT3A leads to better pancreatic differentiation potential is in agreement with a number of pancreatic differentiation studies that use WNT3A in combination with Activin A at the definitive endoderm stage and achieve better yield, insulin expression and functionality after in-vivo maturation that other pancreatic differentiation studies [97].

Finally, our results highlight the insufficiency in analyzing DE markers at the DE stage as an adequate representation of cellular maturation potential. In our experiments, PI3KI consistently showed highest upregulation and yield of DE markers at the end of the DE induction stage. However upon maturation, its potential for *INS* upregulation was lower than that of WNT3A and FGF2. Our correlation analysis also supported this observation, where we found the PP markers to correlate strongly with *INS*, but not the earlier DE markers. This indicates that analysis of PP markers is likely to give us information on the maturation potential of the differentiating cells, but analysis of the DE markers alone is unlikely to reveal such information. In addition, we suggest *PTF1* expression analysis after DE induction to be a potential candidate to determine pancreatic potential. *PTF1* expression showed a high degree of correlation to *INS* expression in our PLSR analysis. Consequently, *PTF1* expression appeared early in conditions resembling pancreatic progression, where *PTF1* expression appears at the prospective pancreatic endoderm stage.

3.4 MATERIALS AND METHODS

3.4.1 hESC maintenance

H1 hESC (WiCell) were maintained in feeder free conditions as previously described [16].

3.4.2 Pancreatic differentiation protocol

Once hESC reached an average colony size of 1 mm in diameter, DE induction media was added for 4 days with media change every day. After 4 days media was replaced with PP (PP) media for 2 days with media change every day. After 2 days, all-Trans Retinoic acid was added to the PP media for 2 additional days with media change every day. Media was then replaced with maturation media. After 2 days DAPT was added to maturation media. Cells were maintained in this media for 1 week with media change every day. Media formulations found in Appendix table 2.

3.4.3 Proliferation and cell death quantification

On day 0 of the protocol, several wells were treated with accutase and starting cell density was estimated using a hemocytometer. 24 hours after initial DE media exposure, cell death was quantified by counting floating cells in the media and normalized with respect to starting cell density. Additionally, the remaining attached cells were harvested with accutase, stained with propidium iodide in PBS at 10ug/ml concentration and the number of dead cells (PI

positive) was quantified by flow cytometry. For quantification of cell number throughout the entire protocol, cells were exposed to alamar blue at day 0 according to manufacturer's instruction for quantification of cell number. This procedure was repeated at the end of each stage of differentiation (days 4,8,15), and cell number was calculated according to as described in the product manual, using Day 0 values as control for each of the stages.

3.4.4 Quantitative polymerase chain reaction

qPCR was performed as previously described [17]. A list of the primers used can be found in the Appendix table 3. ΔCt values were calculated by substracting the respective Ct value for GAPDH from the Ct value of the marker(s) of interest. ΔΔCt values were calculating by subtracting the ΔCt values for undifferentiated cells for the marker of interest from the ΔCt value for the same marker in each group. Relative expression was found by calculating $2^{-\Delta\Delta Ct}$.

3.4.5 Flow cytometry

Flow cytometry was performed as previously described [98] . As a control for non-specific staining, cells were incubated in secondary antibody only. Cells analyzed using an Accuri C6 flow cytometry instrument. Antibodies and concentrations can be found in the supplementary table 3. For cell cycle analysis Cells were harvested and dissociated with Accutase, rinsed, centrifuged and resuspended in ice-cold 70% ethanol and fixed overnight in -20°C. Cells were rinsed and suspended in DNA staining buffer (PBS+0.1% Triton-X+0.2 mg/mL DNAse-free RNAse+0.01 mg/mL/1 million cells propidum iodide) for 25 minutes at RT. Stained cells were then directly analyzed on an Accuri C6 flow cytometer, the output of which being a

histogram of the DNA content for the cellular population in each sample. To accurately determine the fractions of the cellular population in each phase of the cell cycle from these data, Modfit LT (Verity Software House) was applied to the DNA histograms. Modfit identifies the G1 and G2 peaks of DNA histograms acquired by flow cytometry, and fits established cell cycle models to these peaks in addition to the S phase "peak". The area under the curve is calculated via this model, thereby obtaining relative proportions of each cell cycle phase within the population.

3.4.6 Immunocytochemistry

Cells were fixed using 4% parafolmaldehyde for 15 minutes at room temperature and permeabilized using 0.25% Triton X-100 (TX) for 15 minutes. Blocking was performed in 10% donkey serum in 0.05% TX for 30 minutes followed by primary antibody incubation, which was performed overnight at 4°C in blocking buffer with primary antbodies. Secondary antibody incubation was performed for one hour at room temperature in the dark with appropriate antibodies diluted in blocking buffer. Nuclear staining was performed by incubation with Hoescht stain in PBS for 5 minutes. Pictures were taken using Olympus IX81 inverted microscope and Metamorph imaging software.

3.4.7 Statistical analysis

Differentiation results are presented as averages of 6 separate independent experiments. Error bars represent SEM. Kriskal-Wallis test was used to determine statistical significant difference between the DE induction treatments. Additional Mann–Whitney U tests were used for post-hoc comparison with Bonferroni correction of the α.

3.4.8 Mathematical analysis

3.4.8.1 Principal component analysis (PCA)

The gene expression data containing the dynamics of the differentiation markers across the four stages of differentiation and the four conditions was analyzed using PCA. The data was preprocessed by mean centering and variance scaling across each transcription factor. PCA was done on this matrix in MATLAB R2010 by using the princomp option. It was found that the first two PCs explained at least 67% of the variance in the data for all the PC plots in this paper. Therefore, two principal components were retained in the final analysis.

3.4.8.2 Clustering techniques

K-means clustering was used to identify TFs that showed similar patterns of expression across the four stages independently for each condition. MATLAB function kmeans was used alongwith the correlation distance. The quality of the resulting clusters was judged by the Silhouette value (Si). We selected a threshold of 0.6 for Si, and determined the number of clusters k which gave all Si values greater than 0.6. Hierarchical clustering was done on the

entire dataset (all conditions together) to further classify the dynamics. We used the in-built Matlab functions pdist and linkage to perform the analysis on the mean expression data and the results were represented as a clustergram. We also tested the tree generated using different linkage measures and found all the trees to be similar with the cophenetic correlation coefficient greater than 0.9.

3.4.8.3 Partial least squares regression (PLSR)

We performed PLSR to find which of the earlier markers showed the highest correlation with INS up-regulation. The matrix, X, was generated as described in PCA. INS was chosen as the output, Y, and the remaining transcription factors acted as the predictors. We used the plsregress option from MATLAB which uses the SIMPS algorithm. The data was mean centered and variance scaled. For the PLSR plot in Figure 2.7, the R2 values were above 0.995.

4.0 ENDOTHELIAL CELL MEDIATED MATURATION OF HUMAN EMBRYONIC STEM CELLS TOWARDS PANCREATIC ISLET CELL TYPES

4.1 INTRODUCTION

ESC are pluripotent cells that can be propagated in an undifferentiated state indefinitely making them a desirable source of cells for transplantation [99]. These cells can be guided to differentiate into virtually any cell and tissue type by provision of appropriate cues in a directed differentiation approach [100]. In terms of pancreas, directed differentiation consists of stage-wise induction through events known to take place during pancreatic development, beginning with DE (DE) formation. This is typically achieved by modulation of the nodal pathway trough Activin A [101]or more recently, small molecules such as IDE1 and IDE2 [80]; Moreover, it has been demonstrated that supplementing nodal activity by modulating alternative pathways such as WNT3A [71] or PI3K inhibition [102] aids DE induction. DE induction is followed by PP (PP) commitment, marked by the appearance of PDX1 which is the diverging point between pancreatic progression and development of other DE derived tissues [101]. It is well known that appearance of PDX1 is associated to sonic-hedhgog (SHH) inhibition during pancreatic development, therefore can be achieved through addition of cyclopamine in an in-vitro setting [103]. These PP are directed towards endocrine progenitors by addition of retinoic acid [104]. Finally, NGN3 expressing endocrine progenitors are matured towards beta cells trough different

mechanisms including notch inhibition, found during pancreatic development [105], and GLP-1 activation which has been demonstrated to promote regeneration of beta cells through proliferation of already mature β cells and transdifferentiation of ductal PP cells [106].

Several studies, including previous work in our lab, have used this information to develop directed differentiation protocols [71,102]. Many of these existing protocols result in high yield of PP cells. These cells also have the potential for functional maturation upon implantation in diabetic mice models [68]. However, maturing these cells into functional islet-like cells in an in-vitro setting is yet to be demonstrated.

Organogenesis is a complex and dynamic process involving signals from several parallel inputs including chemical, mechanical and from contact with neighboring cells. While there is an increasing trend to recapitulate the entire micro-environmental niche, most of the existing protocols use modulation of individual pathways through targeted molecules and growth factors [107]. In this report we are presenting an alternate strategy for achieving islet specific maturation of hESC derived PP cells. We hypothesize close contact with endothelial cells (EC) during final stages of hESC differentiation will induce islet specific maturation of the hESC derived PP cells. Several reasons lead to this hypothesis, including the fact that the pancreas and aorta develop in close proximity [7] and there is cross-talk between this cell types at several stages of development [108]; that the pancreas develops into a highly vascularized organ and that it has been shown that EC are capable of regulating mature β cell function [109-111].

In this study we recapitulated cell-cell interactions between EC and hESC-derived PP in an *in-vitro* environment. We find that co-culture with different EC (but not fibroblast) results in pancreatic islet-specific differentiation of hESC-derived PP cells without additional chemical induction. The cells further demonstrated response to exogenous glucose levels by enhanced

C-peptide synthesis. Finally, analysis of a comprehensive database of signaling pathways suggests that our co-culture system aligned well with endocrine development and we suggest possible mechanisms involved in the observed phenomenon.

4.2 RESULTS

4.2.1 Multi-stage directed differentiation protocol

hESC where propagated in hESC qualified matrigel coated dishes and maintained in mTeSR1 media until average colony diameter reached 1mm, at which point the hESCs were differentiated following a multi-stage directed differentiation protocol as described in Figure 4.1A. The first stage involved DE induction by exposure to Activin A and inhibition of PI3K signaling by Wortmannin. These treatments lead to significant cell death, particularly on the first day. Surviving cells, however, rapidly proliferated with cell mass being recovered by day 4 of treatment. At the end of DE induction we observed upregulation of DE markers *FOXA2, SOX17* and *CXCR4* by qPCR (Figure 4.1B). Protein expression was further confirmed by immunostaining, which showed strong nuclear expression of SOX17 (Figure 4.1C). Flow cytometry analysis of FOXA2 showed 90% of cells positive for FOXA2 stain (Figure 4.1D). Taken together, these results confirm DE induction by treatment with Activin A and PI3K inhibition.

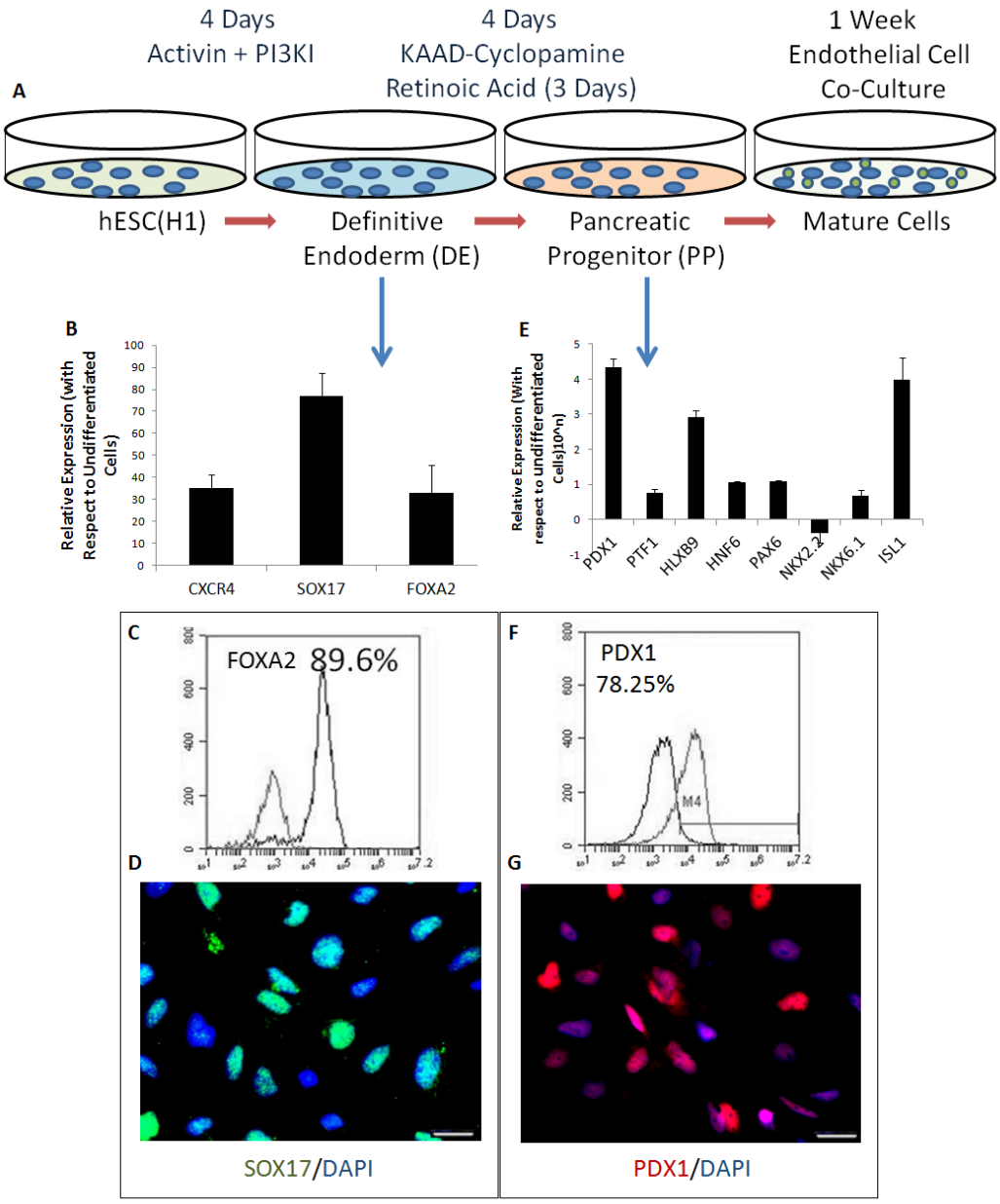

Figure 4.1: Directed Differentiation Protocol.

(A) Schematic representation of multi-stage differentiation system. DE was induced by modulation of nodal pathway simultaneously inhibition of PI3K. PP was achieved by SHH inhibition along with retinol signaling. Maturation was induced by endothelial cell co-culture. (B) qPCR result for DE markers at the end of DE induction. (C) Representative flow cytometry for FOXA2 and (D) immunocytochemistry for *SOX17*. (E) qPCR result for PP markers at the end of PP induction. (F) Representative flow cytometry and (G) immunocytochemistry for PDX1. Scale bar: 25µm

The second stage of our protocol consisted of PP induction by SHH inhibition by exposure to Cyclopamine followed by SHH inhibition and retinoid signaling. At the end of this stage, cells were harvested and analyzed for PP markers. qPCR analysis confirmed high upregulation of PP markers, particularly *PDX1*, *HLXB9* and *ISL1* (Figure 4.1E) which showed roughly 21,000, 800 and 9,500 fold upregulation over undifferentiated cells respectively. PDX1 expression was confirmed at the protein level both by immunocytochemistry and flow cytometry. Staining revealed strong nuclear expression of PDX1 in a large number of the cells (Figure 4.1F) and flow cytometry analysis for PDX1 confirmed 78% of the differentiated cells positive for PDX1 (Figure 4.1G). These results confirm proper differentiation into PP cells by exposure to cyclopamine and retinoic acid following DE induction.

4.2.2 Endothelial cells mediate islet-specific maturation of hESC derived PP Cells

The PP cells obtained by the protocol mentioned above were next subjected to the maturation protocol. The hESC derived PP cells were exposed to nicotinamide containing media for 2 days, after which rat heart microvascular endothelial cells (RHMVEC) were directly added to the differentiating population of hESCs to establish a contact co-culture configuration. Since a contact co-culture requires culturing both the differentiating hESCs and the endothelial cells (EC) in the same media, it is critical to develop a defined media that would support both hESC differentiation and sustain EC survival. RHMVEC are traditionally cultured in FBS containing media while our differentiation protocol in entirely serum-free. In order to maintain completely serum-free condition, the differentiation media was supplemented with growth factors that induce RHMVEC survival including EGF and crude FGF (EndoGro) (henceforth referred to as co-culture media). Despite this, RHMVEC survival was limited with considerable cell death

observed within 5 days of culture. Figure 4.2A shows DiI-Ac-LDL labeled RHMVEC in co-culture with the hESC derived cells. It is observed that while many of the RHMVEC attach to the empty spots in the plate, a significant portion of the cells are in direct contact with the hESC derived PP cells. This was further confirmed by Immunostaining which shows Von Willerbrand factor (VWF) positive EC in direct contact with PDX1 positive PP cells (Figure 4.2B).

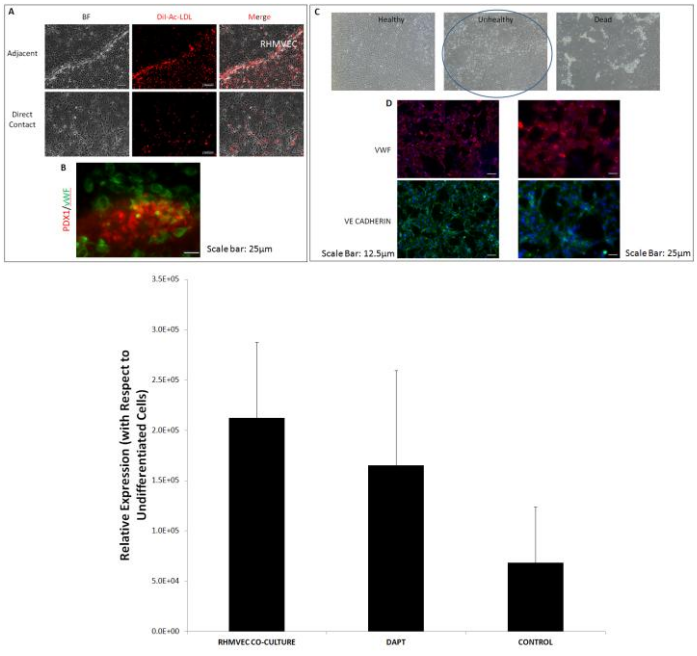

Figure 4.2: Endothelial Cell Induced Maturation co-culture with hESC-derived PP

(A) Contact co-culture of hESC derived PP with Dil-ac-LDL labeled RHMVEC. EC are observed djacent (top) or in direct contact (Bottom) with hESC derived PP. (B) ICC shows VWF positive EC and PDX1 positive hESC-derived PP cells in direct contact. (C)Maintenance of EC in serum free co-culture media leads to EC depletion attributed to absence of serum in media. (D) Before EC depletion ICC confirms expression of EC specific markers.

Having established the co-culture system, we next evaluated the effect of co-culture on the differentiating population of hESC derived PP cells. As described above, the EC are added to the hESC after the PP stage and maintained in the co-culture media until the RHMVEC gets

depleted from the co-culture configuration (around 5 days). At that point the media was switched to regular hESC maturation media, without the EC supplements, and culture was continued for 5 more days to allow for complete depletion of EC. Interestingly, we found that the RHMVEC survived longer when cultured in the presence of hESC-derived PP than when cultured alone (data not shown). Before complete depletion, RHMVEC were stained for EC specific markers VE Cadherin and VWF to confirm maintenance of EC phenotype (Figure 4.2C,D). The cells were harvested after complete EC depletion and PCR analysis showed over 200,000 fold upregulation of *INS* (Figure4.2E). In order to confirm that the observed effect on differentiation is mediated by the EC and not from the modified co-culture media, parallel control culture was maintained in co-culture media without the EC for 5 days and switched to maturation media at the same time as the co-culture group and maintained in this media for the remaining experiment. This control group showed a 68,000 fold upregulation of *INS*, hence confirming the positive role of EC in maturing hESCs to islet-like cells (Figure 4.2E). In the next step we compared the efficiency of differentiation mediated by EC with that of standard procedures of notch inhibition by DAPT treatment [57]. DAPT treatment for 5 days followed by maturation media for 5 additional days resulted in comparable levels of INS up-regulation, without any significant difference (Figure 4.2E).

4.2.3 Co-culture mediated maturation is Specific to endothelial cells

Having confirmed the positive effect of RHMVEC in islet-specific maturation of hESC, we next wanted to investigate if the effect can be reproduced by other ECs as well. Human Umbilical Vein endothelial Cells (HUVEC) were our next choice of EC since it is a very well studied cell of human origin. HUVECs are more robust in culture and, unlike RHMVEC,

survived the entire maturation period, therefore after 5 days in co-culture media the HUVECs were thus labeled with DiO-Ac-LDL and sorted out prior to qPCR analysis. hESC-derived PP cells matured in contact with HUVEC showed almost 700,000 fold upregulation of *INS*, resulting in over 3 fold higher INS gene expression compared to RHMVEC co-culture or notch inhibition by DAPT (Figure 4.3A). As a further precaution, the DiO-Ac-LDL positive sorted populations were also analyzed for *INS* gene expression, which was found to be undetectable. Hence this confirms that the hESCs are maturing into INS expressing cells when co-cultured with endothelial cells.

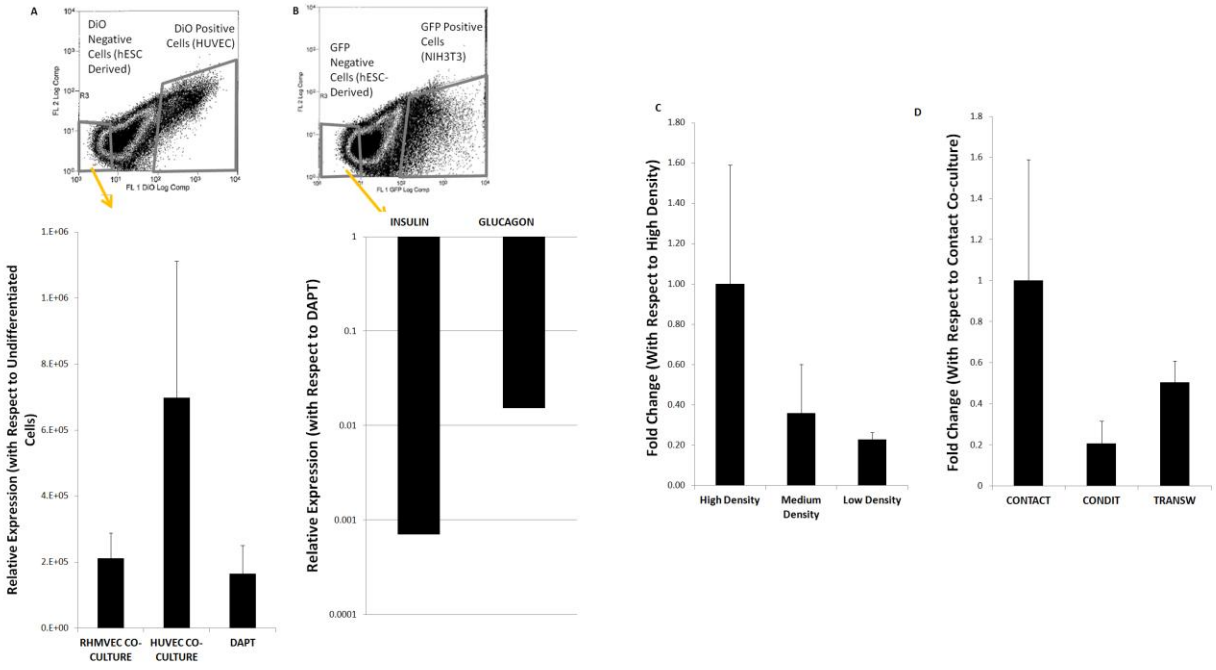

Figure 4.3: Endothelial cells mediate maturation of hESC-derived PPs.

(A) qPCR for *INS* after maturation stage with DAPT, contact co-culture or co-culture media. Higher expression for cells matured by EC co-culture was observed. Co-Culture with (B) HUVEC and (C NIH3T3. Cells were sorted to isolate hESC derived cells and qPCR for *INS* and *GLUC* was performed. qPCR results show that other endothelial cells also mediate insulin upregulation in hESC derived PP, while non-endothelial cells do not. qPCR for the isolated HUVEC and NIH3T3 show no INS in either cell type confirming that insulin upregulation comes from the hESC-derived cell population. qPCR results for cells matured varying EC density (D)or co-culture configurations (E). EC number positively correlates with insulin upregulation. INS expression is upregulated for all co-culture configurations but to a lower extent than contact co-culture. Transwell co-culture elicits higher upregulation than EC conditioned media, suggesting some signals may be short lived.

Our next question was if the effect of the co-culture was specific to ECs or can be reproduced by any other cell type. To test this we performed a parallel co-culture with a fibroblast cell line (GFP-NIH-3T3). Like HUVEC, NIH-3T3 cells survived for the entirety of the maturation stage of the protocol, and the GFP positive fibroblast population was sorted out prior

to qPCR analysis. The negative hESC-derived population was analyzed for *INS* and *GLUC* expression, showed only a minimal 100 fold increase in INS expression (Figure 4.3B). Together, these results confirm that ECs have the potential to induce differentiation of hESC-PP cells into insulin expressing cells and that this effect is specific to EC and is not mediated by other cell types such as fibroblasts.

4.2.4 EC mediated maturation of hESC-PP is augmented by direct contact between cells

Having confirmed that co-culture with EC specifically governs islet-like maturation of the hESC-derived PP cells, we sought to investigate the effect of density of endothelial cell co-culture on differentiation. Since HUVEC was mediating a stronger effect further experiments were performed with HUVEC (Figure 4.3C). ECs were added at a plating ratio of 1:1, 1:2 or 1:10 with respect to hESC-derived PP cells in direct contact and the culture was continued as before. Analysis of the differentiated cells by qPCR after sorting out the ECs confirmed strong *INS* expression under all the co-culture ratios. The effect was, however, strongest with high density of co-culture with *INS* levels being progressively lower for lower co-culture densities (Figure 4.3C).

In order to analyze the mechanism through which the endothelial cells are mediating hESC maturation, we investigated the effect of alternate co-culture configurations on hESC differentiation (figure 4.3D); namely, transwell co-culture in which the EC and the hESC-derived PP cells were plated on adjacent chambers separated by a semi-permeable membrane that allows diffusion of soluble signals, but prevents direct contact. Additionally we tested EC conditioned media where the co-culture media was added to HUVEC (maintaining the 1:1 ratio) for 24 hours

before being added to the hESC-Derived PP with media change in this manner every 24 hours. Both conditions were maintained for 7 days, at which point HUVEC viability started to decrease. qRT-PCR analysis for insulin gene expression under alternate configurations revealed highest up-regulation for contact co-culture, followed by 2 times lower expression in transwell and 5 times lower in conditioned media culture. This indicates that the maturation is mediated by cell-cell contact along with possibly short-lived soluble factors.

4.2.5 Characterization of cells matured by HUVEC

Based on the above analysis, the hESC derived PP cells were co-cultured in direct contact with high density of HUVEC, and the differentiated cells were further characterized for relevant islet-specific maturation. Analysis by RT-PCR for relevant β-cell markers revealed (Figure 4.4A) particularly high upregulation of *GLUT2* reaching 25,000 fold; *NKX2.2*, *NKX6.1* and *ISL-1* also achieved considerable upregulation of 200, 135 and 394 fold respectively.

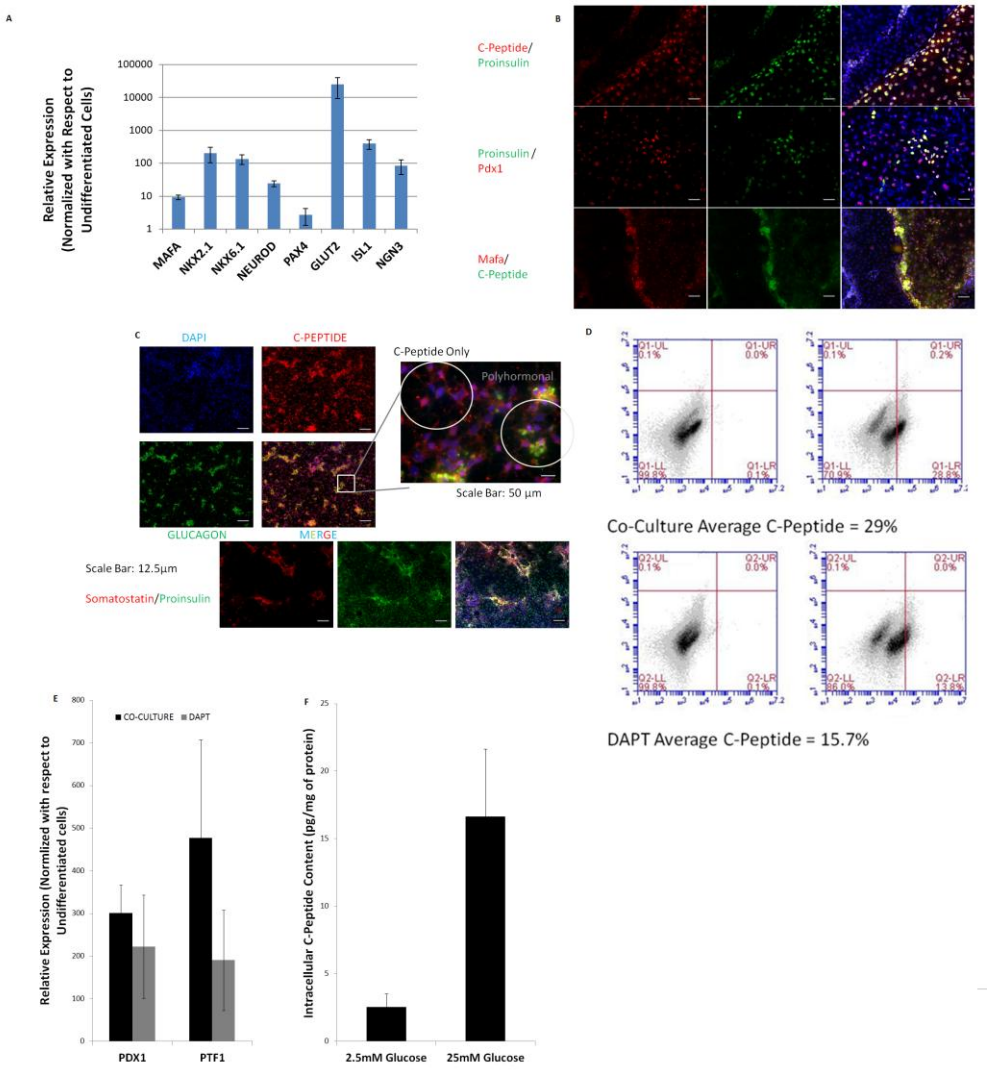

Figure 4.4: Characterization of Endothelial Cell matured hESC-Derived Cells

(A)qPCR for β- cell markers confirms maturation of hESC-derived PP by endothelial cell co-culture method (B)Characterization by ICC shows co-expression of C-Peptide and Proinsulin. Further ICC shows high co-expression of Prosinulin and PDX1 and MAFA and C-Peptide. Scale bar: 12.5µm. (C) ICC for glucagon and c-peptide and somatostatin and proinsulin after EC contact co-culture show populations of poly-hormonal cells as well as populations of cells expressing c-peptide only. (D) qPCR for PDX1 and PTF1 expression show superior upregulation under co-culture maturation conditions. (E) Flow cytometry results indicate 29% of the cells are positive for c-peptide (F) Magpix was used to quantify intracellular c-peptide levels at low (2.5mM) and high (25mM) glucose levels. The results show approximately 6 fold increase in c-peptide upon high glucose stimulation.

Cells differentiated under this condition showed positive staining for PDX1, Proinsulin, C-Peptide and MAFA (Figure 4.4B). We examined whether the resulting cells were polyhormonal by immunocytochemistry (Figure 4.4C). Specifically we co-stained for Glucagon and C-Peptide and somatostatin and Proinsulin. For both cases we found populations of multiple-hormone expressing cells; however we found a significant number of cells expressing insulin in the absence of other pancreatic hormones, representing fully mature cells. Staining for Amylase was found to be negative, suggesting absence of exocrine cells (not shown).

Quantification by flow cytometry showed that about 29% of the cells were positive for C-Peptide, compared to 15% obtained when using notch inhibition as illustrated in Figure 4.4D. The foremost functionality of β-cells is glucose responsive insulin release. Hence glucose responsiveness of the hESC derived cells was analyzed by exposing the cells to 2.5 mM (low) glucose or 25mM (high) glucose media for 4 hours and quantifying intracellular C-Peptide levels (Figure 4.4F). When stimulated in low glucose, the intracellular C-Peptide level was observed to be 2.5 pg/mg of total protein, while at high glucose concentrations these values increased to over 16 pg/mg of total protein, representing an almost 7 fold increase over low-glucose condition. These results suggest that the hESC derived islet-like cells have the capability of modifying insulin biosynthesis in response to external glucose concentration.

4.2.6 Analysis of signaling pathways mediating EC-induced pancreatic maturation

4.2.6.1 Correlation between markers associated with signaling pathways and pancreatic maturation

In order to identify possible pathways that are differentially modulated by the endothelial cells, the gene expression profile at the end of maturation was analyzed using human signal transduction PCR pathway finder. The signal transduction genes were further supplemented with relevant pancreatic markers to form our complete dataset, as represented in Figure 4.5A. Figure 4.5A presents the heatmap of $-\Delta\Delta C_T$ values of the focus genes for two co-culture samples and one transwell sample labeled as samples 1, 2 and 3 respectively. Since, stem cell cultures show high degree of variability, we analyzed each sample independently without taking mean of the fold-changes. Using a threshold of 2-fold up- or down- regulation, the dataset was filtered to select the genes to be focused to further analysis. Among the 95 genes in the dataset, 37 were identified as the focus genes across all the three samples. These focus genes belonged to the following pathways: Hedgehog, JAK/STAT, NFκB, WNT, TGFβ, Hypoxia, PPAR, Notch and p53. Next we wanted to identify any possible association between the signaling transcription factors and the pancreatic markers. Partial least squares regression (PLSR) analysis was performed with each pancreatic marker as the output and the signaling pathway genes as the input. We observed two groups of output markers based on the type of their relationship with the signaling genes as seen from the sign of the regression coefficient. The outputs *INS*, *GCG*, *ISL1* and *NEUROG3* formed group 1 and *NKX2-1*, *NKX6-1*, *NEUROD1* and *GLUT2* formed group 2 and these groups showed opposite relationships to the signaling genes. The regression coefficients for group 1 that contained our primary output of interest, *INS*, are presented in

Figure 4.5B. These regression coefficients denote the independent contribution by each signaling TF to the total output. As seen from the figure, the top five prime contributors were *FCER2*, *ICAM1*, *WISP1*, *EPO* and *FABP1* while the remaining genes gave very small contributions. *FCER2* (JAK1,3/STAT6), *EPO* (Hypoxia) and *FABP*1 (PPAR) showed a negative correlation while *ICAM1* (NFκB) and *WISP1* (WNT) elicited a positive correlation. The regression coefficients for group 2 are presented in Appendix Figure 4.6.

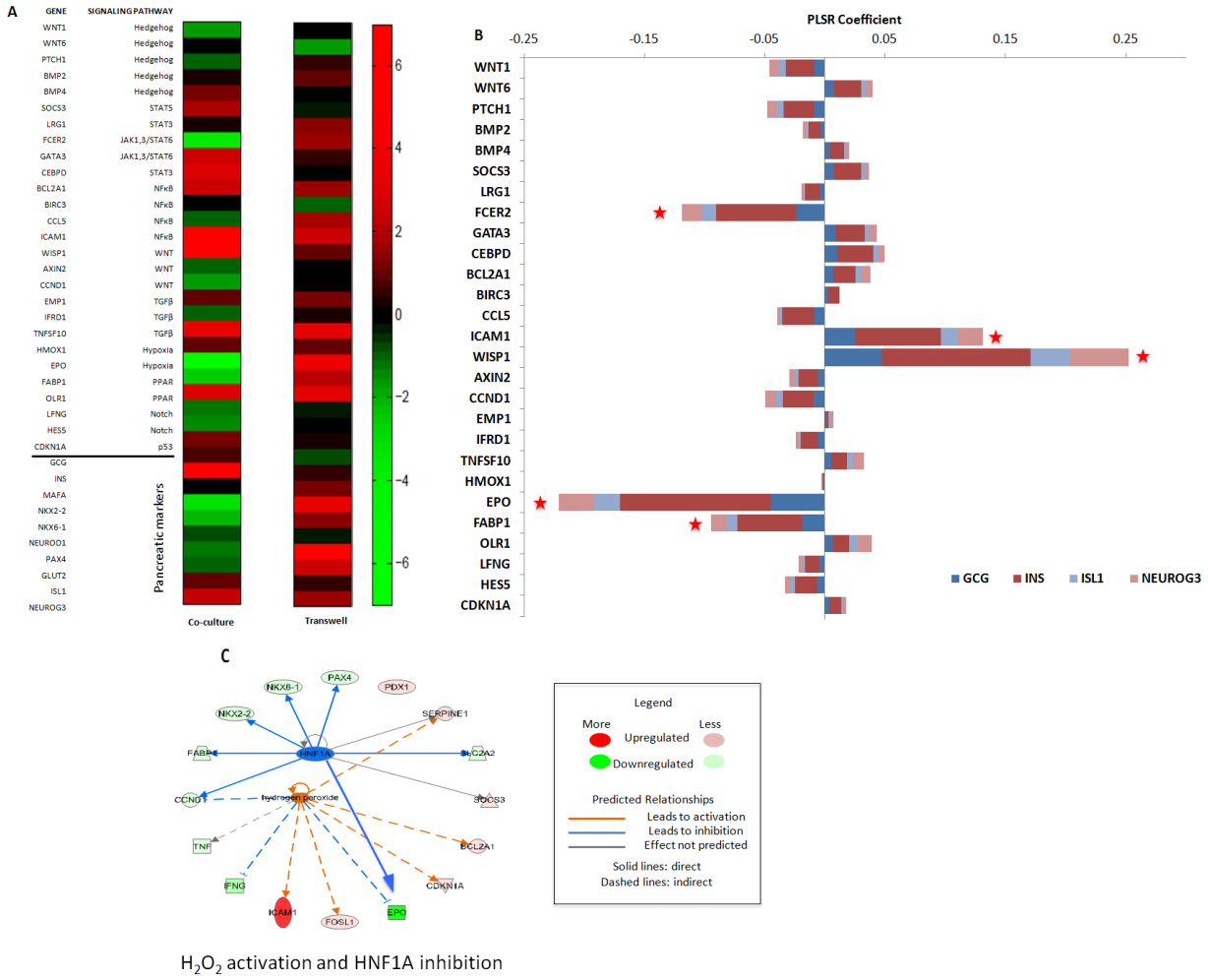

Figure 4.5: Quantitative analysis of signal transduction gene expression during maturation.

(A) Heatmap of PCR gene expression at the end stage of maturation. Each sample is normalized to the respective control medium. A threshold of 2 fold upregulation/downregulation is used to filter the dataset and the $-\Delta\Delta C_T$ values of the focus genes are presented here. The Y-axis contains signaling genes and the pancreas specific markers. Genes in red are up-regulated while those in green are down-regulated. It is seen that co-culture sample 1 shows the highest *INS* levels. (B) PLSR coefficients indicating the correlation between the major pancreatic markers and signaling pathway genes. *INS, GCG, ISL1 and NEUROG3* are taken as the outputs and the signaling pathway genes from (A) are taken as the inputs. The data matrix is log2 transformed before regression analysis. The output markers show identical relationship to the signaling pathway molecules. (C) Upstream regulators of the focus genes in the dataset associated with deactivation of hypoxia mediated signaling in co-culture sample 1.

While this analysis is helpful in identifying independent relationships between each TF in the signaling pathway and the pancreatic markers, it is also informative to analyze the overall activity of pathways constituting these genes. Therefore, an in depth comparison of focus genes in the dataset to the literature was done using Ingenuity Pathway Analysis (IPA) database to infer network level information.

4.2.6.2 Signaling pathways differentially regulated under co-culture configuration

Network analysis was performed for the most representative sample (Sample 1) of co-culture that gave the highest insulin up-regulation. Using the IPA database, the top networks associated with the genes in the dataset were identified and ranked according to the score values. Table 4.1 lists the identified networks with the corresponding scores and focus genes. The top network is associated with endocrine system development and contains 13 genes from the dataset (estimated probability of random gene placement = 10^{-30}; i.e. score = 30). The remaining networks were associated with cell death and survival (score = 16) and cardiovascular system development (score = 14). Thus, based on gene expression, the co-culture dataset contains gene sets that contribute primarily to endocrine cell development. This network of endocrine cell development containing the relevant focus genes is presented in Appendix Figure 4.7. A biological functional analysis was also performed for the co-culture sample that further supported the network analysis. The significant functions are presented in Appendix Figure 4.8. Among the developmental functions, those associated with digestive system and endocrine system are again identified to be important. The molecular and cellular functions included cellular development, cell survival, cellular function and maintenance etc.

Table 4.1: Top networks in the dataset

Key Networks	Focus Molecules	Score
Endocrine System Development and Function, Tissue Morphology, Digestive System Development and Function	*FCER2, FOSL1, INS, LFNG, NEUROG3, NKX2-2, NKX6-1, PAX4, PDX1, PTCH1, SLC2A2, SOCS3, TNSFS10*	30
Cellular Development, Cell Death and Survival, Cancer	*AXIN2, CCND1, FABP1, HES5, GATA3, TNF, WISP1, WNT1*	16
Cardiovascular System Development and Function, Cellular Movement, Cellular Development	*BCL2A1, BMP4, CCL5, CEBPD, EMP1, ISL1, OLR1*	14

Using the IPA database, possible upstream regulators of global gene expression changes in the dataset were then identified. Table 4.2 lists the upstream regulators and their predicted activation status. The z-scores denote the significance associated with this predicted activation status as compared to a random association and scores with an absolute value greater than 2 are considered to be significant. Many of the top regulators are significantly activated in the co-culture sample and only one pathway is significantly downregulated. Among the top upstream regulators, cyclic AMP is predicted to be activated based on the up-regulation of *GATA3*, *CEBPD*, *CDKN1A*, *TNFSF10*, *SOCS3*, *SERPINE1* and down-regulation of *IFNG*, *PTCH1*, *CCND1* and *TNF*. Similarly, hydrogen peroxide (H_2O_2) is also predicted to be activated based upon up-regulation of *SERPINE1*, *BCL2A1*, *FOSL1*, *CDKN1A*, *ICAM1* and down-regulation of *EPO*, *IFNG*, *TNF* and *CCND1*. This is followed by butyric acid and angiopoietin 2. Among down-regulated pathways, only HNF1A upstream regulator was predicted to be significant. HNF1A and H_2O_2 together also form a connected system and interaction between these

molecules are shown in Figure 4.5C by an influence graph with the target genes from the dataset. Overall, the pathway analysis highlights ability of endothelial cells to mediate global gene expression patterns to follow pancreatic organogenesis and identifies the possible signaling pathways that are differentially regulated under the contact configuration.

Table 4.2: Top upstream regulator of gene expression

Upstream Regulator	Molecule Type	Prediction	Target Genes	Z-score	P-value
Cyclic AMP	Endogenous chemical	Up	*TNFSF10, TNF, SOCS3, IFNG, GATA3, CEBPD, CDKN1A, CCND1, PTCH1, SERPINE1*	2.719	6.86×10^{-12}
H_2O_2	Endogenous chemical	Up	*SERPINE1, IFNG, FOSL1, EPO, CDKN1A, CCND1, BCL2A1, TNF, ICAM1*	2.697	2.3×10^{-8}
Butyric Acid	Endogenous chemical	Up	*TNF, ICAM1, GATA3, CDKN1A, CCND1, BCL2A1, SERPINE1, SOCS3*	2.335	1.35×10^{-5}
Angiopoietin 2	Growth factor	Up	*OLR1, ICAM1, CDKN1A, CCL5*	2.0	4.46×10^{-5}
HNF1A	Transcriptional regulator	Down	*SERPINE1, SOCS3, SLC2A2, PAX4, CCND1, NKX6-1, NKX2-2, FABP1, EPO*	-2.0	3.65×10^{-8}

4.3 DISCUSSION

We have described a protocol for efficient differentiation of hESCs to insulin-producing cells using EC as mediators of PP cell maturation. We were able to confirm this effect to be EC specific by using EC from different sources as well as non-endothelial cells as controls. We also tried several co-culture configurations and we observed that contact co-culture leads to higher insulin expression suggesting that some of the signals are short-lived and/or require direct contact between the EC and hESC-derived PP. Characterization of the resulting cells showed higher yield of insulin expressing cells compared to standard method of notch inhibition and cells were found to express mature cell markers.

Alternate strategies have been proposed for inducing DE for pancreatic maturation [Ref]. We initially attempted DE induction by activation of WNT pathway, which results in strong pancreatic progenitor differentiation. However there was less success with EC co-culture in this condition, primarily because the confluence hESC culture at the pancreatic progenitor stage interfered with EC attachment. On the other hand DE induction by Activin A and PI3KI as previously described [69,112] results in significant initial cell death. While the cells gradually recover with continued culture, still the culture is less confluent at the PP stage, thereby favoring EC attachment for contact co-culture.

We performed the co-culture with three different cell-types: two endothelial cells and one non-endothelial cell. Our results confirmed the observed maturation effect to be specific to endothelial cell co-culture. While both the endothelial cells elicit a strong up-regulation of insulin in the differentiating hESCs, the effect was stronger in the human endothelial cell co-

culture compared to the rate heart micro-vascular cells. This could imply that human EC in general are more supportive of human embryonic stem cell differentiation. However, we also observe that the HUVECs are more robust and survive longer in the co-culture configuration, compared to the RHMVEC cells, hence can potentially elicit a stronger effect on the cell maturation.

At the end of our differentiation protocol, functionality was assessed my measuring intracellular C-peptide levels after incubation in low or high glucose media. While this method has not been widely used in other β cell differentiation studies, it is routinely used in β cell biology. The significance of it is that upon glucose stimulation the initial cell response consists of a series of events including increase of post-transcriptional modification of proinsulin into insulin to increase the available pool of intracellular insulin ready for release [113].

We hypothesized that several mechanisms could mediate the observed phenomenon. One possibility is deposition of extracellular matrix by endothelial cells. This is in agreement with both developmental and differentiation studies. In terms of development it has been postulated that while pancreatic cells do not produce ECM, they produce VEGF which attracts endothelial cells. These endothelial cells produce ECM which aids with pancreatic progression trough activation of integrin mediated pathways [Cirulli, 2000; Nokolova, 2006]. In differentiation studies it has been observed that laminin-1 promotes differentiation of pancreatic progenitor cells into insulin expressing cells [Jiang, 1999]. Another possible mechanism by which endothelial cells mediate differentiation is restoration of normoxia, which has been suggested to favor beta cell differentiation [Heinis, 2010]. Related to this, release of nitric oxide from EC has effects that resemble normoxic conditions inhibition of endothelin-1 (Kourembanas, 1993), destabilization of HIF during hypoxic conditions, and interference with hypoxia signaling (Brune, 2007).

In order to investigate the mechanism through which the EC are mediating the maturation of hESC derived PP cells, we analyzed two additional co-culture configuration: transwell and conditioned media. The contact co-culture was found to have the maximal effect, followed by transwell, while conditioned media had a positive but reduced effect on maturation. We further analyzed these conditions using a PCR array for signaling pathway with the objective of identifying possible pathways through which ECs are mediating an effect. Further comparative analysis between the different co-culture configurations will also reveal the specific effect of contact co-culture. For example, C/EBPD was strongly up-regulated under contact co-culture, but not under transwell culture. C/EBPD, which has both anti-apoptotic and anti-inflammatory roles in pancreatic β-cells [31], has been found to be upregulated in hepatocytes cultured on laminin rich extracellular matrix [32]. Upregulation of C/EBPD in our co-culture configuration suggests the possibility of laminin secretion by EC in contact co-culture conditions.

We further analyzed the array data to identify possible mechanisms mediating the maturation process and also a possible correlation between the beta cell maturation markers and signaling pathway molecules. PLSR analysis showed several genes that are highly correlated to insulin expression. Amongst them WISP1 which is expressed in the adult pancreas [114] and has been implicated in increase regenerative ability of beta cells [115]. Also, a high negative correlation was found with FABP1, which in the intestine has been found to be suppressed by expression of PDX1 [116]. Similarly EPO showed a strong negative correlation with insulin expression. EPO is produced and secreted during hypoxic conditions [ref], therefore suggesting a negative correlation between hypoxia and PP maturation.

At this point, most of the analysis done consists of independent pathways and targets, however, we deemed important to analyze the overall activity of pathways constituting these

genes in the IPA database to infer network level information. Detailed pathway analysis revealed several of the differentially regulated genes to be from the signaling pathways belonging to pancreatic organogenesis. Secondly, biological functions associated with cellular survival were also identified to be important. Among the canonical pathways, those mediated by growth factors were strongly associated with the genes in our dataset. Among them, JAK/STAT has been recently implicated in the pancreatic maturation process and increased endocrine differentiation [117]. From the upstream analysis, IPA inferred many upstream regulators that could possibly be activated by endothelial specific signaling. Many of the downstream genes identified by IPA support the close association of H_2O_2 activation and HNF1A downregulation. For example, H_2O_2 is found to inhibit EPO (associated with hypoxia) [118] and it is significantly downregulated in the coculture sample. EPO is also a downstream target of HNF1A [119,120]. Also, at later stages of maturation, HNF1A downregulation due to normoxia is found to favor β–cell differentiation [108]. This effect is due to the close association between endothelial cells and beta-cells during pancreatic organogenesis.

In summary, we have developed a protocol for differentiation of hESC into insulin expressing cells that synthesize insulin in response to exogenous glucose levels. The last stage of our protocol recapitulates cell-cell interactions with endothelial cells as found during pancreatic development. Gene expression analysis showed a close resemblance to endocrine development, thus, by recapitulating cell-cell interaction aspects of the developmental niche we achieved a differentiation model that lines up with endocrine cell formation, and hence can be used as a model for β-cell development.

4.4 MATERIALS AND METHODS

4.4.1 hESC maintenance

H1 hESC (WiCell) were maintained in feeder free conditions as previously described [87]. EC at passages lower than 10 were maintained using MCDB-131 complete (VEC technologies).

4.4.2 Differentiation

Once hESC reached an average colony size of 1mm, DE induction media was added for 4 days with media change every day. After 4 days media was replaced with PP media for 2 days with media change every day. After 2 days, all-Trans Retinoic acid was added to the PP media for 2 additional days with media change every day. Media was then replaced with maturation media for 2 days, after which EC were harvested and added to hESC-PP in serum containing MCDB-131 media overnight . The same media was added to both DAPT control and co-culture media controls. The next day co-culture media or DAPT control media were added with media change every day for up to 10 days. Media formulations found in Appendix table 2.

4.4.3 Quantitative polymerase chain reaction

qPCR was performed as previously described [81]. A list of the primers used can be found in the Appendix table 3.

4.4.4 Immunocytochemistry

Cells were fixed using 4% parafolmaldehyde for 15 minutes at room temperature and permeabilized using 0.25% Triton X-100 (TX) for 15 minutes. Blocking was performed in 10% donkey serum in 0.05% TX for 30 minutes followed by primary antibody incubation, which was performed overnight at 4°C in blocking buffer with primary antbodies. Secondary antibody incubation was performed for one hour at room temperature in the dark with appropriate antibodies diluted in blocking buffer. Nuclear staining was performed by incubation with Hoescht stain in PBS for 5 minutes. Pictures taken using Olympus IX81 inverted microscope and Metamorph imaging software.

4.4.5 Flow cytometry

Flow cytometry was performed as previously described [121] . As a control for non-specific staining, cells were incubated in secondary antibody only. Cells analyzed using an Accuri C6 flow cytometry instrument. Antibodies and concentrations can be found in the Appendix table 4.

4.4.6 Quantification of intracellular C-Peptide

Cells were exposed to low glucose (2.5mM) or high glucose (25mM) in Krebs ringer buffer for 2 hours. After glucose stimulation, cells were harvested and lysed using Bio-Plex lysing system according to manufacturer's instructions. C-Peptide and glucagon were quantified with Bio-Plex Pro Human Diabetes kit following the product manual and analyzed using the Magpix Luminex system.

4.4.7 Statistical analysis

Every result is reported as an average of at least 3 independent experiments. Error bars correspond to standard error and p values were obtained using the Wilcoxon rank-sum test.

4.4.8 Partial least squares regression (PLSR)

We performed PLSR to find correlaton betwenn mature markers and the signaling pathways genes from the PCR array. The mature markers were chosen as the output, *Y*, and the signaling pathway genes as the predictors, *X*. The samples chosen contained both co-culture as well as transwell configurations and the data was normalized with respect to the control sample. From the signaling pathway genes, only those which showed greater than or equal to 2-fold up- or down-regulation were chosen. The data was log2 transformed and the analysis was performed using *plsregress* option from MATLAB (R2010b, Mathworks, Natick, MA). The quality of the regression was acceptable for most of the markers with R^2 greater than 0.8.

4.4.9 Ingenuity pathway analysis (IPA)

Focus genes were analysed using Ingenuity Pathway Analysis Tool (Version 7.6, Ingenuity® Systems) to identify the biological functions, signaling pathways and upstream regulators that were differentially regulated under endothelial cell co-culture. A threshold of 2-fold was used for filtering. This resulted in set of focus genes that contained 42 eligible molecules for the co-culture sample from the 95 genes in the dataset. The top networks and the biological functions were analyzed for these focus genes. The networks were assessed for their significance using the score function (z) with probability of random placement of the gene given as 10^{-z}. The biological functions were ranked using the significance score obtained from Benjamini-Hochberg (B-H) multiple testing correction method (values presented as -log(B-H p-value)). The upstream regulators that may result in the gene expression changes observed in the dataset were tested using overlap p-values obtained from Fischer's Exact test. Also, the state of activation/inhibition was quantified using an activation z-score. The z-score signifies the consistentecy in the direction of increase or decrease of all the downstream genes associated with the upstream regulator. Z-score greater than 2 or less than -2 are significant.

5.0 OVERALL CONCLUSIONS AND FUTURE WORK

5.1 CONCLUSIONS

The studies presented in this dissertation merge together different components of the stem cell niche or native microenvironment to achieve embryonic stem cell differentiation into clinically relevant insulin expressing cells with the potential of being used as alternative therapies to organ transplantation for a number of pathologies of the pancreas, including type 1 diabetes. We accomplish this by studying 1) the effects of substrate mechanical properties in early differentiation events, followed by 2) investigation of chemical modulation of pathways that induce DE specification and lastly, 3) exploitation of cell-cell interaction between hESC-derived PPs and endothelial cells to achieve maturation of the former into functional insulin expressing cells. The results presented here highlight the different components of the stem cell niche which can modulate hESC fate commitment and functionality. Given the current limitations of pancreatic differentiation protocols, this leads us to conclude that all these aspects together and possibly more, need to be modulated and optimized in order to achieve a robust model for pancreatic differentiation. This can also be applied to differentiation of other stem cell types and into any cells or tissue.

In our first study, ESC were cultured in fibrin gels of different compositions and therefore different mechanical and microstructural properties. In the chosen range of substrate

stiffness we found the ectoderm and mesoderm was insensitive to the substrate while the endoderm responded strongly to the different substrates. In this study we measured bulk stiffness of the substrates and concluded endoderm to be preferentially upregulated in softer gels. However, preliminary studies showed that substrates with similar stiffness, but differences in microstructure exhibit different differentiation behavior. This suggests that factors other than stiffness, contribute to differentiation.

In a subsequent study by our group, the microstructural features of these substrates were analyzed in depth. Nine different properties were isolated: fiber connectivity, node density, fiber aspect ratio, fiber diameter, fiber orientation index, pore orientation index, fiber length, pore size and bulk porosity. The correlation of each one of these properties with respect to differentiation was analyzed and fiber orientation was found to have the highest association to endoderm differentiation.

That being said, the effect of substrate stiffness in embryonic stem cell differentiation cannot be completely disregarded. In a more recent study by our group [82] alginate was used at different cross-linking conditions to achieve different stiffness values. All gels were coated with fibronectin and ESCs were allowed to spontaneously differentiate on these substrates. Similar to our fibrin study, endoderm differentiation was more responsive to changes in substrate stiffness. Due to the continuous nature of these gels compared to the fiber structure of fibrin, microstructural characteristics were not considered an important factor, therefore it was concluded that stiffness was the sole mediator of differentiation in this system.

Both studies raise the question of why is endoderm more sensitive to physical changes in the substrate. A very plausible explanation lies in the fact that in both systems the cells fail to spread but aggregate instead. As seen in the fibrin study, endoderm markers are preferentially

expressed at the periphery of the aggregates suggesting that these are the cells that are in direct contact with the extracellular environment, and therefore are more sensitive to changes in it. This leads one to question the sequence of events; do the cells in the periphery get signals from the extracellular environment that directs them into endoderm, or is there an intrinsic mechanism that directs the peripheral cells to become endoderm, which in turn respond to the extracellular environment due to their proximity to it? While in the studies reported here there is not enough data to support the answer to this, it has been seen that endoderm cells are also found in the periphery of embryoid bodies irrespective of the aggregate formation method (appendix figure 10). Since the aggregates seen in our studies are analogous to embryoid bodies, which are a well studied system for gastrulation, we can hypothesize that the peripheral cells become endodermal cells due to signals other than the substrate, but respond to it due to the proximity to it. The observed effect consists of upregulation of endoderm markers in those cells close to the periphery, and not expansion of DE trough proliferation, which by normalization with respect to cell number would show a decrease in other germ layer markers.

Possible mechanism involved in this response still need to be investigated, however, we propose TWIST activation to be a possible mediator. TWIST is a gene involved in gastrulation of *Drosphila* embryos [122], found to be upregulated at the mesendoderm stage [123], responsive to mechanical stimuli [124]and regulated through nuclear translocation of β-catenin [125].

The second study presented here uses growth factors to direct differentiation of hESC. Previous work from our group [57] had developed a pancreatic differentiation protocol using mouse ESC. In order to adapt this protocol to hESC, the first step was proper differentiation into DE cells. A comprehensive literature review showed lack of uniformity in DE induction

mechanism amongst different groups and no evidence that supported one particular method over others. The importance of the study presented here lies in the comparison of widely used DE methods and the conclusion that modulation of pathways at this stage lead to cells with dissimilar pancreatic potential regardless of the fact that they all show expression of DE markers. Furthermore from the observation that even though at the DE stage we were obtaining "better" DE cells from PI3KI as judged by magnitude and yield of DE marker expression, this group failed to achieved good beta cell differentiation, we concluded stage specific marker expression to be an insufficient method of analysis and we suggest an alternative method for assessment of pancreatic potential.

Regression analysis supported our experimental results suggesting that PP markers, instead of DE markers, are better predictors of pancreatic potential. While this statement appears to be intuitive, we suggest looking at PP marker expression at the DE stage, not only the PP stage. From the genes with highest correlation with insulin, we found *PTF1* to be upregulated for both FGF2 and WNT3A induced cells immediately after DE induction. Its magnitude and expression patterns closely resemble those of *FOXA2* and *SOX17* up to the PP stage for those conditions which gave best insulin upregulation. This suggests that expression of *FOXA2*, *SOX17* and *PTF1* shortly after DE induction could be used as a predictor of pancreatic potential. In future studies a verification strategy should be developed for this observation. This can be achieved by creating cell lines with conditional expression of PTF1 so that its expression can be manipulated at desired stages of pancreatic development.

Last, we suggest that method of DE induction primes cells towards specific DE derivatives at later stages of differentiation protocols. This idea is once again supported by subsequent work in our laboratory [126] where a more detailed analysis of DE induction was performed by using a larger catalogue of DE markers and all possible combinations of growth factors (Appendix figure 4). It was observed that BMP4 conditions lead to down-regulation of *CER* and *HNF6*, both of which indicate foregut development, while FGF2 and WNT3 conditions have the opposite effect. This supports the idea that "priming" of potential occurs at the DE stage, with FGF2 and WNT3A priming cells towards forgut development, therefore this cells have higher potential of becoming foregut structures such as the pancreas.

In the last study presented here, the effect of cell-cell interactions is studied by adding EC in direct contact with our hESC-derived PP cells to modulated maturation into insulin expressing cells. We were able to confirm this effect to be endothelial cell-specific by using EC from different sources as well as non-endothelial cells as controls. We also tried several co-culture configurations and we observed that contact co-culture leads to higher insulin expression suggesting that some of the signals are short-lived and/or require direct contact between the EC and hESC-derived PP. Investigation of possible mechanisms associated with this phenomenon was performed using qPCR arrays. From these arrays we found consistent expression patterns for several genes responsive to signal transduction pathways. Regression analysis was performed to find significant correlations between these genes and insulin expression resulting in identification of relevant pathways including the JAK/STAT pathway, hypoxia pathway, NFκβ, WNT and PPAR pathways. We then used IPA database to predict activation status of associated pathways which suggested activation of hydrogen peroxide pathway and inhibition of HNF1A pathway. Consistent with our regression analysis, this points to downregulation of hypoxia, or

restoration of normoxia as a possible mechanism trough which EC mediate maturation of hESC-derived PP. This remains to be further examined, which can be achieved by manipulating oxygen tension in the culture conditions, with confirmation of our results consisting in recapitulation of our current observations at heightened oxygen tension in the absence of endothelial cells.

5.2 FUTURE WORK

In this study we separately evaluate the effect of mechanical, chemical and cell-cell interactions in differentiation of ESC into pancreatic cells. The aim of future studies is to combine these signals together to more closely mimic the complex developmental niche and develop a system for differentiation including ECM, growth factors and cross-talk between different cell types.

Fibrin was picked as a scaffold in our first study for its biocompatibility and ability to be tuned into scaffolds with varying physical properties. Based on the observations from our first and second study, Activin A and WNT3A could be added to hESC encapsulated in soft fibrin gels. By doing this we would study the effects of synergistically using physical and chemical cues to achieve DE induction. Another advantage to this system is the formation of cell aggregates as seen in our fibrin study. It has been postulated that cell aggregates lead to improved differentiation, which has also been observed in studies done in our group. A possible limitation to this however arises from mass transport limitations to the cells at the core of these aggregates. McDevitt's group has shown that embryonic stem cell can be formed into aggregates containing microspheres [127]. Studies by other groups [128] have successfully formed fibrin microbeads. By combining these observations, a possible solution to the mass transfer limitations

of the previously suggested system is formation of stem cell aggregates containing fibrin microbeads with immobilized growth factors.

At later stages of our protocol, endothelial cells can also be used in conjunction with fibrin. Fibrin scaffolds have been postulated as desired candidates for vascular tissue engineering because unlike other materials used for clinical implants, fibrin promotes endothelial cell adhesion and spreading [129]. A possible method is encapsulation of endothelial cells and embryonic stem cell derived PP cells into fibrin gels with immobilized growth factors that promote endothelial cell survival.

APPENDIX A

SUPPLEMENTARY INFORMATION

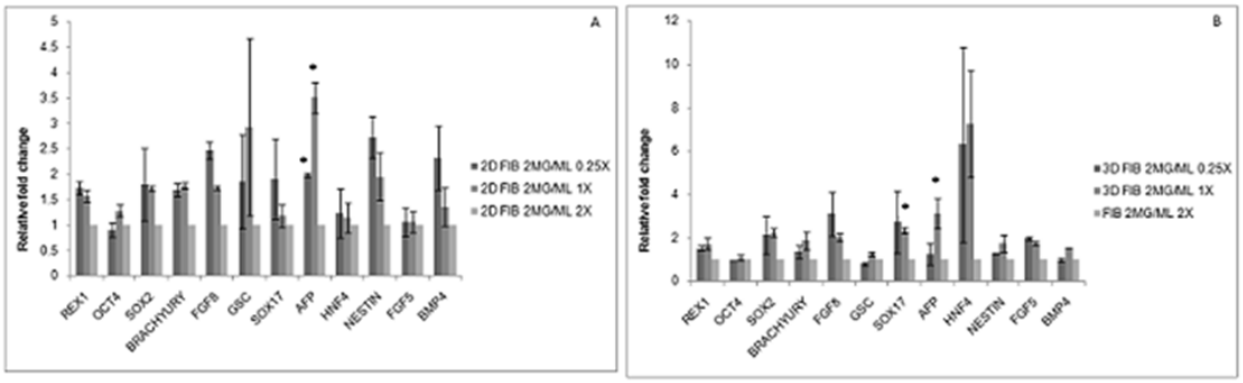

Appendix figure 1. qPCR results for cells plated on gels of 2 mg/ml fibrinogen and various thrombin ratios in 2D (A) and 3D (B) culture formats. Expression levels of ectoderm and mesoderm markers remained relatively constant for all crosslinking ratios. There was significant upregulation of endoderm markers AFP in the 2D culture and Hnf4 in the 3D culture for lower crosslinking groups. * $p < 0.05$ compared to highest stiffness values

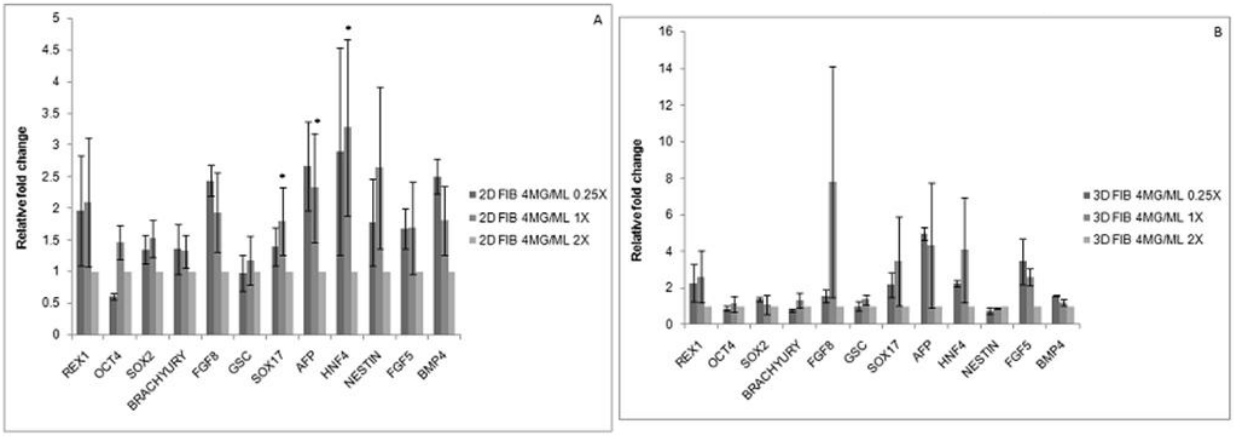

Appendix figure 2. qPCR results for cells plated on gels of 4 mg/ml fibrinogen and various thrombin ratios in 2D(A) and 3D culture formats (B). Most striking difference of marker expression found in 3D formats, where all endoderm markers were significantly upregulated in substrates of lower crosslinking ratios compared to highest crosslinking ratio. Fgfs were also upregulated, but no other mesoderm or ectoderm markers showed a significant difference. * p <0.05 compared to highest stiffness values

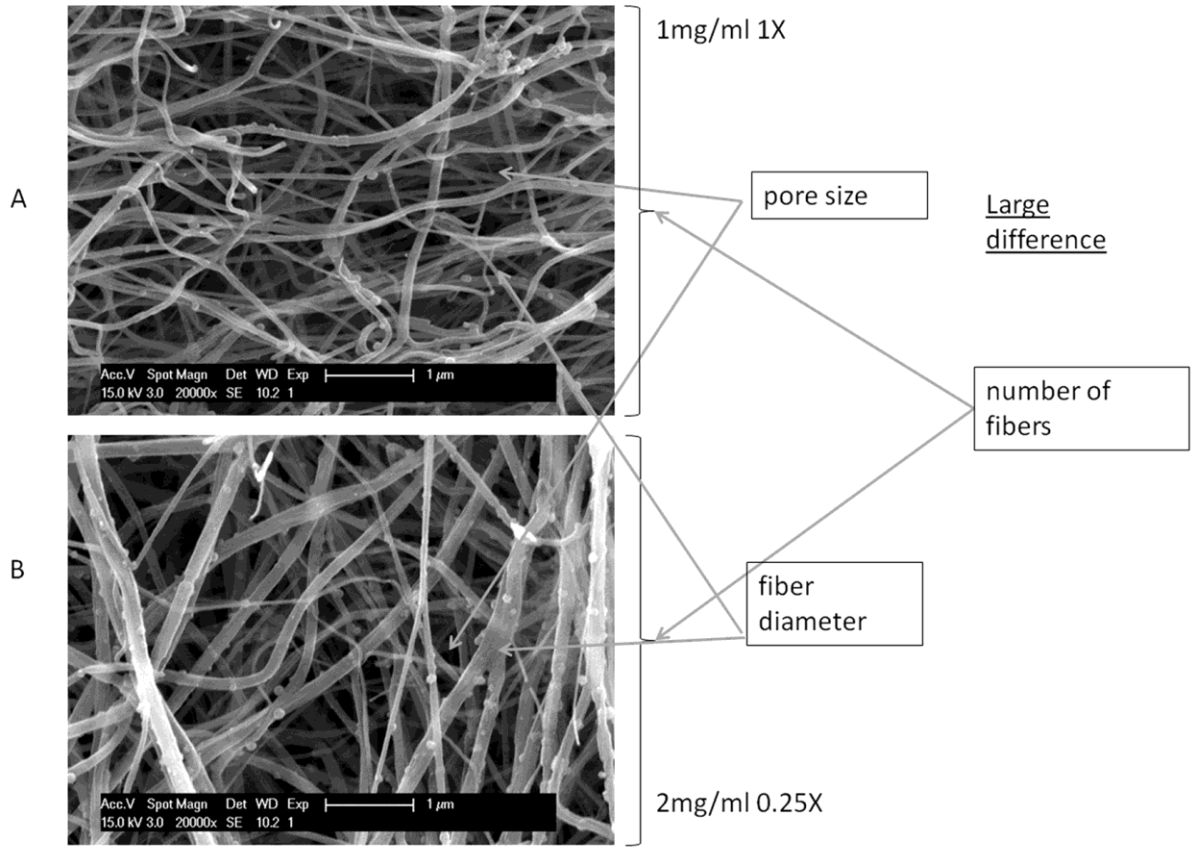

Appendix figure 3. SEM images of 1 mg/ml gels at 1x crosslinking ratio (A) and 2 mg/ml gels at 0.25x crosslinking value (B). Rheology measurements showed comparable stiffness ranges. However, microstructural analysis showed significant differences in characteristics, including node density, pore size distribution and fibre diameter

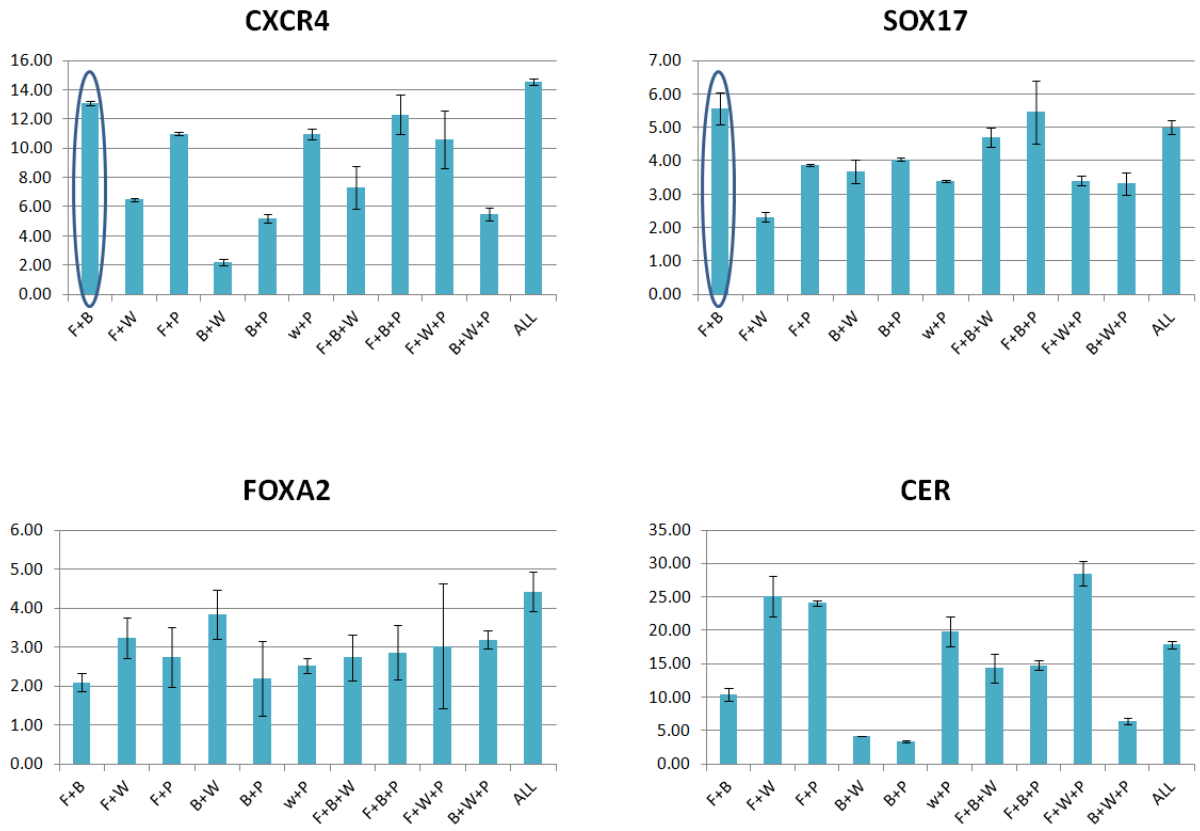

Appendix figure 4: DE induction using Activin A and all possible combinations of molecules used in chapter 3.

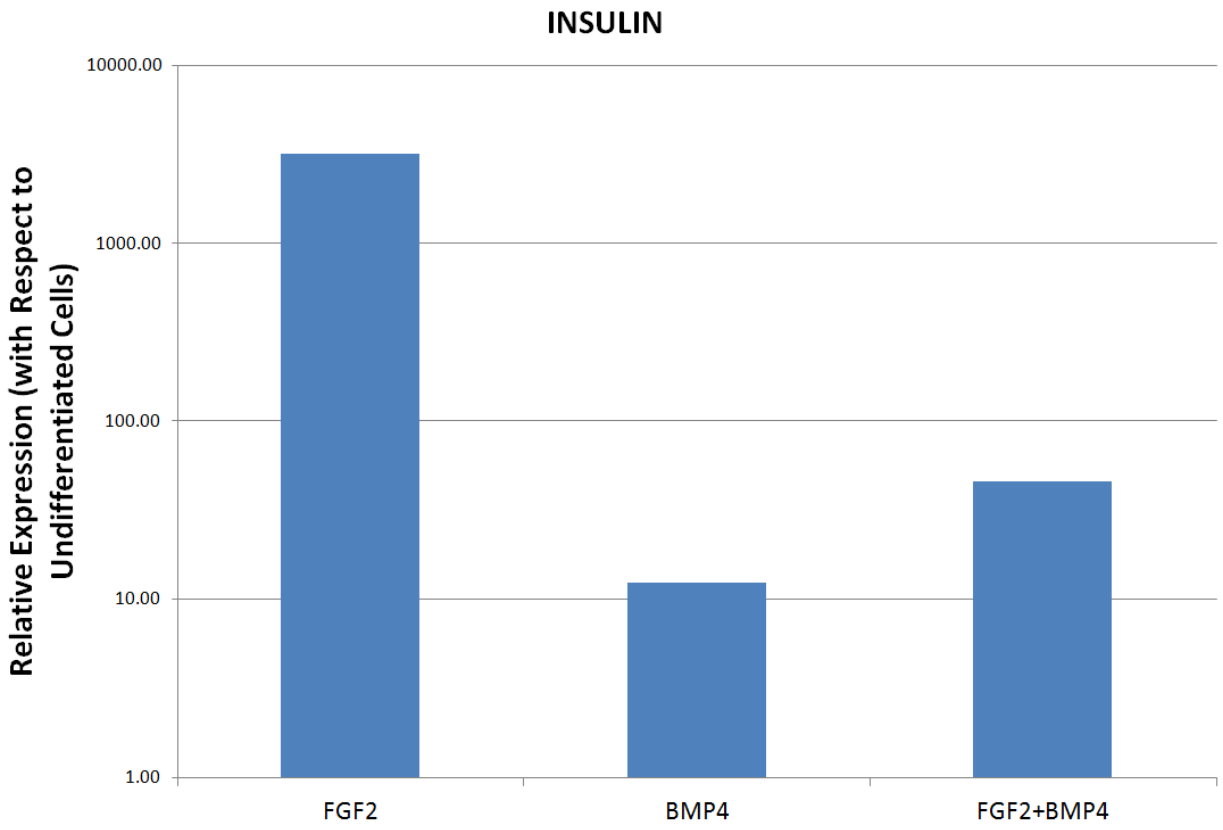

Appendix figure 5: Insulin expression after maturation stage for cells treated with activin with FGF2, BMP4 or both at DE stage

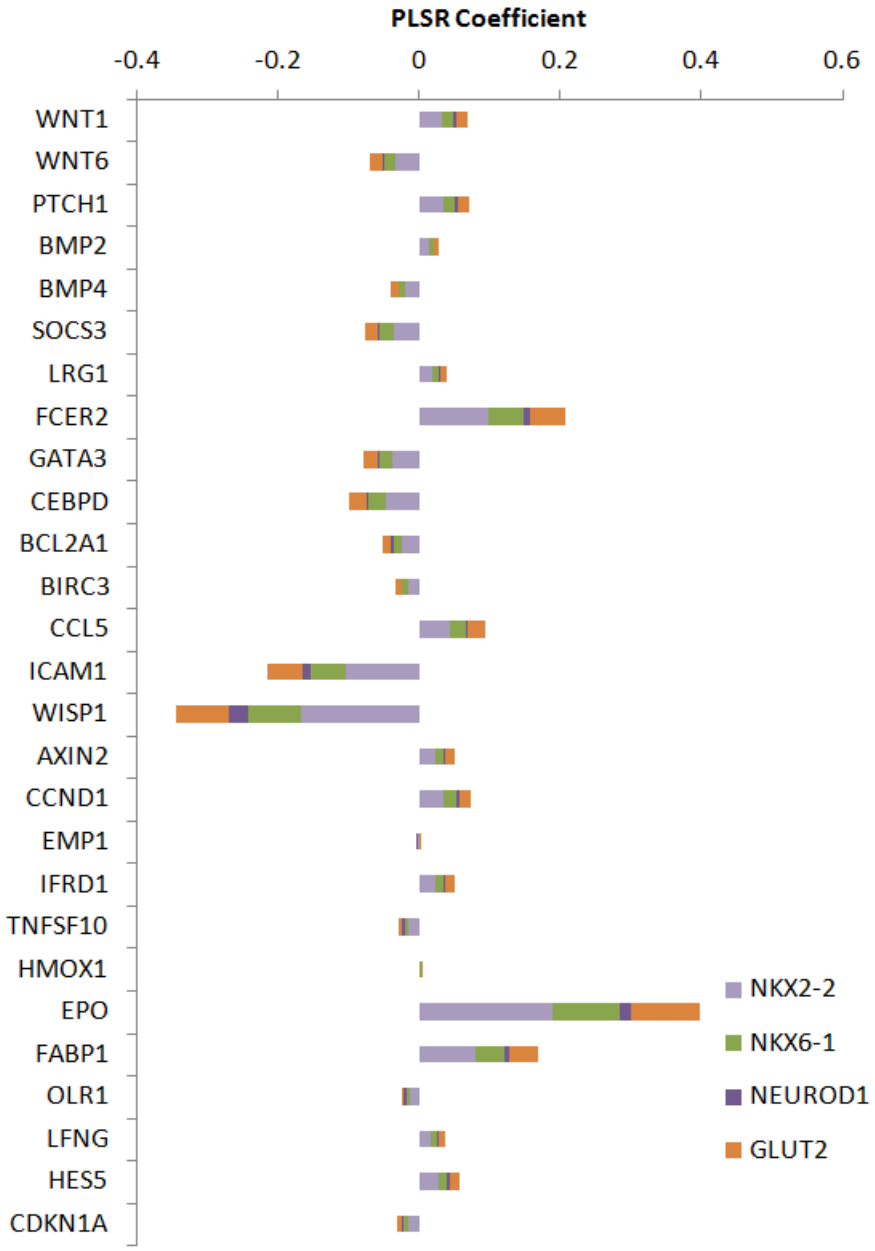

Appendix figure 6: PLSR regression coefficients for group 2 outputs, *NKX2-2*, *NKX6-1*, *NEUROD1*, *GLUT2*.

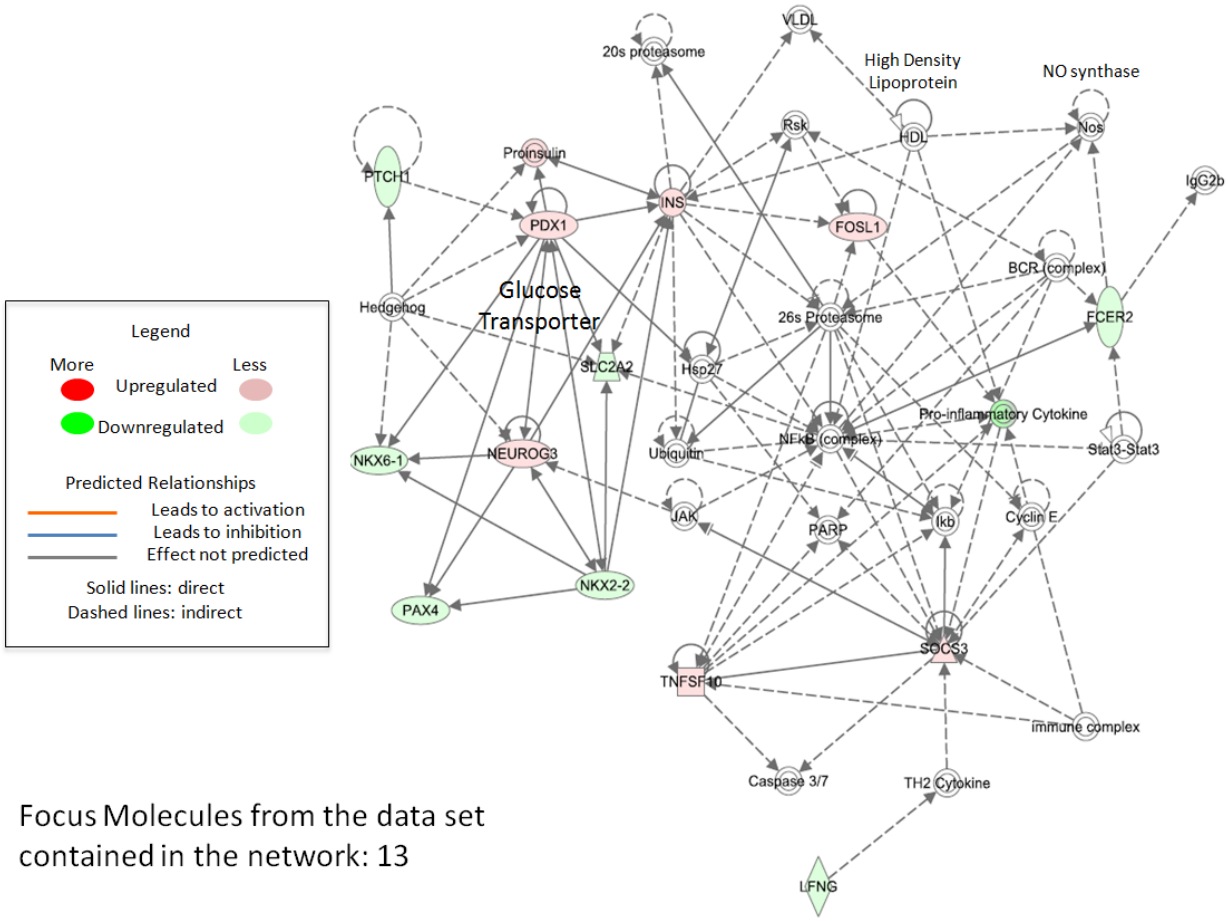

Appendix figure 7 : Top Network associated with endocrine system development as identified by the IPA on the co-culture dataset.

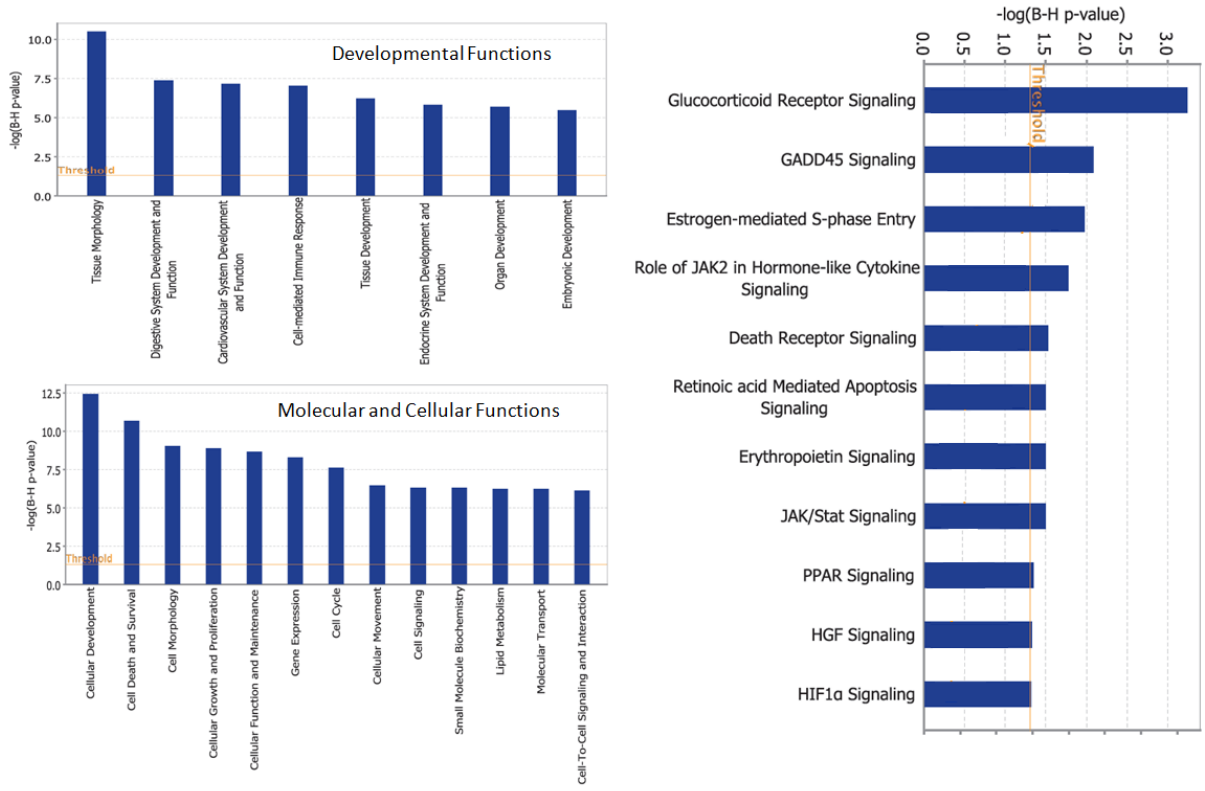

Appendix figure 8. Pathway Analysis for Coculture Sample.(A) Significant biological functions associated with the dataset above the threshold are presented here. Top: Developmental functions, bottom: Molecular and cellular functions. (B) Important canonical pathways associated with gene

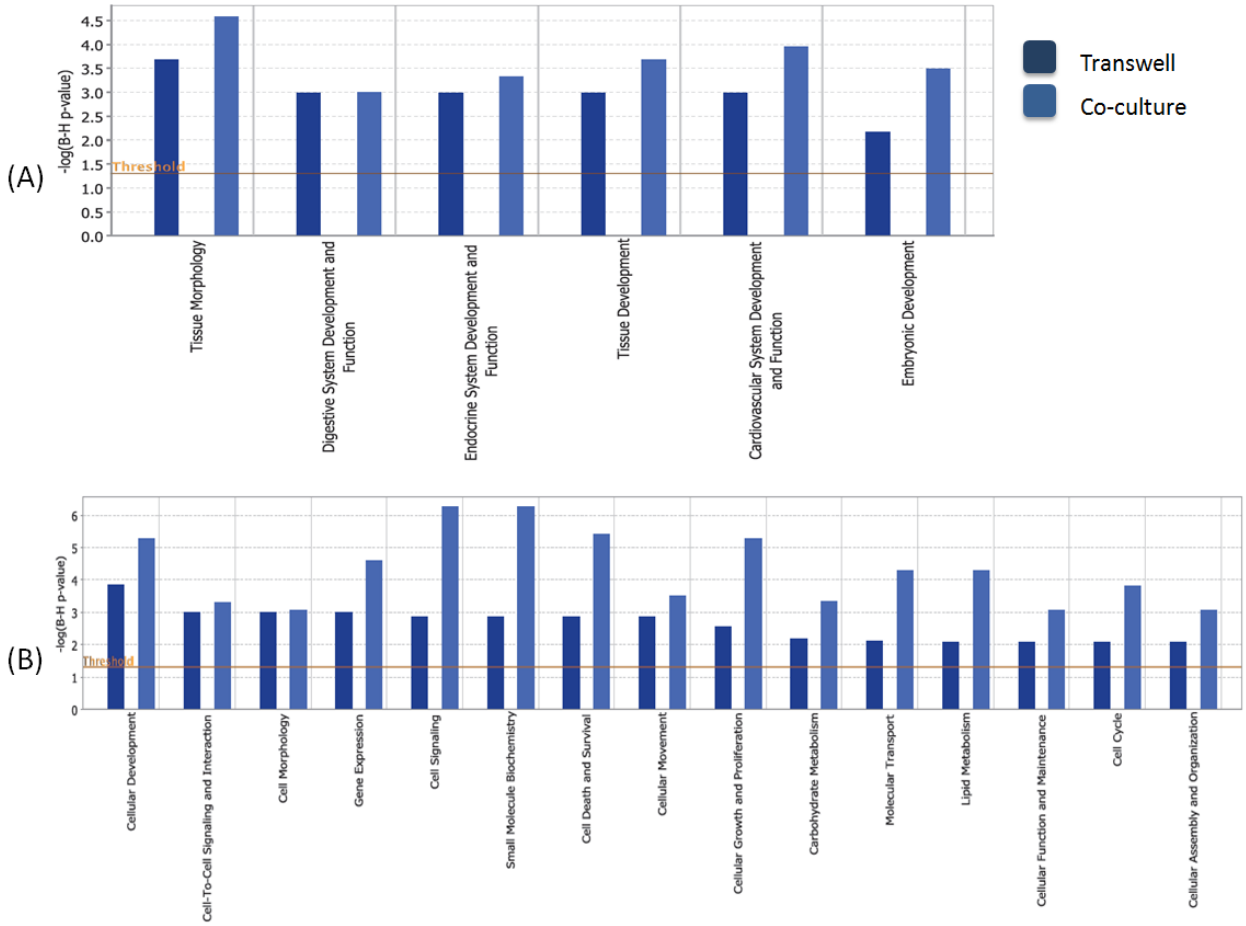

Appendix figure 9: Comparison between Co-culture and Transwell samples. (A) Functions associated with development (B) Molecular and Cellular Functions

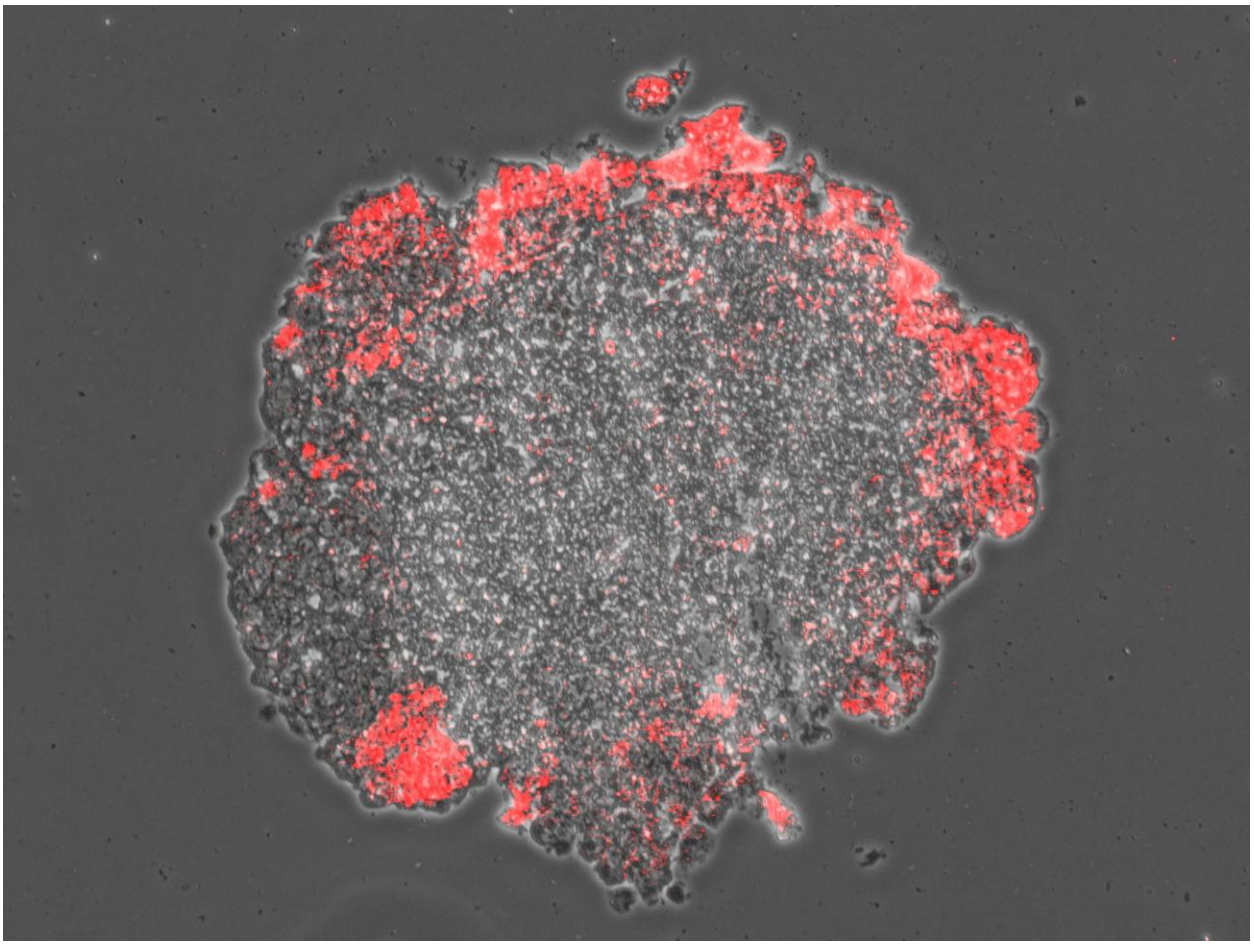

Appendix figure 10: Immunohistochemistry of embryoid body formed by hanging drop method showing peripheral expression of SOX17

Appendix table 1: Primers used for q-RT-PCR in chapter 2

TISSUE	NAME	DIR	SEQUENCE
Control	B-Actin	L	cagcagttggttggagca
		R	tgggagggtgagggactt
PLURIPOTENCY	rex1	L	aaggtcatccacggcaca
		R	tgggagtcatcgcttggt
	0ct4	L	ggagaagtgggtggaggaa
		R	gctgattggcgatgtgag
	sox2	L	ctggactgcgaactggaga
		R	ttggatgggattggtggt
Mesoderm	Brachyury T	L	aagaacggcaggaggatg
		R	gcgagtctgggtggatgta
	FGF8	L	acggcaaaggcaaggact
		R	tgaagggcgggtagttga
	GSC	L	gcaccgcaccatcttca
		R	tcgcttctgtcgtctcca
Endoderm	Sox 17	L	atccaaccagcccactga
		R	acaccacggaggaaatgg
	AFP	L	ctctggcgatgggtgttt
		R	aactggaaggggtgggaca
	HNF4	L	catcgtcaagcctccctct
		R	ccctcagcacacggtttt
Ectoderm	Nestin	L	ggaggatgtggtggaggat
		R	ttcccgtctgctctggtt
	FGF5	L	ttcaagcagtccgagcaa
		R	taggcacagcagagggatg
	BMP4	L	atctggtctccgtccctga
		R	cgctccgaatggcacta

Appendix table 2: Media formulations for pancreatic differentiation protocol used in chapter 3

Stage	Base Media	Supplements	Inducers	Comments
Definitive Endoderm	DMEM/F12	0.2% BSA B27	100ng/ml Activin A *100ng/ml Fgf2 *100ng/ml Bmp4 *25ng/ml Wnt3a *1µM Wortmannin	Day 0-4
Pancreatic Progenitor	DMEM/F12	0.2% BSA B27	0.2µM KAAD-Cyclopamine 2µM All-Trans Retinoic Acid	Day 4-8 Day 6-8
Maturation	DMEM/F12	0.2% BSA B27 25 µg/ml Insulin 50 µg/ml Transferrin 30nM Sodium Selenite	10mM Nicotinamide 30µM DAPT	Day 8-End Day 10-End

** Either/or

Appendix table 3: q-RT-PCR primers used in Chapter 3 and 4

Gene	Primers	Reference
GAPDH	ACGACCACTTTGTCAAGCTCATTTC	D'Amour et al., 2006
	GCAGTGAGGGTCTCTCTCTTCCTCT	
SOX17	CTCTGCCTCCTCCACGAA	Osafune et al., 2008
	CAGAATCCAGACCTGCACAA	
CER	ACAGTGCCCTTCAGCCAGACT	D'Amour et al., 2006
	ACAACTACTTTTTCACAGCCTTCGT	
FOXA2 (Hnf3b)	GGAGCGGTGAAGATGGAA	Osafune et al., 2008
	TACGTGTTCATGCCGTTCAT	
CXCR4	CACCGCATCTGGAGAACCA	D'Amour et al., 2006
	GCCCATTTCCTCGGTGTAGTT	
PDX1	AAGTCTACCAAAGCTCACGCG	Kroon et al., 2008
	GTAGGCGCCGCCTGC	
PTF1	GAAGGTCATCATCTGCCATCG	D'Amour et al., 2006
	GGCCATAATCAGGGTCGCT	
NGN3	CCTTACCCTTAGCACCA	Kroon et al., 2008
	CCCTCTACTCCCCAGTCTCC	
HNF6	TGTGGAAGTGGCTGCAGGA	Zhang et al., 2009
	TGTGAAGACCAACCTGGGCT	
HLXB9	CACCGCGGGCATGATC	D'Amour et al., 2006
	ACTTCCCCAGGAGGTTCGA	
PAX4	TCTCCTCCATCAACCGAGTC	Zhang et al., 2009
	GAGCCACTATGGGGAGTGAG	
PAX6	CGAATTCTGCAGGTGTCCAA	Zhang et al., 2009
	ACAGACCCCCTCGGACAGTAAT	
NKX6-1	AGACCCACTTTTTCCGGACA	Zhang et al., 2009
	CCAACGAATAGGCCAAACGA	
NKX2-2	GGCCTTCAGTACTCCCTGCA	D'Amour et al., 2006
	GGGACTTGGAGCTTGAGTCCT	
ISL1	GATCTATGTCACCTCGCAAGG	Osafune et al., 2008
	TACAACCACCATTTCACTG	
MAFA	CTTCAGCAAGGAGGAGGTCATC	Zhang et al., 2009
	CTCGTATTTCTCCTTGTACAGGTCC	
SOMATOSTATIN	CCCAGACTCCGTCAGTTTCT	Zhang et al., 2009
	ATCATTCTCCGTCTGGTTGG	
GLUT2	AGCTTTGCAGTTGGTGGAAT	Hui et al., 2001
	AATAAGAATGCCCGTGACGA	
INSULIN	AAGAGGCCATCAAGCAGATCA	D'Amour et al., 2006
	CAGGAGGCGCATCCACA	
GLUCAGON	AGGCAGACCCACTCAGTGA	Osafune et al., 2008
	AACAATGGCGACCTCTTCTG	

Appendix table 4: Antibodies used in Chapter 3

Antibody	Source	Application	Dilution
FOXA2	Santa Cruz Biotechnologies sc-20692	Flow	1:500
C-Peptide	Abcam ab14181	Flow/ICC	1:1000/1:500
Alexafluor 488 or 647	Invitrogen	Flow/ICC	1:1000/1:500
SOX17	Santa Cruz Biotechnologies sc-17355	ICC	1:200
PDX1	Santa Cruz Biotechnologies sc-14662, 1:200	ICC	1:200
Hoescht stain	Invitrogen	ICC	1:1000

BIBLIOGRAPHY

1. MacFarlane WM, AJ Bone and M Harrison. (2009). Pancreas Biology, Pathology, and Tissue Engineering. In: *Strategies in Regenerative Medicine*. Santin M ed. Springer Science. pp 261-278.

2. Kahn CR and EP Joslin. *Joslin's diabetes mellitus*. (2005). Lippincott Williams & Willkins, Philadelphia.

3. Marshall MO, HM Thomas, MJ Seatter, KR Greer, PJ Wood and GW Gould. (1993). Pancreatic beta-cells express a low affinity glucose transporter: functional consequences in normal and diabetic states. Biochem Soc Trans 21:164-8.

4. Efrat S, M Tal and HF Lodish. (1994). The pancreatic beta-cell glucose sensor. Trends Biochem Sci 19:535-8.

5. Fridlyand LE and LH Philipson. (2010). Glucose sensing in the pancreatic beta cell: a computational systems analysis. Theor Biol Med Model 7:15.

6. Yovos JG. (2011). The role of α-, δ- and F cells in insulin secretion and action. Diabetes Research and Clinical Practice 93, Supplement 1:S25-S26.

7. Oliver-Krasinski JM and DA Stoffers. (2008). On the origin of the β cell. Genes & Development 22:1998-2021.

8. Blum B, SS Hrvatin, C Schuetz, C Bonal, A Rezania and DA Melton. (2012). Functional beta-cell maturation is marked by an increased glucose threshold and by expression of urocortin 3. Nat Biotechnol 30:261-4.

9. Whitcomb DC. (2008). Pancreatitis. Services UDoHaH ed. National Institute of Health.

10. Castellanos E, J Berlin and DB Cardin. Current treatment options for pancreatic carcinoma. Curr Oncol Rep 13:195-205.

11. Maraschin Jde F. (2012). Classification of diabetes. Adv Exp Med Biol 771:12-9.

12. Silverthorn DU. *Human physiology : an integrated approach*. (1997). Prentice Hall, Upper Saddle River, N.J.

13. Bensellam M, DR Laybutt and JC Jonas. (2012). The molecular mechanisms of pancreatic beta-cell glucotoxicity: recent findings and future research directions. Mol Cell Endocrinol 364:1-27.

14. Shima K, K Shi, A Mizuno, T Sano, K Ishida and Y Noma. (1996). Exercise training has a long-lasting effect on prevention of non-insulin-dependent diabetes mellitus in Otsuka-Long-Evans-Tokushima Fatty rats. Metabolism 45:475-80.

15. McGill JB. (2012). Pharmacotherapy in type 2 diabetes: a functional schema for drug classification. Curr Diabetes Rev 8:257-67.

16. Tavakoli A and S Liong. (2012). Pancreatic transplant in diabetes. Adv Exp Med Biol 771:420-37.

17. Langer RM. Islet transplantation: lessons learned since the Edmonton breakthrough. Transplant Proc 42:1421-4.

18. Lyssiotis CA, LL Lairson, AE Boitano, H Wurdak, S Zhu and PG Schultz. (2011). Chemical Control of Stem Cell Fate and Developmental Potential. Angewandte Chemie International Edition 50:200-242.

19. Cowie CC, KF Rust, DD Byrd-Holt, EW Gregg, ES Ford, LS Geiss, KE Bainbridge and JE Fradkin. (2010). Prevalence of Diabetes and High Risk for Diabetes Using A1C Criteria in the U.S. Population in 1988–2006. Diabetes Care 33:562-568.

20. Jahansouz C, SC Kumer, M Ellenbogen and KL Brayman. (2011). Evolution of β-Cell Replacement Therapy in Diabetes Mellitus: Pancreas Transplantation. Diabetes Technology & Therapeutics 13:395-418.

21. De Vos J, S Assou, S Tondeur, M Dijon and S Hamamah. (2009). Les cellules souches embryonnaires humaines : de la transgression de l'embryon humain à la médecine régénératrice de demain. Gynécologie Obstétrique & Fertilité 37:620-626.

22. Wen Y, B Chen and ST Ildstad. (2011). Stem cell-based strategies for the treatment of type 1 diabetes mellitus. Expert Opin Biol Ther 11:41-53.

23. Van Hoof D, KA D'Amour and MS German. (2009). Derivation of insulin-producing cells from human embryonic stem cells. Stem Cell Res 3:73-87.

24. Abraham S, N Eroshenko and RR Rao. (2009). Role of bioinspired polymers in determination of pluripotent stem cell fate. Regen Med 4:561-78.

25. Engler AJ, S Sen, HL Sweeney and DE Discher. (2006). Matrix Elasticity Directs Stem Cell Lineage Specification. Cell 126:677-689.

26. Lammert E, O Cleaver and D Melton. (2001). Induction of Pancreatic Differentiation by Signals from Blood Vessels. Science 294:564-567.

27. Yoshitomi H and KS Zaret. (2004). Endothelial cell interactions initiate dorsal pancreas development by selectively inducing the transcription factor Ptf1a. Development 131:807-817.

28. Murry CE and G Keller. (2008). Differentiation of Embryonic Stem Cells to Clinically Relevant Populations: Lessons from Embryonic Development. Cell 132:661-680.

29. Chowdhury F, Y Li, Y-C Poh, T Yokohama-Tamaki, N Wang and TS Tanaka. (2010). Soft Substrates Promote Homogeneous Self-Renewal of Embryonic Stem Cells via Downregulating Cell-Matrix Tractions. PLoS ONE 5:e15655.

30. Evans N, C Minelli, E Gentleman, V LaPointe, S Patankar, iM Kallivretak, X Chen, C Roberts and M Stevens. (2009). Substrate stiffness affects early differentiation events in embryonic stem cells. Eur Cell Mater 18:15.

31. Mosesson M, K Siebenlist and M DA. (2001). The structure and biological features of fibrinogen and fibrin. Annals of the New York Academy of Science 936:19.

32. Rosso F, G Marino, A Giordano, M Barbarisi, D Parmeggiani and A Barbarisi. (2005). Smart materials as scaffolds for tissue engineering. Journal of Cellular Physiology 203:465-470.

33. Lim JY, BH Min, BG Kim, HJ Han, SJ Kim, CW Kim, SS Han and JS Shin. (2009). A fibrin gel carrier system for islet transplantation into kidney subcapsule. Acta Diabetol 46:243-8.

34. Kidszun A, D Schneider, D Erb, G Hertl, V Schmidt, E Michael, KT Preissner, G Breier, R Bretzel and T Linn. (2006). Isolated Pancreatic Islets in Three-Dimensional Matrices Are Responsive to Stimulators and Inhibitors of Angiogenesis. Cell Transplantation 15:489-497.

35. Ellis P, B Fagan, S Magness, S Hutton, O Taranova, S Hayashi, A McMahon, M Rao and L Pevny. (2004). SOX2, a persistent marker for multipotential neural stem cells derived from embryonic stem cells, the embryo or the adult. Developmental Neuroscience 26:18.

36. Jin GP, ZY Chang, HR Scholer and D Pei. (2002). Stem cell pluripotency and transcription factor Oct4. Cell Res 12:321-329.

37. Palmqvist L, CH Glover, L Hsu, M Lu, B Bossen, JM Piret, RK Humphries and CD Helgason. (2005). Correlation of Murine Embryonic Stem Cell Gene Expression Profiles with Functional Measures of Pluripotency. Stem Cells 23:663-680.

38. Dziadek M and E Adamson. (1978). Localization and synthesis of alphafoetoprotein in post-implantation mouse embryos. Journal of Embryology and Experimental Morphology 43:289-313.

39. Hudson C, D Clements, RV Friday, D Stott and HR Woodland. (1997). Xsox17[alpha] and -[beta] Mediate Endoderm Formation in Xenopus. Cell 91:397-405.

40. Weber H, B Holewa, EA Jones and GU Ryffel. (1996). Mesoderm and endoderm differentiation in animal cap explants: identification of the HNF4-binding site as an activin A responsive element in the Xenopus HNF1alpha promoter. Development 122:1975-1984.

41. Blum M, SJ Gaunt, KWY Cho, H Steinbeisser, B Blumberg, D Bittner and EM De Robertis. (1992). Gastrulation in the mouse: The role of the homeobox gene goosecoid. Cell 69:1097-1106.

42. MacArthur CA, A Lawshe, J Xu, S Santos-Ocampo, M Heikinheimo, AT Chellaiah and DM Ornitz. (1995). FGF-8 isoforms activate receptor splice forms that are expressed in mesenchymal regions of mouse development. Development 121:3603-3613.

43. Wilkinson DG, S Bhatt and BG Herrmann. (1990). Expression pattern of the mouse T gene and its role in mesoderm formation. Nature 343:657-659.

44. Lobo MT, M Arenas, FJ Alonso, G Gomez, E Bazán, C Paíno, E Fernández, B Fraile, R Paniagua, A Moyano and E Caso. (2004). Nestin, a neuroectodermal stem cell marker molecule, is expressed in Leydig cells of the human testis and in some specific cell types from human testicular tumours. Cell and Tissue Research 316:369-376.

45. Monsoro-Burq AH, D Duprez, Y Watanabe, M Bontoux, C Vincent, P Brickell and N Le Douarin. (1996). The role of bone morphogenetic proteins in vertebral development. Development 122:3607-3616.

46. Rathjen J, J Lake, M Bettess, J Washington, G Chapman and P Rathjen. (1999). Formation of a primitive ectoderm like cell population, EPL cells, from ES cells in response to biologically derived factors. J Cell Sci 112:601-612.

47. Blombäck B and N Bark. (2004). Fibrinopeptides and fibrin gel structure. Biophysical Chemistry 112:147-151.

48. Weisel JW. (2004). The mechanical properties of fibrin for basic scientists and clinicians. Biophysical Chemistry 112:267-276.

49. Duong H, B Wu and B Tawil. (2009). Modulation of 3D Fibrin Matrix Stiffness by Intrinsic Fibrinogen–Thrombin Compositions and by Extrinsic Cellular Activity. Tissue Engineering Part A 15:1865-1876.

50. Ho W, B Tawil, JCY Dunn and BN Wu. (2006). The Behavior of Human Mesenchymal Stem Cells in 3D Fibrin Clots: Dependence on Fibrinogen Concentration and Clot Structure. Tissue Eng. 12:9.

51. Banerjee A, M Arha, S Choudhary, RS Ashton, SR Bhatia, DV Schaffer and RS Kane. (2009). The influence of hydrogel modulus on the proliferation and differentiation of encapsulated neural stem cells. Biomaterials 30:4695-4699.

52. Antoine M, W Wirz, CG Tag, M Mavituna, N Emans, T Korff, V Stoldt, AM Gressner and P Kiefer. (2005). Expression pattern of fibroblast growth factors (FGFs), their receptors and antagonists in primary endothelial cells and vascular smooth muscle cells. Growth Factors 23:87-95.

53. West AF, M O'Donnell, RG Charlton, DE Neal and HY Leung. (2001). Correlation of vascular endothelial growth factor expression with fibroblast growth factor-8 expression and clinico-pathologic parameters in human prostate cancer. Br J Cancer 85:576-583.

54. Canham MA, AA Sharov, MSH Ko and JM Brickman. (2010). Functional Heterogeneity of Embryonic Stem Cells Revealed through Translational Amplification of an Early Endodermal Transcript. PLoS Biol 8:e1000379.

55. Gibson JD, CM Jakuba, N Boucher, KA Holbrook, MG Carter and CE Nelson. (2009). Single-celltranscript analysis of human embryonic stem cells. Integrative Biology 1:540-551.

56. Ko H. (2008). Design, synthesis, and optimization of nanostructured calcium phosphates (nanocaps) and natural polymer based 3d non-viral gene delivery systems In: *Department of Biomedical Engineering, .* Carnegie Mellon University, Pittsburgh, PA.

57. Banerjee I, N Sharma and M Yarmush. (2010). Impact of co-culture on pancreatic differentiation of embryonic stem cells. Journal of Tissue Engineering and Regenerative Medicine:n/a-n/a.

58. Van Hoof D, KA D'Amour and MS German. (2009). Derivation of insulin-producing cells from human embryonic stem cells. Stem Cell Research 3:73-87.

59. Wen Y, B Chen and ST Ildstad. (2010). Stem cell-based strategies for the treatment of type 1 diabetes mellitus. Expert Opinion on Biological Therapy 11:41-53.

60. Kubo A, K Shinozaki, JM Shannon, V Kouskoff, M Kennedy, S Woo, HJ Fehling and G Keller. (2004). Development of definitive endoderm from embryonic stem cells in culture. Development 131:1651-1662.

61. Kim SK and RJ MacDonald. (2002). Signaling and transcriptional control of pancreatic organogenesis. Current opinion in genetics & development 12:540-547.

62. Zaret KS and M Grompe. (2008). Generation and Regeneration of Cells of the Liver and Pancreas. Science 322:1490-1494.

63. Xu X, VL Browning and JS Odorico. (2011). Activin, BMP and FGF pathways cooperate to promote endoderm and pancreatic lineage cell differentiation from human embryonic stem cells. Mechanisms of Development 128:412-427.

64. Phillips BW, H Hentze, WL Rust, QP Chen, H Chipperfield, EK Tan, S Abraham, A Sadasivam, PL Soong, ST Wang, R Lim, W Sun, A Colman and NR Dunn. (2007). Directed differentiation of human embryonic stem cells into the pancreatic endocrine lineage. Stem Cells Dev 16:561-578.

65. Teo AKK, Y Ali, KY Wong, H Chipperfield, A Sadasivam, Y Poobalan, EK Tan, ST Wang, S Abraham and N Tsuneyoshi. (2012). Activin and BMP4 Synergistically Promote Formation of Definitive Endoderm in Human Embryonic Stem Cells. Stem Cells 30:631-642.

66. Bakre MM, A Hoi, JCY Mong, YY Koh, KY Wong and LW Stanton. (2007). Generation of Multipotential Mesendodermal Progenitors from Mouse Embryonic Stem Cells via Sustained Wnt Pathway Activation. Journal of Biological Chemistry 282:31703-31712.

67. D'Amour KA, AG Bang, S Eliazer, OG Kelly, AD Agulnick, NG Smart, MA Moorman, E Kroon, MK Carpenter and EE Baetge. (2006). Production of pancreatic hormone-expressing endocrine cells from human embryonic stem cells. Nat Biotech 24:1392-1401.

68. Kroon E, LA Martinson, K Kadoya, AG Bang, OG Kelly, S Eliazer, H Young, M Richardson, NG Smart, J Cunningham, AD Agulnick, KA D'Amour, MK Carpenter and EE Baetge. (2008). Pancreatic endoderm derived from human embryonic stem cells generates glucose-responsive insulin-secreting cells in vivo. Nat Biotech 26:443-452.

69. McLean AB, KA D'Amour, KL Jones, M Krishnamoorthy, MJ Kulik, DM Reynolds, AM Sheppard, H Liu, Y Xu, EE Baetge and S Dalton. (2007). Activin A Efficiently Specifies Definitive Endoderm from Human Embryonic Stem Cells Only When Phosphatidylinositol 3-Kinase Signaling Is Suppressed. STEM CELLS 25:29-38.

70. Ptasznik A, GM Beattie, MI Mally, V Cirulli, A Lopez and A Hayek. (1997). Phosphatidylinositol 3-kinase is a negative regulator of cellular differentiation. J Cell Biol 137:1127-36.

71. D'Amour KA, AG Bang, S Eliazer, OG Kelly, AD Agulnick, NG Smart, MA Moorman, E Kroon, MK Carpenter and EE Baetge. (2006). Production of pancreatic hormone-expressing endocrine cells from human embryonic stem cells. Nat Biotechnol 24:1392-401.

72. Zhang D, W Jiang, Y Shi and H Deng. (2009). Generation of pancreatic islet cells from human embryonic stem cells. Sci China C Life Sci 52:615-621.

73. Ameri J, A Stahlberg, J Pedersen, JK Johansson, MM Johannesson, I Artner and H Semb. (2010). FGF2 specifies hESC-derived definitive endoderm into foregut/midgut cell lineages in a concentration-dependent manner. Stem Cells 28:45-56.

74. Lee DH, JJ Ko, YG Ji, HM Chung and T Hwang. (2012). Proteomic Identification of RREB1, PDE6B, and CD209 Up-Regulated in Primitive Gut Tube Differentiated From Human Embryonic Stem Cells. Pancreas 41:65-73.

75. Bramswig NC and KH Kaestner. (2011). Transcriptional regulation of α-cell differentiation. Diabetes, Obesity and Metabolism 13:13-20.

76. Gosmain Y, C Cheyssac, MH Masson, A Guérardel, C Poisson and J Philippe. (2012). Pax6 Is a Key Component of Regulated Glucagon Secretion. Endocrinology 153:4204-4215.

77. Servitja J and J Ferrer. (2004). Transcriptional networks controlling pancreatic development and beta cell function. Diabetologia 47:597-613.

78. Bone HK, AS Nelson, CE Goldring, D Tosh and MJ Welham. (2011). A novel chemically directed route for the generation of definitive endoderm from human embryonic stem cells based on inhibition of GSK-3. Journal of Cell Science 124:1992-2000.

79. Kunisada Y, N Tsubooka-Yamazoe, M Shoji and M Hosoya. (2012). Small molecules induce efficient differentiation into insulin-producing cells from human induced pluripotent stem cells. Stem Cell Research 8:274-284.

80. Borowiak M, R Maehr, S Chen, AE Chen, W Tang, JL Fox, SL Schreiber and DA Melton. (2009). Small Molecules Efficiently Direct Endodermal Differentiation of Mouse and Human Embryonic Stem Cells. Cell Stem Cell 4:348-358.

81. Jaramillo M, SS Singh, S Velankar, PN Kumta and I Banerjee. (2012). Inducing endoderm differentiation by modulating mechanical properties of soft substrates. J Tissue Eng Regen Med.

82. Candiello J, SS Singh, K Task, PN Kumta and I Banerjee. (2013). Early differentiation patterning of mouse embryonic stem cells in response to variations in alginate substrate stiffness. J Biol Eng 7:9.

83. Xu X, VL Browning and JS Odorico. Activin, BMP and FGF pathways cooperate to promote endoderm and pancreatic lineage cell differentiation from human embryonic stem cells. Mechanisms of Development.

84. Mfopou JK, B Chen, I Mateizel, K Sermon and L Bouwens. (2010). Noggin, Retinoids, and Fibroblast Growth Factor Regulate Hepatic or Pancreatic Fate of Human Embryonic Stem Cells. Gastroenterology 138:2233-2245.

85. Nostro MC, F Sarangi, S Ogawa, A Holtzinger, B Corneo, X Li, SJ Micallef, I-H Park, C Basford, MB Wheeler, GQ Daley, AG Elefanty, EG Stanley and G Keller. (2011). Stage-specific signaling through TGFβ family members and WNT regulates patterning and pancreatic specification of human pluripotent stem cells. Development 138:861-871.

86. Johansson KA, U Dursun, N Jordan, G Gu, F Beermann, G Gradwohl and A Grapin-Botton. (2007). Temporal Control of Neurogenin3 Activity in Pancreas Progenitors Reveals Competence Windows for the Generation of Different Endocrine Cell Types. Developmental Cell 12:457-465.

87. Mathew S, M Jaramillo, X Zhang, LA Zhang and I Banerjee. (2012). Analysis of alternative signaling pathways of endoderm induction of human embryonic stem cells identifies context specific differences. BMC Syst Biol 6:154.

88. Yu P, G Pan, J Yu and JA Thomson. (2011). FGF2 sustains NANOG and switches the outcome of BMP4-induced human embryonic stem cell differentiation. Cell Stem Cell 8:326-334.

89. Vallier L, T Touboul, Z Chng, M Brimpari, N Hannan, E Millan, LE Smithers, M Trotter, P Rugg-Gunn, A Weber and RA Pedersen. (2009). Early cell fate decisions of human embryonic stem cells and mouse epiblast stem cells are controlled by the same signalling pathways. PLoS ONE 4:6082.

90. Sinner D, S Rankin, M Lee and AM Zorn. (2004). Sox17 and β-catenin cooperate to regulate the transcription of endodermal genes. Development 131:3069-3080.

91. Liu P, M Wakamiya, MJ Shea, U Albrecht, RR Behringer and A Bradley. (1999). Requirement for Wnt3 in vertebrate axis formation. Nat Genet 22:361-365.

92. Schneider VA and M Mercola. (2001). Wnt antagonism initiates cardiogenesis in Xenopus laevis. Genes & Development 15:304-315.

93. Singh AM, D Reynolds, T Cliff, S Ohtsuka, AL Mattheyses, Y Sun, L Menendez, M Kulik and S Dalton. (2012). Signaling Network Crosstalk in Human Pluripotent Cells: A Smad2/3-Regulated Switch that Controls the Balance between Self-Renewal and Differentiation. Cell Stem Cell 10:312-326.

94. Tsaniras SC and PM Jones. (2010). Generating pancreatic β-cells from embryonic stem cells by manipulating signaling pathways. Journal of Endocrinology 206:13-26.

95. Zorn AM and JM Wells. (2009). Vertebrate endoderm development and organ formation. Annual review of cell and developmental biology 25:221-251.

96. White J and S Dalton. (2005). Cell cycle control of embryonic stem cells. Stem Cell Rev 1:131-8.

97. Becker KA, JL Stein, JB Lian, AJ van Wijnen and GS Stein. (2010). Human embryonic stem cells are pre-mitotically committed to self-renewal and acquire a lengthened G1 phase upon lineage programming. J Cell Physiol 222:103-10.

98. Task K, M Jaramillo and I Banerjee. (2012). Population based model of human embryonic stem cell (hESC) differentiation during endoderm induction. PLoS One 7:32975.

99. De Vos J, S Assou, S Tondeur, M Dijon and S Hamamah. (2009). Les cellules souches embryonnaires humaines : de la transgression de l'embryon humain à la médecine régénératrice de demain. Gynécologie Obstétrique & Fertilité 37:620-626.

100. Yechoor V and L Chan. (2010). Minireview: β-Cell Replacement Therapy for Diabetes in the 21st Century: Manipulation of Cell Fate by Directed Differentiation. Molecular Endocrinology 24:1501-1511.

101. Raducanu A and H Lickert. (2012). Understanding Pancreas Development for β-Cell Repair and Replacement Therapies. Current Diabetes Reports 12:481-489.

102. Zhang D, W Jiang, M Liu, X Sui, X Yin, S Chen, Y Shi and H Deng. (2009). Highly efficient differentiation of human ES cells and iPS cells into mature pancreatic insulin-producing cells. Cell Res 19:429-38.

103. Kim SK and DA Melton. (1998). Pancreas development is promoted by cyclopamine, a Hedgehog signaling inhibitor. Proceedings of the National Academy of Sciences 95:13036-13041.

104. Chen Y, FC Pan, N Brandes, S Afelik, M Sölter and T Pieler. (2004). Retinoic acid signaling is essential for pancreas development and promotes endocrine at the expense of exocrine cell differentiation in Xenopus. Developmental Biology 271:144-160.

105. Hu H, L Zhou, A Awadallah and W Xin. (2012). Significance of Notch1-signaling Pathway in Human Pancreatic Development and Carcinogenesis. Appl Immunohistochem Mol Morphol.

106. Xu G, DA Stoffers, JF Habener and S Bonner-Weir. (1999). Exendin-4 stimulates both beta-cell replication and neogenesis, resulting in increased beta-cell mass and improved glucose tolerance in diabetic rats. Diabetes 48:2270-6.

107. Champeris Tsaniras S and PM Jones. (2010). Generating pancreatic beta-cells from embryonic stem cells by manipulating signaling pathways. J Endocrinol 206:13-26.

108. Villasenor A and O Cleaver. (2012). Crosstalk between the developing pancreas and its blood vessels: An evolving dialog. Seminars in Cell & Developmental Biology 23:685-692.

109. Paget MB, HE Murray, CJ Bailey, PR Flatt and R Downing. (2011). Rotational co-culture of clonal β-cells with endothelial cells: effect of PPAR-γ agonism in vitro on insulin and VEGF secretion. Diabetes, Obesity and Metabolism 13:662-668.

110. Sabra G and P Vermette. (2012). A 3D cell culture system: Separation distance between INS-1 cell and endothelial cell monolayers co-cultured in fibrin influences INS-1 cells insulin secretion. Biotechnology and Bioengineering:n/a-n/a.

111. Johansson Å, J Lau, M Sandberg, L Borg, P Magnusson and PO Carlsson. (2009). Endothelial cell signalling supports pancreatic beta cell function in the rat. Diabetologia 52:2385-2394.

112. Zhang D, W Jiang, M Liu, X Sui, X Yin, S Chen, Y Shi and H Deng. (2009). Highly efficient differentiation of human ES cells and iPS cells into mature pancreatic insulin-producing cells. Cell Res 19:429-438.

113. Wicksteed B, C Alarcon, I Briaud, MK Lingohr and CJ Rhodes. (2003). Glucose-induced Translational Control of Proinsulin Biosynthesis Is Proportional to Preproinsulin mRNA Levels in Islet β-Cells but Not Regulated via a Positive Feedback of Secreted Insulin. Journal of Biological Chemistry 278:42080-42090.

114. Pennica D, TA Swanson, JW Welsh, MA Roy, DA Lawrence, J Lee, J Brush, LA Taneyhill, B Deuel, M Lew, C Watanabe, RL Cohen, MF Melhem, GG Finley, P Quirke, AD Goddard, KJ Hillan, AL Gurney, D Botstein and AJ Levine. (1998). WISP genes are members of the connective tissue growth factor family that are up-regulated in Wnt-1-transformed cells and aberrantly expressed in human colon tumors. Proceedings of the National Academy of Sciences 95:14717-14722.

115. Bell GI, HC Broughton, KD Levac, DA Allan, A Xenocostas and DA Hess. (2011). Transplanted Human Bone Marrow Progenitor Subtypes Stimulate Endogenous Islet Regeneration and Revascularization. Stem Cells and Development 21:97-109.

116. Chen C, R Fang, L-C Chou, AW Lowe and E Sibley. (2012). PDX1 regulation of FABP1 and novel target genes in human intestinal epithelial Caco-2 cells. Biochemical and Biophysical Research Communications 423:183-187.

117. Gutteridge A, JM Rukstalis, D Ziemek, M Tie, L Ji, R Ramos-Zayas, NA Nardone, LD Norquay, MB Brenner, K Tang, JD McNeish and RK Rowntree. (2013). Novel pancreatic endocrine maturation pathways identified by genomic profiling and causal reasoning. PLoS One 8:e56024.

118. Canbolat O, J Fandrey and W Jelkmann. (1998). Effects of modulators of the production and degradation of hydrogen peroxide on erythropoietin synthesis. Respiration Physiology 114:175-183.

119. Ke Q and M Costa. (2006). Hypoxia-Inducible Factor-1 (HIF-1). Molecular Pharmacology 70:1469-1480.

120. Metzen E, U Berchner-Pfannschmidt, P Stengel, JH Marxsen, I Stolze, M Klinger, WQ Huang, C Wotzlaw, T Hellwig-Bürgel, W Jelkmann, H Acker and J Fandrey. (2003). Intracellular localisation of human HIF-1α hydroxylases: implications for oxygen sensing. Journal of Cell Science 116:1319-1326.

121. Task K, M Jaramillo and I Banerjee. (2012). Population based model of human embryonic stem cell (hESC) differentiation during endoderm induction. PLoS One 7:e32975.

122. Thisse B, M el Messal and F Perrin-Schmitt. (1987). The twist gene: isolation of a Drosophila zygotic gene necessary for the establishment of dorsoventral pattern. Nucleic Acids Res 15:3439-53.

123. Thisse B, C Stoetzel, C Gorostiza-Thisse and F Perrin-Schmitt. (1988). Sequence of the twist gene and nuclear localization of its protein in endomesodermal cells of early Drosophila embryos. EMBO J 7:2175-83.

124. Farge E. (2003). Mechanical induction of Twist in the Drosophila foregut/stomodeal primordium. Curr Biol 13:1365-77.

125. Wozniak MA and CS Chen. (2009). Mechanotransduction in development: a growing role for contractility. Nat Rev Mol Cell Biol 10:34-43.

126. Mathew S, M Jaramillo, X Zhang, LA Zhang, A Soto-Gutierrez and I Banerjee. (2012). Analysis of alternative signaling pathways of endoderm induction of human embryonic stem cells identifies context specific differences. BMC Syst Biol 6:154.

127. Bratt-Leal AM, RL Carpenedo, MD Ungrin, PW Zandstra and TC McDevitt. (2011). Incorporation of biomaterials in multicellular aggregates modulates pluripotent stem cell differentiation. Biomaterials 32:48-56.

128. Gorodetsky R, RA Clark, J An, J Gailit, L Levdansky, A Vexler, E Berman and G Marx. (1999). Fibrin microbeads (FMB) as biodegradable carriers for culturing cells and for accelerating wound healing. J Invest Dermatol 112:866-72.

129. Kumar TR and LK Krishnan. (2002). Fibrin-mediated endothelial cell adhesion to vascular biomaterials resists shear stress due to flow. J Mater Sci Mater Med 13:751-5.